Novel reagentless chronopotentiometric method for assessing antioxidant activity using chemically modified working electrode

Doctoral thesis

PhD

Author:

Lawrence Kinyua Muthuri

Doctoral School of Chemistry,

Department of Physical Chemistry and Materials Science

Doctoral Supervisors:

Prof. Dr. Géza Nagy

Co-Supervisor:

Dr. Lívia Nagy

Head of the Doctoral School:

Prof. Dr. Attila Felinger

University of Pécs, 2023.

Contents

Acknowledgement

I would like to first express my kind regards and gratitude to my supervisors, Prof. Géza Nagy and Dr. Livía Nagy who have greatly contributed to my growth as an electrochemist. Their invaluable guidance and the privileged opportunity to work with them on my study subject will forever be cherished.

Accolades to the Doctoral School of Chemistry University of Pécs, initially under the leadership of Prof. Ferenc Kilár and subsequently Prof. Attila Felinger. My studies would not have been possible without the immense support of Stipendium Hungaricum scholarship program in Hungary.

Finally I give thanks to God for good health and firm mind. I cannot forget my wife, my children, my parents and as well as the close family members who prayed for my success.

Motivation

Approximately three decades ago, I visited a dentist for routine examination in a small town upcountry in Kenya. At the dentist's office, the orderly and precise protocols that accompany clinical procedures impressed me so much that, I finally broke the news to my parents. "I would like to be a dentist". This wish did not come true in exact sense, however that visit ignited in me the desire to be a medic, a scientist or to be in a profession that would involve solving problems using a learned skill. At that time, I did not know that scientific research would be so invigorating.

At the early age, academic research was still unheard to me. Actually, I did not know anyone who did research. Later on, I chose an alternative profession guided by the reality that only a couple of slots were available at the medical school in my country. Ideas of seeking alternative universities in Eastern Europe were suggested. Meanwhile, I was offered the opportunity to study science at a University in the city. This fitted into my second desire, a first dream came true. At the undergraduate level, I studied biochemistry and zoology as my combination for first degree. I did not intend to specialize too early. In the wisdom of a young post high school lad, specialization at the undergraduate level appeared restrictive, therefore the option of taking a major was put off till such a time when I could study for a master of science degree.

With good scientific qualifications, an opportunity arose to serve in a chemist's laboratory. That laboratory provided analytical services for food, water and environmental samples (in various matrixes) employing mainly the conventional analytical techniques. It is while doing laboratory analysis that my interest was drawn to chemical pollution concerns. To interrogate this concern further, I enrolled for a master's program in environmental science. When I had the opportunity to undertake PhD studies in the application of electrochemical sensors, there was no turning back. In September 2019, just before the pandemic, I began work on my PhD under supervision of Prof. Géza Nagy and Dr. Lívia Nagy in Pécs, Central Europe. This was a second dream come true.

The opportunity to gain additional academic and practical knowledge fitted perfectly into my plans. Though I was forty years old with a fairly young family, I found solace in the fact that communication technology was advanced and readily available in our days. Therefore, it would be possible to multitask in paying bills, doing basic parenting and study all at the same time via online platforms.

Generally, I have a passion for solving real life challenges through innovative solutions. In relation to my current studies, certain substances that are foreign to the bodies of living organisms (xenobiotics) are known to trigger excessive free radical production. This can lead to oxidative stress and in some cases pathological state or illness. However, it also known that physiological systems use antioxidants to counteract the possible harmful effects of radical species. This concern fueled my interest to use antioxidant species in my laboratory measurements.

In addition, many modern chemist's laboratories use conventional methods for the analysis of foods, physiological and environmental samples. This was a second challenge that led to my interest in method development. In reality, many of the conventional technologies are expensive, require specialized training of laboratory staff and in most cases cannot be used on site to obtain instant results. An attractive option to close this gap was adaptation of less costly, simple, fast and convenient technology to detect chemical species. Electrochemistry offered the ideal option, in particular advanced electrochemical sensors.

1 Introduction

At the end of August 2019, I started my research work far from my home and family as a Stipendium Hungaricum supported foreign student at the University of Pécs. It was not an easy time especially because, the COVID-19 pandemic regulations slowed down the experimental work. There were quite long periods when entering or staying in the labs was seriously limited. Despite these difficulties, I found a research field that I greatly enjoyed cultivating. The successes I achieved with my experiments gave sufficient compensation for the hard times I faced often. In this work, I am summarizing the results obtained in the last, almost four years.

My thesis deals with development of a novel method that hopefully in the future, will find application in everyday practice of quantitative analytical chemistry and possibly get listed in the broad techniques of electro-analysis.

The broad objective of this study was development of a new "Reagentless" chronopotentiometric method for measurement of antioxidant activity of samples using all-solid-state chemically modified working electrodes.

The specific objectives were,

- To introduce and experimentally determine the working principle of a novel method for antioxidant activity measurements.
- To use different methods in immobilizing Meldola Blue mediator containing stable redox layers on the surfaces of different carbon electrodes.
- To study the properties such as the thickness of MB, activity of MB, number of confined MB molecules and the stability of the mediator layer using different methods
- To use model calculations for explaining the expected dependence of analytical signal on different measuring parameters.
- To study and test different carbon electrodes such as GC, Pencil, GC with GO docking layer with chemical modifications.
- To investigate the analytical signal provided by the method in case of different antioxidant species and to use gallic acid equivalence for expressing collective antioxidant activity value.

- To make preliminary SECM measurements for studying the redox activity of MB layer on modified carbon electrodes.
- To test the applicability and reproducibility of measurement results of the method for assessing antioxidant activity of pure antioxidants and real fruit juice samples.
- To prove that the confined redox reagent gets renewed in a controlled potential step of the method. Therefore no addition of reagent is needed for the sample–reagent interaction. The novel method can be considered as "reagentless" one

Looking at the history of instrumental analysis, it can be concluded that in the beginning, electrochemical methods played fundamental roles. Their invention and application started as early as in the second part of the nineteenth century. The Faraday law based electrogravimetry was introduced in 1864 by Wolcott Gibbs[1]. A book was published about these methods[2] by 1882. The other Faraday laws based electroanalytical method, the coulometry had also been proceeded early[3]. Hungarian scientists pioneered in developing coulometric titrations[4].

Kohlrausch and Nippoldt [5] developed an alternating current method for conductometry that could be used for decoupling interfering polarization potential. The early use of conductometry for detecting end points of titrations were summarized by Kolthoff[6].

Thinking about pH measurements, potentiometry seems to be the most often employed method of instrumental analysis even in our days. The Nernst equation that potentiometry is based on was formulated by Walther Hermann Nernst in 1889[7]. Potentiometry at a broad scale was used in practice and has been taught in analytical chemistry courses. It is used mainly in, end point detection of acid base, redox measurements and precipitate titrations using different electrodes like hydrogen-, Pt-, Ag- etc. The major steps in potentiometry however, were made in developing different selective potentiometric (ion selective) sensors.

In 1909 Sørensen introduced the pH scale, but for measuring it, potentiometric method and selective pH measuring electrode were needed. Accordingly, development of pH sensing glass electrode was the most important step. Max Cremer[8] used the first glass bulb membrane in potentiometry and noticed the electrode potential - pH dependence. Haber and Klemensiewicz[9] are most often mentioned as developers of the selective pH

measuring glass electrode. Because of the high resistance of this sensor, no appropriate instrument existed in the first decades of the twentieth century for its application. Arnold Beckman, the founder of the Beckman Company developed and marketed from 1935, the first easy to use pH meter instrument. Later, other ion selective potentiometric electrodes were worked out and introduced in practice of analytical chemistry, however the glass electrode is the sensor that still shows an exceptionally best character up till today.

The invention of dropping mercury electrode brought in great potential for working out potent methods for metal analysis[10]. The dynamic ranges of the new, so called polarographic methods far overpassed the other contemporary ones that existed concerning the lower limit of determination, accuracy and reproducibility. For organic analysis, different carbon electrodes and different voltammetric techniques cyclic voltammetry (CV), differential pulse voltammetry (DPV) and square wave voltammetry (SWV) were already at hand in the middle of last century.

From the early times that have been mentioned in this text, the development of electroanalytical methods still goes on at a high pace in different laboratories. A high number of reports appear about new and improved methods, instruments, electrodes and about advantages of their applications. Regardless of these, the real every day applications of electroanalytical methods is getting more and more overpassed by other more recent methods like chromatography, atom absorption spectroscopy (AA), inductively coupled plasma spectroscopy (ICPS), ICP with mass spectroscopy (ICP-MS,) , luminescence spectroscopy, mass spectrometry, enzyme linked immunosorbent assay (ELISA) etc. The reason is obvious. By the fast development of electronic and information sciences, the automation of those methods have become more and more productive.

There are however, several areas where the electroanalytical methods still compete well with the mentioned ones. As example, we can mention the measurements with ultra-micro electrodes in assessing local concentration data in living biological organisms or in gathering local chemical information for scanning electrochemical microscopy studies.

Similarly, when very low concentration of certain species has to be measured, then inverse voltammetric methods can give help. The application of cost effective, online or at site (in-situ) methods using selective electrochemical sensors gives electroanalytical methods a huge comparative advantage. For example, highly selective biosensors can be employed at different environmental spots and living or working in space locations. Essentially, Chillawar et al.[11] in their review note that the "electroanalytical methods have several uses in the study of enzyme catalysis, free radicals, coordination chemistry, environmental monitoring, industrial quality management, solar energy conversion and determination of low concentrations of electrochemically active species in samples". This is in addition to the advantages of rapidity, low cost, environmentally friendly, sensitivity, simplicity and reliability.

I started my experimental work by investigating properties and applications of chemically modified voltammetric graphite electrodes. It was fascinating learning how modification with size exclusion films, coating with different nanomaterials, among them catalysts can extend the applicability of earlier developed electrodes. Furthermore, I could see, how much and how easily certain electrochemical methods can be used in electrode modification techniques.

Some of the chemical modification materials for electrode in electroanalytical work include conductive polymers such as Poly(2,3-dihydrothieno-1,4-dioxin)-poly(styrene sulfonate)- (PEDOT:PSS), 2D graphene derivatives (e.g. Graphene oxide). Others of particular interest are the phenoxazines and phenothiazines [12] which have good coupling to graphite electrodes and very fast charge transfer rate. The chemical modification introduces the advantage of lowering the standard potential (E^o) of the base electrode upon modification. With E^o of the mediator, the heterogeneous electron transfer can occur within the potential range. In his way, the redox catalysis of the test species is made possible.

Some examples of the phenoxazines are; Meldola Blue, Neutral red/phenazin-5-ium (3-amino-7-dimethylamino-2-methylphenazine hydrochloride), phenothiazines include;

phenothiazin-5-ium/Toluidine Blue O (7-amino-8-methylphenothiazin-3-ylidene)-dimethylammonium chloride), Nile blue A/ [9-(diethylamino)benzo[*a*]phenoxazin-5-ylidene]azanium sulfate and Methylene Blue/ [7-(Dimethylamino)phenothiazin-3-ylidene]-dimethylazanium chloride, Prussian Blue a ferrous ferrocyanide oxidation product, crystal violet a triarylmethane dye, etc.

To fit my objective of studying various antioxidant activity, consideration was made of the formal potential, stability on electrode, solubility at neutral pH and ecological friendliness. Based on these concerns, I settled on Meldola Blue for my studies.

Working with carbon electrodes modified with a reversible redox mediator layer, it was learned that the confined mediator layer could easily be electrochemically brought into its oxidized or reduced redox state. This guided us into investigating on the applicability of the mediator layer as an analytical redox reagent. Early results showed that the confined reagent, after the analytic reaction, could be brought into its initial state by controlled potential electrolysis implying reversibility. Furthermore, potentiometry could be used to detect the progress of the reaction. These encouraged us to experiment with working out practically applicable "reagent less" analytic methods. Based on literature information and on earlier, or recent experimental findings we concentrated our efforts in dealing with determination of the action of reductive species in liquid samples.

The antioxidant activity (AOA) is a collective property. It is related to reaction rate. Higher activity shows higher reaction rate in radical quenching or electron exchange. In our work a reagent less method was worked out. It uses for gaining analytical signal the rate of a heterogeneous redox reaction by detecting the initial change of open circuit redox potential in the first few milliseconds. The reagent reacting with the analyte is a reversible redox mediator confined on the surface of a carbon working electrode. A controlled potential step is used for setting the redox state of the reagent. It needs to be mentioned here that most of the advanced electrochemical workstations are equipped with potentiometric measuring program that is capable of executing the measuring protocol. It is hoped that the obtained signal can be used well for estimating the

antioxidant activity of certain samples. My dissertation introduces the method, shows the experiments and findings obtained in the way of its development. Results are shown for proving applicability.

Antioxidants are substances of different structure, action, or origin that can slow or prevent oxidation of other oxidizable species being present. This means that any compound**,** mineral, nutraceutical, or herb that protects against certain damages from reactive oxygen species, including free radicals, single oxygen atoms and hydrogen peroxide are called antioxidants. They can be products of physiologic reactions proceeding in living cells (endogenous antioxidants) or can get into the system from exogenous sources. Endogenous antioxidants are responsible to keep the redox potential balance optimal for physiologic processes in living tissues. This balance can be influenced by clinical treatment or by appropriate nutrition. Addition of appropriate antioxidant to nutrition, beverage and to certain industrial products can avoid their early aging or spoilage. Some very active endogen antioxidants are actually enzymes, while high number of molecules with a variety of chemical structure belongs to the group of non-enzymatic antioxidants.

The best-known enzymatic antioxidants are the glutathione peroxidase, the catalase and the superoxide dismutase. The vitamin E (α-tocopherol) is a popular non-enzymatic, lipid soluble antioxidant similarly to carotenoids, while vitamin C (L-ascorbate) is the most common water soluble one. Flavonoids (benzo-γ-pyrone derivatives) are having both antioxidant and chelating properties.

Antioxidant molecules containing thiol group(s) are listed in an important subgroup. The tripeptide glutathione, the α-Lipoic acid (1, 2-dithione-3-pentanoic acid), and the melatonin (N-acetyl-5-methoxytryptamine) are most often mentioned as members of this group.

2 Literature review

My research largely focused on electrochemical measurement of antioxidant activity in pure samples using a novel chronopotentiometric method at neutral pH. The oxidants (free radicals) which are oxidised species, were "mimicked" by the oxidized form of the redox mediator immobilised on the chemically modified carbon working electrodes. The thin mediator film was brought to the oxidised form using controlled potential. Therefore, it is necessary to do a literature review in regard to the importance of oxidants in physiology, food and general environment as well as the counter effect of both endogenous and exogenous antioxidants in the maintenance of a homeostatic balance and prevention of food spoilage.

2.1 Oxidants

Many excellent reviews [13] [14] [15] [16] have dealt with the issues of oxidants/free radicals in regard to the role played by these reactive species. In the physiological environment, free radicals or reactive species which are oxidants may result from normal essential metabolic processes aimed at cellular signalling or as a reaction to xenobiotics such as air pollutants, toxic chemicals, ionising radiation, drugs, pesticides, ozone (O_3) and other toxic substances. The most studied oxidants / reactive species/ free radicals include those derived from oxygen, reactive oxygen species (ROS), derived from nitrogen, reactive nitrogen species (RNS), derived from sulphur reactive sulphur species (RSS), derived from chlorine reactive chlorine species (RCS) and derived from bromine reactive bromine species (RBS). Physiological processes such as those in the respiratory chain, phagocytosis, cytochrome P450 system in microsomes of liver cells, in prostaglandin synthesis, inflammation and exercise are additional sources of metabolic sources of free radicals.

2.1.1 Enzymatic generation of free radicals

Several reviews in this section have highlighted the dual role[17] of free radicals in physiology. Radicals are generated through the normal processes, however an excess can lead to a pathological state. Kaur et al. [18] in their review highlights the contribution of various xenobiotics in the proliferation of free radicals in organisms. The review by Furukawa [19] points out the process that produces physiological superoxide, nitric oxide

radical, peroxynitrite, and the role of H_2O_2, Fe, Cu and Zn in the related enzymatic processes. The generation of ROS initiates with the rapid uptake of O_2 followed by the activation of NADPH oxidase and the generation of the superoxide ion molecule ($^{\bullet}O_2^-$) in a reaction catalysed by catalase. The $^{\bullet}O_2^-$ is then converted to H_2O_2 in a process involving superoxide dismutase enzyme. The main source in physiological conditions of superoxide ion ($^{\bullet}O_2^-$) is the mitochondria in eukaryotic cells. It is a product of the electron transport chain.

$$\text{Step 1.} \quad 2O_2 + NADPH \rightarrow 2\,{}^{\bullet}O_2^- + NADP + H^+$$

$$\text{Step 2.} \quad 2\,{}^{\bullet}O_2^- + 2H^+ \rightarrow H_2O_2 + O_2 \qquad (1)$$

Other enzymatic sources of free radicals in physiological conditions include cytochrome P450, oxidoreductase and xanthine dehydrogenase enzyme activity. Hydrogen peroxide is a source of superoxide and is therefore a precursor molecule. However, H_2O_2 is permeable to the cell membrane (lipid bilayer) and therefore relieves the oxidative stress. H_2O_2 is converted to water through the activity of glutathione peroxidase and catalase. An imbalance in $^{\bullet}O_2^-$ and H_2O_2 can lead to the formation of $^{\bullet}OH$. This is dangerous in that this reaction is catalysed by free ferrous ions in Fenton reactions.

$$^{\bullet}O_2^- + Fe^{3+} \rightarrow O_2 + Fe^{2+}$$

$$H_2O_2 + Fe^{2+} \rightarrow {}^{\bullet}OH + OH^- + Fe^{3+} \qquad (2)$$

The review article by Muijsers et al.[20] explains how nitric oxide synthase system generates the nitric oxide radical ($NO^{\bullet}$) which is a reactive nitrogen species. For example, in the presence of oxygen and NADPH, the amino acid L-arginine is a precursor for the $NO^{\bullet}$

$$\text{L-Arginine} + O_2 + NADPH \rightarrow NO^{\bullet} + \text{citrulline} \qquad (3)$$

The continuous generation of $NO^{\bullet}$ through the nitric acid synthase system can make copious amounts of the species available. The $NO^{\bullet}$ modulates each other with the $^{\bullet}O_2^-$. They combine to form peroxynitrite ($ONOO^-$) which is a strong oxidant. The main target

is aromatic amino acid residues. This may inactivate enzymes by modifying their peptide structure. Peroxynitrite however acts as a signalling molecule as well.

2.1.2 Lipid peroxidation

Lipid peroxidation in physiological conditions happens through a free radical mechanism involving initiation, propagation, and termination stages. In the initiation stage, free radicals are formed, this is followed by the propagation stage where lipid radicals react with oxygen to form peroxyl radicals. The peroxyl radicals further react with other lipid molecules to form more lipid radicals and unstable hydrogen peroxide (H_2O_2) as well as secondary products. The peroxyl radical $FOO^{\bullet}$ acts as carriers of the chain reactions. Finally in the termination stage, various radicals react to form non radical products [21]. The other important product of lipid peroxidation is aldehydes which can diffuse from the site of production to cause damage in other parts of the cell. The process involving the fatty acid radical ($F^{\bullet}$) progresses as follows;

Initiation

$$FH \rightarrow F^{\bullet} + H^{\bullet}$$

Propagation

$$F^{\bullet} + O_2 \rightarrow FOO^{\bullet}$$

$$FOO^{\bullet} + FH \rightarrow F^{\bullet} + FOOH$$

Termination

$$F^{\bullet} + F^{\bullet}$$

$$FOO^{\bullet} + FOO^{\bullet}$$

} forms non-radical products

$$F^{\bullet} + FOO^{\bullet}$$

4

Food rich in unsaturated fatty acids and cholesterol may undergo lipid peroxidation. At high temperatures for example, lipids may undergo peroxidation where foul smelling epoxides, ketones, acids and aldehydes are formed[22]. All these processes and products may affect the taste and the quality of food.

2.1.3 Protein oxidation

Protein oxidation on the other hand mainly depends on amino acid composition and structure. The sulphur containing amino acids such as cysteine forms a thiyl radical ($PS^{\bullet}$), thiylperoxyl radical ($PSOO^{\bullet}$) or a disulphide bond (PSSP).

The process of protein oxidation progresses as follows;

$$PSH + \bullet OH \rightarrow PS\bullet + H_2O$$

$$PS\bullet + O_2 \rightarrow PSOO\bullet$$

$$PS\bullet + PS\bullet \rightarrow PSSP$$

5

The aromatic amino acids are susceptible to free radical attack by oxygenation of the aromatic ring[23]. The hydroxyl radical $^{\bullet}OH$ is highly reactive and attacks base pairs of deoxyribonucleic acid (DNA), proteins and lipids thereby causing damage resulting into injury and diseases.[24]

2.2 Antioxidants: classification, action mechanism and current research

A common broad classification is into natural and synthetic as Table 1 shows. The natural is further broken into endogenous and exogenous.

Table 1. A table of the different classes of antioxidants

<table>
<tr><th colspan="2">Natural</th><th>Synthetic</th></tr>
<tr><td colspan="2">Endogenous</td><td rowspan="4">Phenolic structures
Butylhydroxyanisol (BHA)
Butylhydroxytoluene (BHT)
Tert- butylated hydroquinone (TBHQ)
Propyl gallate (PG)
Nano antioxidants</td></tr>
<tr><td colspan="2">Enzymatic</td></tr>
<tr><td><u>Primary defense enzymes</u>
Superoxide dismutase (SOD),
Glutathione peroxidase, Catalase</td><td><u>Secondary defense enzymes</u>
Glucose-6-phosphate-dehydrogenase
Glutathione reductase</td></tr>
<tr><td colspan="2">Non enzymatic</td></tr>
<tr><td colspan="2">Low molecular weight</td><td>oxides</td></tr>
<tr><td><u>Lipophilic</u>
Plasmalogen, Lipoic acid,
Ubiquinone</td><td><u>Hydrophilic</u>
Uric acid, Glutathione,
Conjugated bilirubin,
Melatonin, Amino acids.</td><td>Metallic Nanoparticles
Antioxidant functionalised NPs</td></tr>
<tr><td colspan="3"><u>Metal-binding proteins</u>
Ferritin, Albumin, Metallothionein, Ceruloplasm</td></tr>
<tr><td colspan="3">Exogenous</td></tr>
<tr><td colspan="3"><u>Polyphenols</u>
Anthocyanidins, Cyanidins and Petunidin, Flavones, Flavonols, Isoflavonoids, Flavanones, Flavanones, Flavonoids, Phenolic acids-(Hydroxybenzoic acids: Gallic acid, Ellagic acid, Protocatechuic acid. Hydroxycinnamic acid: Ferulic acid, p-Coumaric acid, Caffeic acid)</td></tr>
<tr><td colspan="3"><u>Trace elements</u>
Se, Mn, Cu, Zn and Fe</td></tr>
<tr><td colspan="3"><u>Vitamins and derivatives</u>
L-ascorbate, Tocopherols, Tocotrienols, Retinol</td></tr>
<tr><td colspan="3"><u>Carotenoids</u>
α- and β-Carotene, Zeaxanthin, Lutein, Lycopene, β-Cryptoxanthin</td></tr>
</table>

The endogenous group is further divided into enzymatic and non-enzymatic. According to their operating mechanism, the enzymatic are either primary or secondary. The non-enzymatic antioxidants include the metal binding proteins such as metallothionein. The exogenous group include the polyphenols, trace elements, vitamins and carotenoids. Synthetic ones have either a phenolic structure or have a nanomaterial component [25] [26].

The antioxidants action mechanisms vary depending on the class. In the interaction, most often an electron or H atom is exchanged. Sometime the metal redox centre of the oxidant is complexed by the antioxidant molecule in this way its action is hindered. The antioxidants also can inhibit the chain reactions that lead to the generation of free radicals. Fig.1 shows the major mechanisms of antioxidant action.

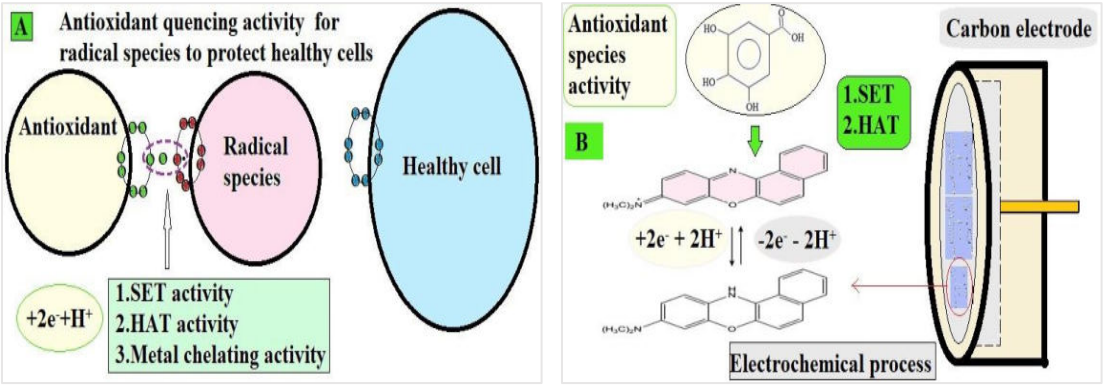

Fig. 1. Illustration (A) shows the SET,HAT and chelation action mechanisms of antioxidants in scavenging for free radicals close to a healthy cell under physiological conditions. Illustration (B) shows a related SET and HAT activity between an electrochemically oxidised layer of MB on a carbon electrode and an antioxidant species (the basis of my experiments).

Reasearch on the behaviour, the roles, the characterization of different antioxidant species, as well as methods for their analysis is getting increasingly into the focus of interest in our days. Extremely high number of publications appear year by year. Giving a comprehensive view about them is far over the scope of my work. In the field dealing with electroanalytical antioxidant measurement too, highly active research has been going on. Fig. 2 shows the number of scientific publications that appeared over a twenty-five year period in ScienceDirect and 25 years in Web of Science citation databases as an example.

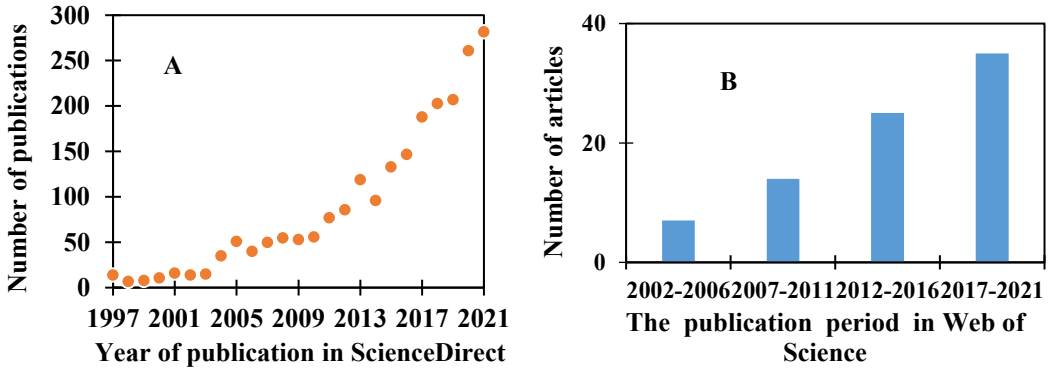

Fig. 2. (A) The graph shows the number of publications in ScienceDirect citation database. The search criteria was “antioxidants in electrochemistry” searched as the keywords. (B) The graph shows the number of publications from chemistry journals in Web of Science citation database for five-year intervals (1997 to 2021). The search was done for the topic "antioxidants in electrochemistry".

The search results shown in Fig. 2 (A) in science direct citation database was done by typing the key words “antioxidants in electrochemistry” as the keywords. The year of publication was 2002 to 2021. The total number of publications meeting this criterion was 2224 for all article types, publication titles and subject areas.

Fig. 2 B shows the results of a more selective search in Web of Science citation database with “antioxidants in electrochemistry” as the topic. The number of records was 433. The selection criteria was set to 1997 to 2021 (395 records), further selection to articles and review articles under document type (388) and finally selection into electrochemistry category (82), the first records meeting the entire criterion appeared after 2002. From the total of 82 records a bar graph is was made in 5 year intervals. This reveals a growing interest in antioxidant research within electrochemistry.

2.2.1 Enzymatic antioxidants

Belinskaia et al.[27] noted in their review that blood is more frequently exposed to oxidants than intracellular fluid. From this fact, serum albumin plays a core role in normal and oxidative stress conditions. Enzymatic antioxidants convert free radicals into H_2O_2 then to H_2O through processes that involve cofactors such as Cu, Zn, Mn and Fe. Primary defence enzymes include superoxide- dismutase (SOD), glutathione peroxidase, and catalase. Secondary defence enzymes include glucose-6-phosphate dehydrogenase (G-6-PDH) that supplies H^+ in the cytosol and glutathione reductase. They act mainly by reducing levels of the non-radical lipid hydroperoxides intermediates and H_2O_2. This prevents lipid peroxidation and ensures that the cell membrane lipid bilayer is maintained.

$$2H_2O_2 \rightarrow 2H_2O + O_2 \text{ catalysed by catalase}$$

$$ROOH + 2GSH \rightarrow ROH + GSSG + H_2O \text{ involves glutathione antioxidant}$$

6

The superoxide ion is not permeable in the mitochondrial membrane hence the accumulation[28]. Superoxide dismutase (SOD) is a metalloenzyme that helps to decrease the concentration of radicals in living tissues. It catalyzes recombination of oxygen

radicals, avoids formation of reactive species like hydrogen peroxide and triplet oxygen. Cu ions were found to induce glutathione transferase activity in cells and a proportionate decrease in reactive oxidising species[29]

2.2.2 Non-enzymatic antioxidants

On the other hand, the non-enzymatic antioxidants disrupt the chain reaction process in lipid peroxidation and protein oxidation. This class includes vitamins, trace elements, carotenoids, polyphenols, metal binding proteins and the synthetic compounds[26].

2.2.2.1 Vitamins

Eggersdorfer et al.[30] gave a review of the vitamins including discovery, isolation, elucidation and first synthesis. In my research, the water soluble, electron donor, L-ascorbate was among the pure materials used in antioxidant studies. It was first isolated by Albert Szent-Györgyi (Fig.3) in 1931 from Hungarian red pepper [31].

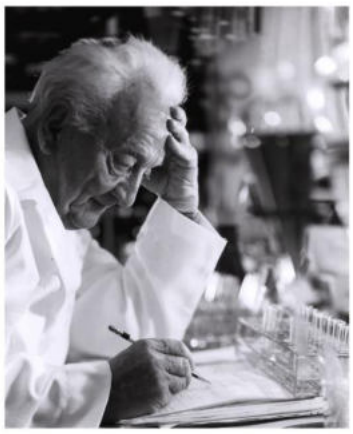

Fig. 3. A photograph of Albert Szent-Györgyi who isolated L-ascorbate

Vitamin C/ L-ascorbate coverts to ascorbate radical by donating an electron to the lipid radical, consequently the chain reaction is terminated. This is followed by the rapid reaction of two ascorbate radicals to form dehydroascorbate which lacks antioxidant activity. To put it back into antioxidant state, two electrons are added in the presence of oxidoreductase to convert it back to ascorbate as illustrated in Fig.4.

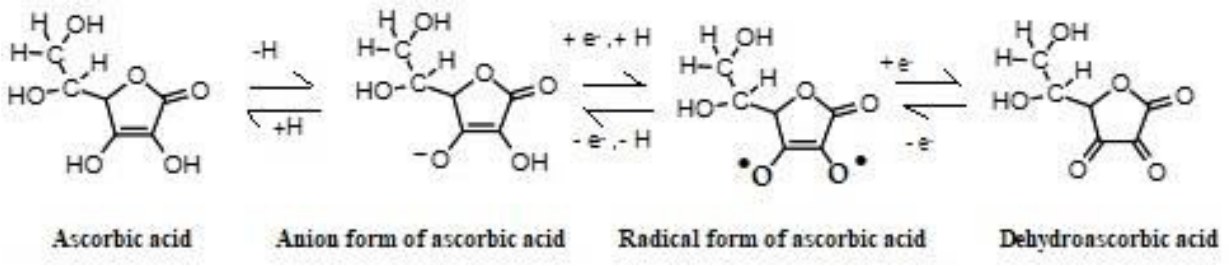

Drawn using https://chemdrawdirect.perkinelmer.cloud

Fig. 4. An illustration of the oxidation and reduction of L-ascorbate

Some vitamins such as α-tocopherol (vitamin E) are fat soluble and act by breaking the chain reaction during lipid peroxidation reactions in low density lipoprotein generation and in cell membrane by capturing the lipid peroxyl radical. The tocopherol radical[24] is quite stable therefore largely not reactive, thereby serving as a good antioxidant

$$LOO^{\bullet} + \alpha\text{-tocopherol-OH} \rightarrow LOOH + \alpha\text{-tocopherol}-O^{\bullet} \quad (7)$$

In addition, vitamin E radical can be converted back to vitamin E by the donation of a proton from vitamin C (see Fig. 5). In turn, the dehydroascorbate form is reduced to L-ascorbate by dehydroascobate reductase in the presence of GSSG-GSH system [33]

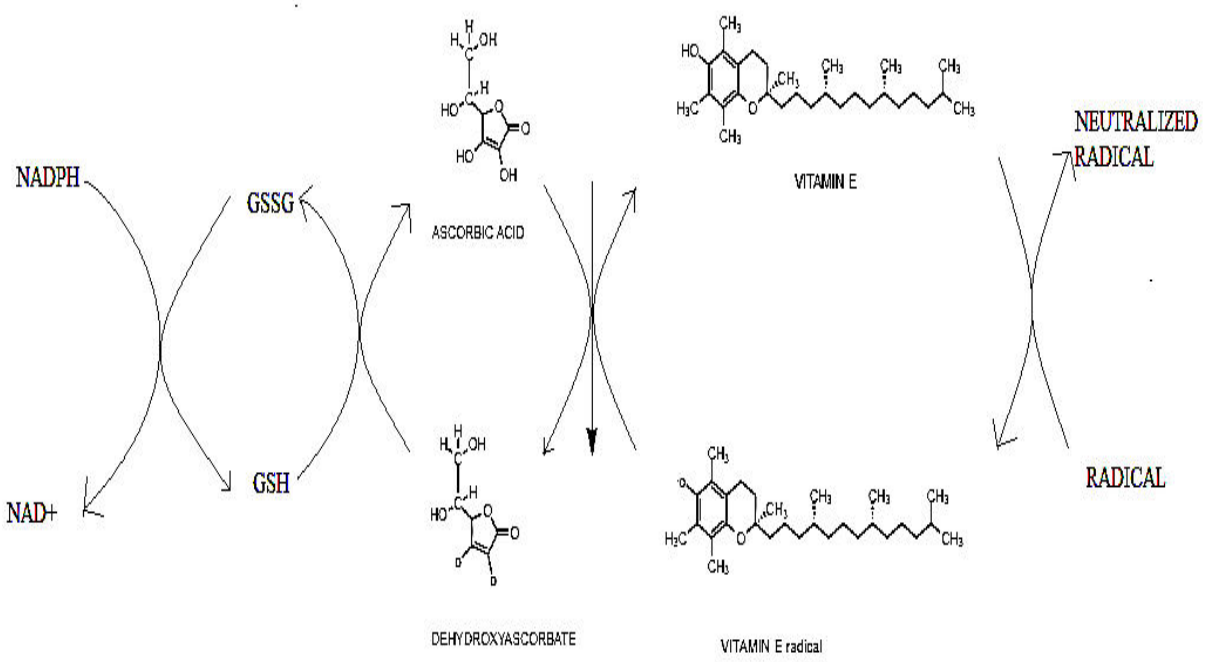

Drawn using https://chemdrawdirect.perkinelmer.cloud and paint tool

Fig. 5. A scheme showing the conversion of vitamin C to dehdroascorbate in the presence of glutathione and the donation of a proton by L-ascorbate to vitamin E radical to convert it back to vitamin E

2.2.2.2 Polyphenols

In my research, polyphenols played a central role as test antioxidants as analytes against the oxidised working electrodes. Polyphenols are characterized by multiple phenol units and play an important role in free radical scavenging as antioxidants[34]. The many articles and reviews in this section have appeared detailing the role of dietary polyphenols and the antioxidant activity. For example, the action aimed at chemoprevention of oxidative stress and protection against protein, lipid and DNA damage that is implicated in human disease[35] . To extend shelf life in foods, the review by Papuc et al. [36] indicates that polyphenols are largely useful in the inhibition of oxidative process as radical scavengers, reducing agents for metmyoglobin in meat and as lipoxygenase inhibitors. The mechanism involves chelating of metal cofactors for enzymes thereby forestalling

the generation of ROS. Other examples include flavanols or catechins in tea, wine, beer and chocolate as well as several cereals[37] [38]. Hydroquinone a phenol compound is a

strong antioxidant naturally found in propolis[39] of bees that may be a constituent of honey and in some mushrooms. It is used as a skin treatment compound. Hydroquinone antioxidant activity has been reported in vitro by Giner et al. in their review article and the pharmacological potential has been proposed[40]. The bioflavonoids are found largely in fruits and vegetables.

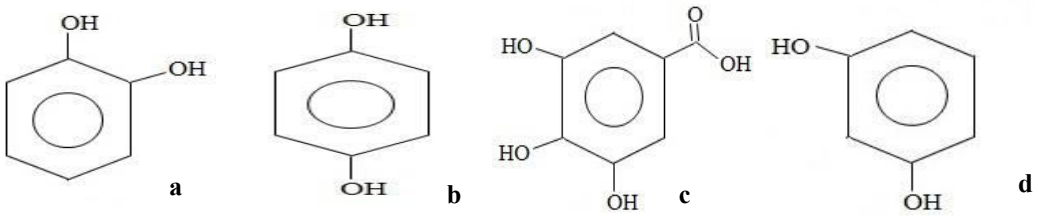

Fig. 6. An illustration of (a) catechol, (b) hydroquinone, (c) gallic acid and (d) resorcinol respectively

The phenolic acids such as, hydroxycinnamates also known as phenylpropanoids include ferulic, caffeic, synaptic, coumaric acid and their derivatives scavenge for hydroxyl radical, superoxide ion radicals, organic radicals, peroxyl radicals, peroxynitrite and singlet oxygen. They act by chain breaking and as reducing agents[41]. Hydroxybenzoic acids include ellagic acid, benzoic acid, protocatechuic acid and gallic acid [42]. Fig.6 shows gallic acid, resorcinol, pyrogallic acid and pyrocatechol. I drew the structures illustrated in Fig.6. Pyrocatechol is derived from the decarboxylation of gallic acid while catechol is a product of the decarboxylation of protocatechuic acid[43].

2.2.2.3 Carotenoids

In their review, Fiedor et al.[44] reveal that carotenoids are fat soluble antioxidants and are known to scavenge peroxyl radicals by reacting to form radical adducts. This terminates the chain reactions and prevents lipoproteins and lipid cell membrane damage. Lycopene for example has strong antioxidant activity that quenches the singlet oxygen radical. Carotenes have been cited to have anti-tumour activity both *in vitro* and *in vivo* by Tanaka et al.[45] in their review. They also point out the possible preventive and therapeutic role in some cancers. They cite chemoprevention with carotenes as a useful possibility.

2.2.2.4 Metal-binding proteins

Metal ions such as Fe and Cu have been cited to mediate the generation of free radical species superoxide anion radical ($O_2^{\bullet -}$) and H_2O_2 by Fenton reactions [46] [47].

$$[\text{Ligand-Fe}]^{2+} + H_2O_2 \rightarrow [\text{Ligand-Fe}]^{3+} + OH^- + OH^{\bullet}$$

$$[\text{Ligand- Fe}]^{3+} + O_2^{\bullet -} \rightarrow [\text{Ligand- Fe}]^{2+} + O_2$$

8

Metallothionein antioxidant protein has proven benefit when over expressed in cells facing reactive oxygen species induced oxidative stress [48] Metallothionein is further implicated in the prevention of DNA damage by efficient removal of superoxide anion and direct binding of reactive oxygen species [49].

2.2.3 Antioxidants in physiology and human health

In the review article on oxidative stress, Durakova associates it to the damage in the molecular species such as lipids, proteins and nucleic acids[50]. The lipid peroxidation reactions and protein oxidation showed in equations 4 and 5 from the previous section occur not only in foods but also in physiological conditions. In addition, damage to DNA has been associated with ROS which induces strand breaks and nucleotide base modification. Free radicals have been implicated in carcinogenesis, mutations and transformations in biological systems[13].

The reactive species or free radicals and resultant oxidative stress have been associated with the pathogenesis of cancer, diabetes, autoimmune diseases, neurodegenerative disorders, aging, hypertension, Parkinson's disease, Alzheimer's disease, cardiovascular disease and other pathological conditions [51] [52]. Some antioxidants such as vitamin C and E, quercetin, epigallicatechin-3-O-gallate, ellagic acid, lycopene, genistein, catalase, glutathione,

coenzyme Q10 have been reported to be pharmacologically and therapeutically active against some oxidative stress related conditions[23]. Exogenous antioxidants such as vitamin C, vitamin E, polyphenols and carotenoids[53] augment the role of endogenous antioxidants such as glutathione, bilirubin, uric acid, coenzyme Q10, ferritin,

metallothionein, melatonin, L-carnitine and alpha-lipoic acid in stabilizing free radicals and achieving homeostasis[16].

Toxic substances offset the free radical oxidant–antioxidant balance in humans and other organisms causing various pathological conditions. Oxidative stress is an aggregate effect of the failure of the free radical - antioxidant balance in physiological conditions. It is a physiological disorder that is the change of the balance between the production and termination of reactive species resulting in increased concentration. The free radical to antioxidant equilibrium in the cell is achieved through homeostasis, however depending on the surrounding cell environment, the breakdown of this natural balance due to either an excess of free radicals or loss of antioxidants leads to an increase in harmful reactive species consequently a pathological state occurs [54]. Antioxidants play an important role in seeking free radicals and offsetting oxidative stress that is capable of modifying biomolecules and causing tissue damage[25] [50].

2.2.4 Antioxidants in the foods

In their review, Carocho et al. [55] emphasize the role of antioxidants in the conservation of food without alteration of taste and colour. Food oxidation occurs mainly through lipid peroxidation and protein oxidation. The dietary habits of populations have an impact on health. Some of these impacts relate to aging and aging related illness. Lipid peroxidation and protein oxidation products with toxic potential may be formed during food growing, processing, preservation or storage and preparation for consumption. These products obviously find their way into the gastrointestinal tract, followed by the entry into the blood stream and eventually get added to the pool of free radicals within cells and cell organelles such as the mitochondria [56] .

Plants in particular are known to have several classes of compounds that offer antioxidative properties. These compounds include carotenoidics, phenolics, antocyanidics, falvonics, vitamins, enzymes, cofactors and unsaturated fatty acids. The plant extracts have been explored for possible prophylactic as well as therapeutics uses[34]. Efficacy depends on structure, concentration, nature of substrate, the presence of

compounds that act synergistically with antioxidants, presence of other free radicals and the physical conditions in which the antioxidant is exposed to[51].

Other compound mainly the phenolics and phytochemicals, antioxidant minerals and antioxidant vitamins act through a variety of mechanisms among which are scavenging for ROS, binding of metal ions, absorption of UV radiation and deactivation of singlet oxygen and conversion of H_2O_2 into non radical moieties[24].

2.3 Antioxidants measuring methods for activity or capacity

Species with different structures, sizes and roles are listed in the group of antioxidants. Oxidoreductase enzymes, large protein molecules like catalase, superoxide dismutase, glutathione peroxidase make one type of them. Some proteins without catalytic action like albumins, ceruloplasmin, and ferritin also can act as antioxidant. A high number of small size antioxidant molecules take part in physiological reactions for example, L-ascorbate, glutathione, uric acid, phenol derivatives, carotenoids, tocopherol, etc. Some hormones (estrogen, melatonin, and angiotensin) are usually mentioned in making up the forth group. As it is obvious, the antioxidants of highly different nature have different affinity for taking part in different redox reaction with different radicals ($O_2^{\bullet -}$, $^1O_2$, $HO^{\bullet}$, $NO^{\bullet}$, and $ONOO^-$) or with different oxidant molecules (ROS). The mechanism and rate of interaction can depend on the nature of the different reactants that are present and on their concentrations. Different antioxidants present in samples can interact affecting the total antioxidant action. Synergic, antagonistic, or just simple additive changes can be resulted [57]. Furthermore in biological samples, the participating reactants can be localized or linked to some structures of the sample item like fruits or living physiological tissues. Therefore it cannot be expected that a single, universal assay can be worked out that can be used generally for showing accurately the measure of power of the antioxidants in different kind of complex matrices.

2.3.1 Conventional antioxidant activity measuring methods

Two different parameter are usually used to characterize antioxidant quality of samples, e.g. food products. One is the antioxidant activity (AOA) while the other is antioxidant

capacity (AOC). The activity is related to reaction rate, higher activity shows higher reaction rate in radical quenching or electron exchange. While capacity shows how many radical or oxidant species can be eliminated by one antioxidant molecule. Methods used for determination of AOA or AOC can be based on electron transfer (ET mechanism) reactions or hydrogen atom transfer mechanism (HAT).

Excellent reviews appeared [26] , [58] , [59] about methods used for assessing antioxidant characters in different samples. A systematic review appeared about effects of antioxidants, mechanism of free radical generation, damages caused by ROS species, about classification of antioxidants, Furthermore it introduces several electrochemical nano sensors[60] applicable for assessing certain antioxidant species.

The three-antioxidant assessment mechanism highlighted are as follows:
The first mechanism is exemplified by the oxygen radical absorbance capacity (ORAC) assay that is based on HAT. In this mechanism, the antioxidant gives hydrogen atom for the generated fluorescence radical. This reaction decreases the fluorescence that is detected and used for the quantification. Azo compounds [61] like AAPH (2,2′-azobis(2-amidinopropane) dihydrochloride) are used for generating peroxyl radicals. Trolox (6-hydroxy-2, 5, 7, 8-tetramethylchroman-2-carboxylic acid) that is a water-soluble analog of vitamin E is used as standard. The Trolox equivalent antioxidant capacity (TEAC) is used as an unit expressing the measured values like Trolox Equivalents (TE), e.g. μmolTE/100 g[62]. For improving reliability in case of different samples, several varieties of the method have been worked out.

The second mechanism such as the DPPH (2, 2-Diphenyl-1-picrylhydrazyl) radical scavenging assay is frequently and uses ET based method. That means that the antioxidant gives electron to the DPPH. The method is popular since the DPPH is a stable, commercially available chromogen radical. No radical generation step is needed in the measuring protocol, simply, only the absorbance change at 517 nm is to be detected [63], [64]. As the antioxidant is reduced, a colour change occurs from purple to yellow this is followed by spectrophotometry through the change of absorbance at 517 nm[65].

‘‘Cupric ion reducing antioxidant capacity’’ (CUPRAC) method is an often used spectrophotometric method for total antioxidant capacity (TAC) measurements. It is based on ET mechanism. Özyürek and coworkers[66] published a detailed review about varieties of it. In this method bis (neocuproine) copper (II) chelate is the reagent that is reduced to Cu (I)-chelate by action of different antioxidants. For quantification, the absorbance of the green species is measured at 450 nm. A version of the CUPRAC method employing electrochemical detection[67] has been also worked out.

Some of the other ET mechanism based methods use Fe^{3+} complex as reagent. The antioxidants reduce the Fe^{3+} to Fe^{2+} and the change is detected with photometric[68] or electrometric way. These methods are called Ferric reducing antioxidant power (FRAP) assays. As ligand for complexing the Fe^{3+}ions, different species have been employed. Among them several method varieties use tripyridyltriazine (TPTZ). Potassium ferricyanide (K_3 Fe[CN]$_6$) has also been found good as a FRAP reagent[61]. When it is used, then Prussian blue is the product of reduction. A variation of the method [69] use coulometric titration for antioxidant measurement. Titrant of Fe $[CN]_6^{3-}$ is electrochemically generated. It reacts with the antioxidant titrating it. The electric charge is used as analytical signal. Brainina et al.[70] used chronoamperometric detection.

Current – electrode potential curves recorded in voltammetric experiments also can reflect the electron donor power of different species, being present. It means that voltammetry can be used for antioxidant activity measurements[71]. In ideal conditions, the peak current (ip_a) of the anodic wing of the CV shows the concentration of certain antioxidant while the peak potential (E_{pa}) reflects the oxidizing potential. Unfortunately, interference of other electroactive species, and electrode fouling brings in uncertainties enough that makes simple voltammetric measurements not generally used in antioxidant measurements.

The third mechanism of antioxidant action is based on chelating capacity of certain species like flavonoids. As it is well known, certain metal ions like Fe^{3+} take part in or catalyze redox reactions in which aggressive radicals are formed. Chelators forming stable complexes with the metal ions can reduce the oxidizing or radical forming action[72]. For measuring antioxidant chelating capacity ferrous ions from ferrous sulfate

are interacted with the antioxidant sample and the change of the absorbance is detected. The metal chelation capacity of antioxidants is expressed as ethylenediaminetetraacetic acid (EDTA) equivalent.

Oxidative stress is an imbalance between the free radical production and the antioxidant defense. The antioxidant capacity or activity of foods and beverages are important parameters that have influence on the commercial value. Because of the differences in chemical nature of species as well as the diverse reactions that proceed during the interaction between radicals or other oxidant and the protective antioxidant, several different measuring method have to be employed for getting a reliable characterization.

In their work, Rivero-Perez et al. [73]used and compared the results of different methods for assessing the antioxidant capacity of wines. Among them TAC (total antioxidant capacity), oxygen radical absorbance capacity, ferric reducing/antioxidant power, hydroxyl and superoxide radical scavenger activities, and biomarkers of oxidative stress methods such as lipid peroxidation inhibition and inhibition of damage to DNA. As well as determination of total polyphenol level (TPP) of wines.

The ABTS cation assay for physiological samples has been done by production of metmyoglobin radical. The $ABTS^{\bullet+}$ is formed by reacting ABTS (2, 2'-azino-bis (3-ethylbenzthiazoline-6-sulfonic acid) with ferryl myoglobin radical that is produced by interaction of metmyoglobin and hydrogen peroxide. The absorbance is detected at 405 nm[74]. For example, the Merck Company commercializes an ABTS Antioxidant Assay Kit for metmyoglobin. Its function is based on the interaction of radical $ABTS^{+}$ a green cation and the antioxidant. The color of the radical decreases as a result of the interaction. The other ABTS radical discoloration assay at 734 nm requires generation of the $ABTS^{\bullet}$ radical is based on the trolox equivalent and is less preferred[75]

In a different CUPRAC method, the antioxidants reduces cupric radical $^{\bullet}Cu^{2+}$ to Cu^{+} cuprous ion that forms a chelate with a colorimetric probe. Its absorbance is measured at 570 nm. The Total Antioxidant Capacity Assay Kit of the Merck uses a complex of Cu^{2+}

as reagent, similar to the CUPRAC method. With the kit, both small molecule and protein antioxidants can be determined. If needed however, a protein mask can be employed that prevents Cu^{2+} reduction by protein, enabling the analysis of only the small molecule antioxidants. Trolox, a vitamin E analog is used as standard.

Folin-Ciocalteau reducing capacity assay (FC)[76] involves an electron transfer from the phenolic compound to the FC reagent . The total phenolics in a sample are measured. This SET test possibly involves Mo^{6+} ion which is reduced to Mo^{5+} by accepting an electron donated by the phenolic antioxidant. This forms a blue chromophore. The FC reagent absorbance is at 750 nm and results are given as the gallic acid equivalent

2.3.2 Classical electroanalytical methods

Electroanalytical methods that mainly utilize the electrical properties of solution such as current, potential and conductance in an electrochemical cell[77]. The methods are broadly classified into interfacial and bulk techniques. The electrode interface based techniques include potentiometry and potentiometric titration which are considered static with current at open circuit, while the dynamic techniques utilize a current greater than zero[78]. In dynamic techniques, the potential is controlled and the current is measured e.g. amperometry and voltammetry[79].

A large portion of antioxidant species are electroactive[80], consequently, under optimal conditions, the concentration of antioxidant species can be directly determined by the use of suitable electrochemical methods[81],[82],[83]. square wave voltammetry (SWV)[84],Cyclic voltammetry (CV) [65], [75], differential pulse voltammetry (DPV) [85] ,[86], amperometry[87] have been used successfully for the determination of the quantity or identity of antioxidants species. The so called electrochemical index (EI) [88] obtained from voltammetric curves has been reported for the characterization of the antioxidant properties of samples in solution.

A higher concentration of antioxidant species, gives a high value of the anodic peak current Ip_a, while a species with low E_{pa} can is considered to easily take electrons from

the redox reaction partners. In that case, a higher EI (μA/mV) value implies that a higher antioxidant capability is associated with the measured species. Where several antioxidants are present, the EI can be expressed as the cumulative value or the sum of the values obtained from the relevant CV peaks as follows.

$$EI = \frac{I_{pa1}}{E_{pa1}} + \frac{I_{pa2}}{E_{pa2}} \ldots + \frac{I_{pan}}{E_{pan}}$$

9

Furthermore, potentiometric procedures have been also reported , and applied successfully [89] over and above the different current detecting, voltammetric methods, (CV, SWV, DPV, amperometry). In these current detecting methods, a reference buffer solution is usually used and the corresponding measured redox potential difference that takes place between the reference buffer solution and the test sample [90] is utilized as the signal. The mediator redox couples, which are often applied such as potassium ferricyanide/ferrocyanide have the role of stabilizing the potential. Whenever an interaction of the sample with the buffer solution occurs, redox potential changes take place [91], [92]. This shift in the redox potential (ΔE) serves as the analytical signal. The redox potential value can obviously indicate the electron exchange activity of antioxidants.

2.3.2.1 Electrodes in voltammetric analysis

In our days different kinds of electrodes are frequently used in voltammetric analysis. Several reviews e.g. [93],[94] have emerged in regard to the preparation techniques, properties as well as application of these electrodes in various spheres of analytical chemistry. The electrochemical index determination (EI) can be obtained by electroanalytical methods. The results correlates well with conventional spectrophotometric methods such DPPH radical scavenging assay, ABTS radical scavenging assay and Folin-Ciocalteau reaction used in total phenol determination. The Antioxidant activity is usually expressed as EC_{50}, μmolTE/g of Trolox and gallic acid equivalent (GAE) for the three spectrophotometric methods respectively[88].

2.4 Carbon electrodes and sensors

In my work different carbon electrodes have been studied, modified chemically, and employed in working out analytical methods. Therefore in the "literature section" only carbon electrodes are surveyed. In our days the most frequently applied voltammetric working electrodes are made of carbon based materials. High number of reviews[93],[94] has been published about preparation techniques, properties and about applications of them in different areas of analytical chemistry. There are various forms of carbon which could be applicable as electrodes. These include, diamond, graphene, highly oriented pyrolytic graphite (HOPG), graphene nanoribbon, porous carbon and carbon nanotube. Graphene is considered to be a semi-metal[95]. The fermi level can be shifted by introducing electrons including electrochemical doping. The HOPG is a highly pure man-made graphite with a 45^{o} angulation of graphite sheets. Carbon nanotubes are one dimensional structures of graphene. Graphene nanoribbons are derived from graphene with metallic and conducting properties with high electron mobility. Diamond is an ideal carbon electrode for its hardness properties. Porous carbon is made through pyrolysis and activation. It was found to have micro-poles of varying sizes where molecules lodge. Carbon paste electrodes and screen printed carbon electrodes have been applied in electrochemistry. Glassy carbon (GC) is a commonly used carbon electrode too[93] [95] .Since the appearance of the excellent book of N.R.Adams about electrochemistry at solid electrodes[96] most of the monographs[97] [98] dealing with different areas of electrochemistry also take longer or shorter sections about introduction of different carbon electrodes.

2.4.1 Classification and application of carbon electrodes

Depending of the structure of the carbon matter used for making them the base electrodes can be classified in four different groups. One type of the electrodes is made of graphite matter of highly oriented parallel sp^2 crystal layers. The matter made with high temperature pyrolysis from hydrocarbons that are called Pyrolytic Graphite (PG). Further treatment with high temperature and pressure results in Highly Oriented Pyrolytic Graphite (HOPG) that can contain layers with crystallites as large as 1 μm. The electrodes made from these are PG or HOPG electrodes respectively.

Electrodes listed in a separate group are made of random oriented polycrystalline carbon matter containing small crystallites. Commercial graphite powder, spectroscopic graphite rods, particle matter obtained by home grinding etc. are used for making them. The carbon paste electrodes introduced by Adams[99] is a well-known, often employed version. The wax impregnated spectroscopic rod is a less frequently used one, while high variety of screen printed flat cells containing composite working electrodes made of polycrystalline carbon particulate matter and appropriate binder are on the market. This includes the pencil graphite electrodes.

Owing to mechanical properties like hardness, compactness, low electric resistance and compatibility with different solvents Glassy Carbon (GC)[100] has been proved excellent stuff for making voltammetric working electrodes. It is available commercially in form of rods, plates, disc, etc. In analytical chemistry commercial CG electrodes or electrodes home-made from commercial GC rods are broad scale use. GC electrodes made the third sub group of the carbon electrodes.

The micro or ultra-micro carbon electrodes [101]form fourth group of the carbon electrodes. Most often their measuring surface is made of carbon filament that is embedded in certain body, very often in a glass capillary. The filaments[102] are made with heat treatments from different matters. They are mass produced in different sizes (diameter 5-33μm) and mass used in manufacturing composite structures used in making advanced matters for transportation industries or for sporting appliances hockey sticks, tennis racquets, archery bows, bicycle frames, golf clubs, etc. Insignificant parts of the fibers are used for making electrodes. The carbon fiber microelectrodes have similar properties as GC electrodes. They gained application in experimental life sciences and in scanning electrochemical microscope (SECM) studies.

Pencil electrodes are getting considerable attention[103] [104] owing to their low cost, availability and to reports published about their use in voltammetric analysis. Graphite materials have both metallic and non-metallic properties. Pencil graphite is readily available commercially. It is composed of 65% graphite, 30% clay and binder material which can be wax, resins or high polymers. Pencil graphite generally have an electrical

resistance below 5 ohms. The material composition influences the pencil graphite properties whenever it is used as an electrochemical electrode. Clay confers specific ion exchange and structural properties such as degree of disorder and morphology [105]. The graphite reinforced carbon (GRC) was first reported by Aoki et al. who indicated advantages over commonly used carbon electrodes such as carbon paste, Glassy carbon, carbon fiber and pyrolytic graphite. The GRC[106] later named pencil graphite electrode (PGE) [107] therefore has comparative advantages over other common carbon electrodes in having lower background currents, better reproducibility of results, an electroactive surface area that is adjustable. The electrode is cheap, easily disposable, and mechanically rigid, can be miniaturized, and has strong adsorption, wide potential window -0.8 to 0.8, 1.0 to 0.8 and -0.8 to 0.6 V vs. SCE for H_2SO_4, KCl and NaOH respectively.

The irregular surface morphology of PGE is associated with the very good electrochemical activity. The PGE surface microstructure involving the edge and basal planes characteristics was studied using scanning electron microscopy (SEM), X ray photoelectron spectroscopy (XPS) for oxygen to carbon ratio as well as aluminum to silica levels, Raman spectroscopy for edge plane density (D) compared to the in-plane characteristics and cyclic voltammetry to determine electron transfer kinetics. The harder pencils were composed of more aluminum and silica with electron transfer rates comparable to Glassy carbon electrodes[107].

The use of commercial pencil leads in fabricating working electrodes for application in voltammetric analysis from the early report of Aoki et al.[106] to date is increasingly getting into the focus of interest. Several reports e.g.[104] and ground breaking reviews[105],[103] have appeared in regard to favourable electrochemical properties, affordable, ease of surface renewal and environment friendly nature of pencil graphite material at the point disposal after use of these electrodes.

Measurements of purines complexes have been reported using pencil graphite electrodes[108]. The cheap disposable electrode has been used in determination of trace metals, vitamin C in commercial fruit juices, genetic nucleotides, haemoglobin,

catecholamines, salixyclic acid , caffeine, O_3 in water and determination of samples of human genetic origin [107].

2.4.2 Chemically modified electrodes

I worked out, studied and employed a novel antioxidant assessing method. It needed a working electrode of special character. In my experiments chemical modification of different kinds of carbon electrodes were carried out to prepare an appropriate sensor. Accordingly, for my research the literature dealing with chemically modified electrodes (CME) gave basic help. In this section a short review is given about the happenings in this very important, relatively new research field. The group of chemically modified electrode was characterized by the IUPAC committee as follows:

"Compared with other electrode concepts in electrochemistry, the distinguishing feature of a CME is that a generally quite thin film (from a molecular monolayer to perhaps a few micrometers-thick multilayer) of a selected chemical is bonded to or coated on the electrode surface to endow the electrode with the chemical, electrochemical, optical, electrical, transport, and other desirable properties of the film in a rational, chemically designed manner"[109].

So it means that with application of a special chemical modification the basic electrodes can be furnished with certain nature that improves their value. The modification sometimes just can enhance some of their practically important features, but sometimes it can bring in new abilities that make them applicable playing novel roles.

The pioneer of the research dealing with chemically modified electrodes, Royce W. Morray published an early quite detailed review about modification of surfaces[110]. In it he showed methods of doing the modification, results and methods analyzing the modifying layer structures as well as the reactions of some confined modifying layer etc. Ever since the development, study and application of chemically modified electrodes are getting more and more in the focus of interest of research schools dealing with electrochemical-, electro-analytical-, electrochemical technology problems. Very high

number of papers, among them monographs reviews[111] appeared about developments in these fields.

A review about different chemically modified electrodes worked out for analysis of paracetamol, the broadly used drug for treatment of numerous cold and flu remedies was published by Boumya and coworkers[112]. They concentrate on how to use nanomaterials, like carbon nanotubes, graphene, graphene oxide, reduced graphene oxide, metallic nanoparticles (NP), fullerene, conducting polymers as well as their composites as modifiers. They discuss the methods for modifying different carbon electrodes among them carbon paste-, Glassy carbon-, spectral graphite-, screen printed carbon electrodes. The electrodes modified with a thin graphene layer were found to have improved performance as published in several report[113], [114], [115]. A more robust electron exchanged rate properties, improved stability of the modified electrode during measurement, as well as more active layers for docking particular species used in electrode modification were observed. In its application pencil graphite electrode gives a good linear range in response[116] to concentration and a significant lower limit of detection.

Different polymeric metal complexes have been successfully used in forming modifying layers on different sensors. Metal organic frameworks (MOFs) with their different active groups attached to porous structures can be beneficial enhancing selective adsorption of analytes, catalyze analyte-sensor interaction, or stabilize the traction of the modifying film. Pournara et al. gave an excellent review about them[117].

The modification of working electrode surface can result in changes that enable applications in solving special tasks that the base electrode cannot do, or cannot do well[118]. Accordingly based on the role of the applied surface layer, different groups of the chemically modified electrodes can be separated. Very often the surface layer increases the selectivity of the determination carried out with the electrode. The sensitivity and lower limit of determination also can be improved using appropriate surface modification[119]. In doing industrial scale electrolysis, the energy consumption can be beneficially reduced by applying confined catalysts on the electrode surfaces.

Immobilized electro catalysts can avoid electrode fouling caused by insoluble product of the heterogeneous electrode process. In different cases electrochemically inactive species can be assessed electrochemically if appropriate catalyst is attached onto the working electrode surface.

The discussion of the literature about chemically modified electrode can be organized sorting by the chemical structure, size of the layer or way of immobilization. In this case electrodes with inorganic, organic, nanomaterials or composite modifiers, as well as modified with adsorptive forces, chemical bindings, electropolymerization etc. can be separated. An extensive group of highly selective chemically modified electrodes made for chemical analysis, the group of biosensors is usually handled separately.

The research dealing with ways of surface modification, with electrochemical characterization and with application of the modified surfaces, electrodes is one of the most actively cultivated field of electrochemistry and material sciences. Enormous number of reports appear yearly about results achieved in the field. I rather concentrate my efforts on experimental work than trying to give a comprehensive review about the literature of this field. Here I just go over the literature shortly mentioning a few "iconic" steps.

2.4.2.1 CME with improved selectivity

The voltammetry does not excel in selectivity. Any species electroactive in the applied electrode potential window would contribute to the current signal. One group of voltammetric enzyme electrodes use oxidoreductase enzyme for recognizing the analyte molecules. It catalyzes the reaction of the electro inactive analyte and the product or the reagent is detected voltammetrically. The enzyme catalysis is selective however, other electroactive species present in the samples would interfere. In the work of Nagy. L[120], a putrescine measuring amperometric biosensor was developed. It function was based on the catalytic effect of putrescine oxidase enzyme. It catalyzes the oxidation of putrescine by oxygen dissolved in the sample. In the reaction H_2O_2 is produced that is detected by the base sensor. In order to avoid interference of other species an electrochemically

prepared poly-phenylene diamine layer was employed on the electrode surface. It allowed passing through the small H_2O_2 molecule and reacting on the base sensing element but blocked the passing the bigger molecules like L-ascorbate. This kinds of size exclusion modifying layer have been employed in many other cases[121] [122] [123] [124] .

In certain cases perm selective layer employed on electrode surface was found satisfactory in eliminating interferences of some matrix components. Monoamine neurotransmitter species like dopamine, norepinephrine and serotonin are electroactive. As it was reported in famous early paper of Adams[125], the human extracellular liquid of the central neural system is with its constant temperature, pH and electrolyte content is a good voltammetric background electrolyte. Therefore it was supposed that with application of appropriate microelectrode and voltammetric technique, local concentration of the neurotransmitters can be assessed in different areas of the living brain. Unfortunately however several endogenous molecules are also electroactive and their concentration is, or can be much higher than that of the neurotransmitters. It was noticed however, that at the physiological pH of the extracellular liquid (pH =7.3) the monoamines are in their cationic form, but the main interfering species L-ascorbate, ureate, oxidized transmitters are anions. Therefore employing thin, appropriate poly-ionic membrane on the surface of carbon microelectrode could eliminate the interfering effect of anionic species. Nafion [126] [127] [128] film was tested and was found useful as selectivity providing electrode modifier. Nafion is a cation exchange polymer. It is actually a sulfonated Teflon based fluoropolymer-copolymer. It blocks the transport of anions but lets the cations pass through to the carbon surface. The perm selective Nafion layer eliminates the interferences caused by the electroactive anionic species and allows voltammetric estimation of local concentration of monoamine neurotransmitters.

2.4.2.2 CME-s with improved sensitivity and lower limit of determination

There different kinds of modification can be employed for improving these two important analytical qualities of working electrodes. Increasing the actual area of the measuring surface is one of them. It can be done by attaching some conductive porous layer or confining particulate matter that can take part in the electrode reaction. The

improvements also can be achieved by coating the measuring surface with a special layer that selectively extracts the analyte from the sample solution. Different kinds of interactions between modifying layer component and analyte can be responsible for the extraction. Most often selective complex formation, electrostatic-, hydrophilic-, hydrophobic interactions, action of molecular imprinted sites [129] are mentioned. The enhanced local concentration at the measuring surface could produce higher signal. The third and most often used sensitivity improving modification is employing electro catalyst containing layer on the electrode surface. The catalyst can enhance the rate of electron exchange reaction that also can result in higher current in voltammetric measurements.

Furthermore, there are two very important goals in voltammetric analysis that can be achieved by employing catalyst containing modifying layer on voltammetric working electrodes. On one hand chemical reaction of the analyte catalyzed by the surface layer can make local changes that can be detected by the base sensor. That allows assessing species that cannot be detected by the basic sensing element. For illustration we can mention here the numerous groups of electroanalytical biosensors. Selective action of biologic modifying components highly extended the set of analytes measurable with electrochemical sensors. High number of biosensors have been made with bio catalytic that means enzyme containing layers. In the work by Csóka and coworkers[130], an elaborate enzyme sensor was made combining a selective layer for recognition and measurement as well as a non-interference portion on the working electrode. The enzymes employed included invertase, mutarotase, and catalase and glucose oxidase. The profiles of oxygen and hydrogen peroxide were measured and the glucose oxidase activity for sucrose and glucose concentration were made successfully.

The other aim that catalytic modification could help achieving is avoiding electrode passivation. It is a well-known phenomenon that happens when the products of certain electrochemical reactions are not well soluble in the media employed. The resulted product(s), often polymers, can stay on the electrode surface decreasing the electrochemical surface area, insulating it. In several cases with modifying layer containing reversible electro catalyst- that means mediator- the electrode fouling could be

avoided. The mechanism of the action is obvious. The mediator reacts chemically with the detected species in a chemical redox reaction and at the base electrode surface and the mediator is regenerated electrochemically. In these reactions the product of the analyte reaction does not get to the base electrode so no electrode fouling can happen.

Nanomaterials have been very extensive tested in making CME-s[131]. They were found useful in enhancing electroactive surface area. They can enhance significantly analyte adsorption allowing improved lower limit of determination or sensitivity. They can provide sites for linking catalyst onto the electrode surface or can have catalytic action of their own. Very extensive literature deal with carbon based-, metal based- nanomaterial modified surfaces and nanopore containing modifying layers. Reports have been made about methods used successfully for immobilizing[132],[133] ,[134] GO on a GCE surface. A big number of reports had been published about improved performance of electrodes that were modified with the nano-size, single layer graphene[135] [113] [114] [115]. The advantages that were observed from the modification included an enhanced electron exchange rate, improved stability as well as more active layers for docking certain electrode modifying species. Furthermore simple methods for electrodeposition of graphene matter [132,133] had been worked out.

The chemically modified electrodes are made by coating a conducting or semiconducting material with a suitable modifier[108]. The chemical modification is often done by formation of a layer on the functionalized electrode surface. Consequently the surface gives some specific properties such as improved selectivity, improved electron exchange rate, a lower detection limit, robust catalytic action, better stability, prevention of surface fouling etc. Carbon electrodes chemically modified with a reversible electro catalyst layer, could be used advantageously in clinical chemistry[113],[136], as fabrication of different amperometric biosensors[137],[138] etc. The modified electrode is attached to a transducer to convert the electrochemical interaction with an analyte into an electrical signal. The capabilities, and suitability of voltammetric methods has improved tremendously through such ways as introduction of chemically modified electrodes[110],[117],[139],[140], [11],[141].

2.4.3 Glassy carbon and pencil graphite electrodes modified with MB

In my research, the chemical modification of Glassy carbon, spectral graphite and pencil graphite was done and the consequent characteristics were investigated. The preparation and application of chemically modified electrodes is an active area of research currently. Some of the procedures adopted in various studies for modification[142] [143] include drop casting, chemisorption, covalent attachment, electrochemical deposition, electrochemical polymerization and paste mixing. Drop casting involves the deposition of the modifier and binder on the surface of a functionalized electrode to obtain a film. Electrochemical deposition[134] utilizes electrochemical techniques to deposit material such as nanoparticles on the electrode surface. Electrochemical polymerization[116] on the other hand use electrochemical process to deposit a thin film to form an activated polymer layer on the electrode.

Gorton and co-workers [144]while working with various organic mediators revealed that a species (Fig.7) called Meldola Blue (MB)+ (N,Ndimethyl-7-amino-1,2-benzophenoxazinium ion) could catalyse the oxidation of NADH. An electrode surface that was immobilised with a thin MB film did not lose activity even over a long time of amperometric NADH measurements.

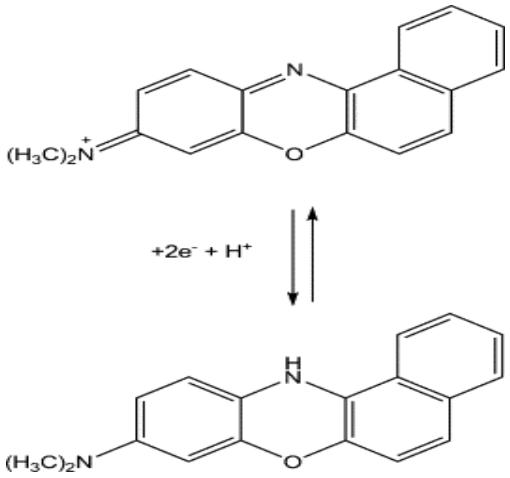

Drawn using https://chemdrawdirect.perkinelmer.cloud

Fig. 7.The chemical structure of Meldola Blue and the redox states

Immobilization of MB redox mediator on GCE surface can be done in several ways. Among them adsorption, covalent linkage, entrapment or polymerization are the most

often employed [145]. In our experiments adsorption and electrochemical polymerization of MB monomer were used for forming the catalytic layer[112] [146].

2.5 Chronopotentiometric measurements

Within this short section the variety of different methods in literature that can be listed into the group of chronopotentiometric measurements are were reviewed. Actually, the term chronopotentiometry (CP) is generally used for identifying all electrochemical measuring methods that use electrode potential – time dependence for evaluation. This section is a build up to the new antioxidant measuring method that this thesis deals with. This new method uses the recorded electrode potential – time dependence for obtaining analytical signal. That means that for the analysis, the electrode potential is measured in time, therefore "chronopotentiometric" measurement is made.

2.5.1 Variety of chronopotentiometric techniques

In some of the measurements the open cell potential against a reference electrode (E - t recording at $i \approx 0$) is followed in time for indicating the progress of certain chemical reaction[147] [148]. This is often employed for end point indication of acid-base-, redox-, complexometric- or precipitate titrations.

In other methods, controlled current is employed between two appropriate electrodes inside the measuring cell, and the cell voltage is followed in time (E – t recording at $i \neq 0$). Obviously as long as electrode processes of species being present can carry the adjusted current, then small cell voltage appears, while in their absence it grows to the level needed for the next reaction. As an example, we can mention the indication of end point of iodometric titrations with two polarized Pt electrodes[149]. In this case, continuous solution stirring and between two identical electrodes small constant DC current is employed. The cell voltage is followed. As long as both I^- and I_3^- ions making the reversible redox couple are present, then, a small voltage appears; however, when the titrant takes away the I_3^- then the voltage sharply increases indicating the end point.

Different constant current ($i \neq 0$) chronopotentiometric[150] methods employing other than amperostatic current control have been worked out. One of them imposes a current pulse in quiescent solution and follows the electrode potential in time. By the current step, the investigated electrode process is started and the concentration of the reacting species starts decreasing at the electrode surface. The linear diffusion transport competes with the electrode process. A slow change of the electrode potential can be observed as the activity ratio of the oxidized and reduced form of the reacting species is changing. However, when the activity of the reacting form approaches to zero, then other process has to be started to carry the set value of the current. This is reflected by rapid potential shift. The time between starting the pulse and the rapid potential shift is called transition time (τ) and i is the current density. The potential at $\tau/4$ time corresponds to the condition when the activity of the oxidized and reduced species are equal at the electrode surface, while under linear diffusion competing with the complication free electrode process, the Sand equation gives the value of $i\tau^{1/2}$. In the equation, n is the number of electrons, F is the faraday constant, D is diffusion coefficient of the analyte, i_- is the current density (i/A), A is the area and C is the concentration.

$$i\tau^{1/2} = \frac{nFA\pi D^{1/2}C}{2} \qquad (10)$$

This method is mostly used for studying electrode reactions. Changing the value of $i\tau^{1/2}$ by the employed current (i) indicates different complication of the electrode process. It can show chemical reaction proceeding before the electron transfer step. Furthermore, catalytic action, inhibition or adsorption involved in the overall electrode process can also be studied by the method.

Comparing the traditional potentiometry and current pulse chronopotentiometry in case of certain redox titration, the chronopotentiometric method showed advantages in the titration of materials in lower concentration regions and in the analysis of small volumes where reproducible stirring is difficult [151].

In the middle of the last century chronopotentiometric methods employing several different shaped current controls have been developed and tested. Among them current reversal chronopotentiometry[152],cyclic chronopotentiometry[153], programmed current chronopotentiometry[154] should be mentioned. Regardless of their certain demonstrated advantages [155] in our days they are not often employed. It is especially true concerning their usage in analytical chemistry.

The application of CP for following the stripping process has been proved very advantageous[156] The invention of inverse voltammetric methods also opened up a new application field of the chronopotentiometry (CP) measuring technique in analytical chemistry [157] [158] [159]. These inverse- or also called stripping methods excel in providing good analytical performance in trace level metal analysis. The detection limit provided in case of different metals can be in the range of 10^{-11}-10^{-10}M. As it is well known, in stripping analysis two discrete experimental steps are employed [160]. In the first step the analyte sample components are accumulated/pre-concentrated on the surface of the working electrode. This critical step is responsible for achieving the extremely low range of determinations.

Three different ways of this pre-concentration are generally carried out. In anodic stripping methods (ASV) controlled potential electrochemical reduction is employed, while in cathodic stripping voltammetry (CSV) electrochemical oxidation is employed. In adsorptive stripping procedures (AdSV) a complexing agent is used that adsorbs on the electrode surface and it accumulates the analyte by complexing it. The second step is the stripping, when the pre-concentrated analyte is stripped away from the electrode and the resulting amount of stripped analyte is detected. On one hand, it can be done by employing different voltammetric techniques, like differential pulse voltammetry and square-wave voltammetry. On the other hand, it has been pointed out that use of CP for following the stripping process is possible[156] . In this case, an oxidant, most often, mercuric ions is added into the solution to strip off the accumulated reduced analyte. Alternatively, a small constant oxidizing current is used for the stripping process. As the different species leave the electrode surface, the electrode potential is followed in time

(CP step) [161] [162]. The process is followed as one deposited metal species leaves the electrode surface and a characteristic electrode potential - time curve is obtained. It looks similar to a redox potentiometric titration curve. Actually the deposited analyte is titrated off by the constant flow of electron acceptor (oxidant) or by the current. The higher the amount of the deposited analyte, the longer the time needed to strip it off. In order to make the evaluation easier dt/dE – E function is derived and used for quantification.

Chronopotentiometry is a method that is seldom used in practice of analytical chemistry. Usually when it is employed, a small, constant current is applied in the measuring cell and the potential of the working electrode is followed in time against a reference electrode. A version of potentiometric stripping analysis (PSA) also employs recording electrode potential-time dependence. In those methods a controlled reductive potential step is used when certain metal components get deposited onto the working electrode. In the second, chronopotentiometric step, a small constant current or oxidative reagent re-oxidises the deposited species [163]. The redox potential-time curve, or the $\Delta t/\Delta E$ –t function is used for evaluating the concentration of different species [164].

3 Materials, equipment and methods

3.1 Materials

3.1.1 Chemicals

The antioxidant L-ascorbate (AA) see Fig.4 and 100% ethanol was obtained from Szkarabeusz (Hungary).

Hydroquinone, resorcinol and pyrogallic acid (see Fig.6) were products of Reanal,(Hungary), while 99% pure pyrocatechol and 98% pure gallic acid (see Fig.6) were obtained from Sigma Aldrich,(Japan and China) respectively.

The 7-dimethylamino-1,2-benzophenoxazine, Meldola Blue (MB) the redox mediator (see Fig.7) used as electro catalyst was purchased from Aldrich,(Milwaukee, USA).

The 99.5% pure 1nm single layer graphene oxide (GO) for modifying the Glassy carbon electrode surface by electrodeposition was obtained from Nanografi (Turkey).

The $[K_3Fe(CN)_6]$ for preparing the redox couple was obtained from Kemika,(Croatia).

The $NaHPO_4.H_2O$ and $Na_2HPO_4.2H_2O$ used for making the 0.25 M phosphate buffer, pH =7.0 and 0.1M pH=8.0 phosphate buffer background electrolyte were products of Reanal (Hungary).

The different sizes of alumina from Bueler (Lake Bluff, IL USA) used as polishing slurry for Glassy carbon electrodes and Pt electrodes. The polishing slurry of 1 μm, followed with 0.3 μm and finalized with 0.05 μm sized particles.

In order to keep the dissolved oxygen out of the electrochemical cell, it was purged with 4.0 nitrogen gas that was a product of Linde (Hungary).

The silver conductive paste was obtained from Sigma Aldrich (South Korea) for the contact between pencil and copper wire in PGEs.

The KCl was a product of Reanal (Hungary), 0.5M was used as solvent for $[K_3Fe(CN)_6]$, 0.1M was used as supporting electrolyte and as the electrolyte during the activation of electrodes. Saturated KCl was the electrolyte in Ag/AgCl reference electrode.

Ferrocene methanol and hexamine ruthenium (III) chloride were obtained from Aldrich and Sigma Aldrich Inc. (USA) respectively.

The H_2SO_4 used in making the 0.5M solution of $[K_3Fe(CN)_6]$ was a product of Merck,(Germany).

The apple and red pepper fruits were obtained from the local market (Pécs, Hngary).

The ion exchanged water having less than $6x10^{-8}$ S/cm specific conductivity was employed for making all aqueous solutions used in this work. All chemicals were of analytical grades. They were used as obtained, without any further purification.

3.1.2 Electrodes

The $1cm^2$ Pt wire is embedded into a glass casing and used as the counter electrode. It was fabricated in the electrochemistry laboratory of the University of Pécs, Hungary. The Pt wire for making the microelectrodes for microscopy were a product of GoodFellow (Cambridge, England).

The working electrodes included the rotating Glassy carbon disk electrode (GCE) a product of Pine Instruments (Durham, NC, USA).

The homemade pencil graphite electrode (PGE) with the outer diameters of 0.2 mm HB was from Ain Stein HB Pentel (Japan), the 0.5 mm HB was from Pentel Hi-polymer,(Japan) and 0.5 mm 2B was a product of Staedtler (Germany).

The 10 cm long borosilicate glass capillaries with 2 mm outer and 1.16 mm inner diameter for making the miniaturized PGEs were a products of Sutter Instruments, (USA).

The Glassy carbon rods used in making the working electrodes were purchased from Alfa Aescar, GmbH (Germany).

The reference electrodes were a commercial Ag/AgCl electrode with saturated KCl, Radelkis, (Hungary) and a Low profile silver/silver chloride reference electrode (74 mm long) obtained from Equilabrium SAS (France).

The fine sandpaper a product of Klingspor (Germany) and the grinding paper size P80 for electrode fabrication was obtained from Bueler (USA).

The scanning electrochemical microscope targets were made from 2 mm and 5 mm spectral graphite obtained from Elektrokarbon Zavod (Slovakia).

The mould was made of Epofix Resin obtained from Struers (USA).

3.1.2.1 Platinum electrode

A homemade Pt electrode sealed in borosilicate glass capillary was fabricated by heating the glass on a flame. A copper wire was inserted into the glass bore till it made contact with the opposite end of the Pt wire. A soldering wire was melted within the glass bore to make a contact between the copper wire and the Pt electrode. This Pt electrode was applied in both voltammetric and chronoamperometric measurement of the electrochemical surface area (ECS) based on the fact that the ECS area is equivalent to the geometric area in the case of platinum electrode.

The counter/ auxiliary electrode was 1 cm long 3.5 mm outer diameter Pt wire with about 1cm^2 surface area. The electrodes were mechanically wet polished stepwise with slurries containing alumina particles of 1, 0.3 and 0.05 μm respectively for a clean surface.

3.1.2.2 Glassy carbon electrode

Home fabricated working electrodes were made by cutting a 10 mm long cylinder from Glassy carbon rod, OD 5 mm obtained from Alfa Aescar (GmbH, Germany). This was fixed into the center of a cylindrical electrode body (outer diameter 10 mm, length 10 cm) of Pine instrument rotating electrode or in a rotating electrode tip of Radiometer rotating disc electrode stand made of hard polyvinyl chloride (PVC) or Teflon, respectively. In the rotating disc assembly of Pine instruments, the built-in spring provided electric contact. Into the internal shaft of the PVC body, a copper wire was introduced as electric contacts, for the Radiometer fabrication. The surface of the fixed Glassy carbon discs facing out were carefully wet polished stepwise with slurries containing alumina particles of 1, 0.3 and 0.05 μm. Between each polishing steps, the electrodes were thoroughly rinsed by sonication in deionized water for 5 minutes and finally in ethanol for 5 minutes.

As an alternative to the home fabricated GC electrodes, the rotating GC disk electrode of Pine instrument was utilized. Conventional beakers (volume 50 and 100 cm^3) were used as three electrode measuring cell, with Ag/AgCl reference electrode from Radelkis (Hungary) and a platinum plate of about 1 cm^2 surface area as the counter electrode.

3.1.2.3 Fabricated pencil graphite electrode

In making the working electrodes, about 10 cm long borosilicate glass capillaries were sealed by melting the glass. This was done to allow for creation of a vacuum within the capillary. In conditions of a vacuum, oxidation of the carbon would not take place when heated to seal the glass. Into the sealed end of the glass tube, 2.5 cm length of each PGE with the outer diameter 0.2 mm HB, 0.5 mm HB, or 0.5 mm 2B, was forced all the way down to the bottom on the sealed part. This was done manually by dropping the capillary tube closed side down several times through a long narrow tube tapping it to a solid surface. The reason for this was to have the graphite close to the end of the glass so that with minimal planar grinding, the disk would be exposed.

The sealed glass capillary with pencil graphite in it was then connected to the vacuum pump and using electric heating coil, the capillary was heated to seal part of the pencil graphite rod in the glass for about a 0.75 cm length without oxidizing it. The sealing by heat was preferred to ensure that the properties of the graphite remained as opposed to use of epoxy as the casing.

An electrical contact was made by covering the exposed end of the carbon with silver paint or mercury, followed by introduction of a sturdy copper wire. This approach ensured that the brittle carbon material was not subjected to mechanical damage. The copper wire was further set with super glue onto the glass capillary on the opposite end to ensure that no movement would occur to break the contact or the carbon electrode material. The empty end of the sealed glass was then taken off by breaking followed by smooth filing with fine sand paper to remove excess glass. This was followed by fine smoothening of the surface using grinding paper. A clean pencil disk electrode surface was consequently ready for use. The obtained surface of 0.2 mm HB, 0.5 mm HB and 0.5 mm 2B pencil discs was polished and beveled in order to get a pointy shape. The fabricated electrodes were tested for successful contact by recording cyclic voltammograms in

5 mM $K_3[Fe(CN)_6]$ solution dissolved in 0.5 M KCl electrolyte. These electrodes were employed as working electrodes for various measurements. A commercial Ag/AgCl Gel

Reference Electrode was employed. The polished bare 0.2 mm HB, 0.5 mm HB and 0.5 mm 2B HB PGE surfaces were then activated by making 80 cycles between -0.5 V and 3 V at a scan rate of 5 V/s in 0.1 M KCl to functionalize the surfaces ready for chemical modification. The home-made pencil graphite electrodes were used as working electrode for the estimation of total antioxidant activity in samples. In these measurements, a 50 ml beaker with at least 20 ml of phosphate buffer served as the measuring cell.

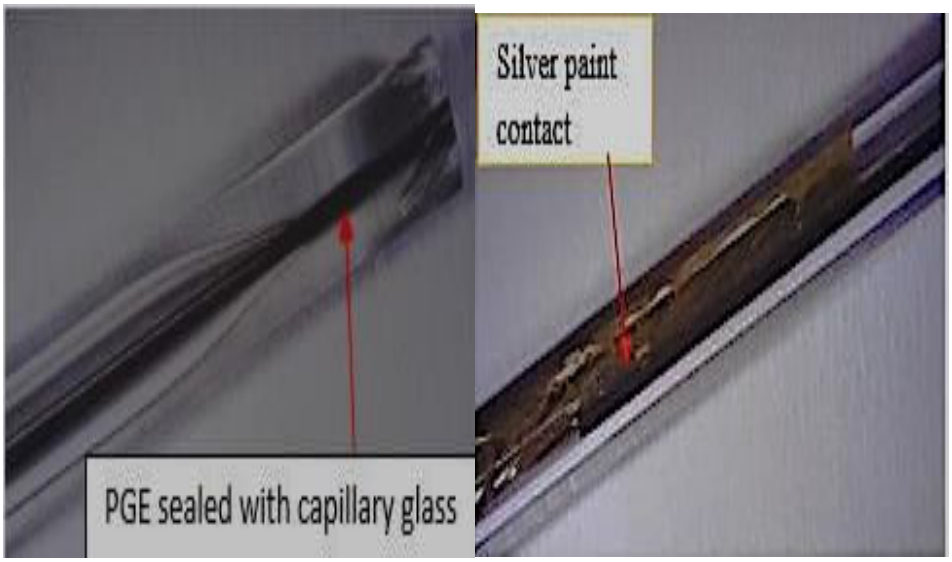

Fig. 8. A picture of the homemade PGE sealed in borosilicate glass with a silver paint contact to conducting wire.

3.1.3 Equipment

To weigh the very small and precise quantity of chemical for preparing the samples, buffers and electrolyte, the microgram limit weighing balance used was the product of Sartorius research Göttingen (Germany).

The hand-held Digital Multimeter MS 8250B was used for making potential and circuit tests on fabricated electrodes. It was a product of Mastech (USA).

The pH meter and the) reference buffers pH 4, 7 and 10 were products of Mettler Toledo (Hungary) and Merck (Germany) respectively.

The Vacuubrand GMBH+CO KG vacuum pump from, Labokraft Kft (Hungary) was used in creating the vacuum during the sealing of carbon rods in borosilicate glass.

The Hyundai HYD80I inverter was used for generating direct current for heating the wire filament for sealing the borosilicate glass under vacuum conditions.
The deionized water was prepared using Elix® essential water purification system, Merck KGaA, Darmstadt (Germany), for use as solvent in various electrochemical measurements. The water bath and Clifton sonicator was obtained from Fisher Scientific (England).

The electrochemical measurements to determine antioxidant activity and characterization of electrodes were carried out using two instruments. The first one was a Pine research WaveDriver200 Bipotentiostat/galvanostat with EIS electrochemical workstation, controlled by AfterMath 1.5.9644 software from Pine Research Instrumentation (Durham, NC, USA). It was equipped with a rotating disk electrode, Pine model AFMSRCE. The second instrument was an electrochemical workstation Auto lab POTSTAT 12 controlled by GEPES 4.9.005 software from Echochemie (Netherlands). It had a Radiometer rotating disc electrode stand with a rotation speed control unit CTV 101, from Radiometer (Copenhagen). These were used with the fabricated rotating disk electrode.

A homemade scanning electrochemical microscope with a step motor driven for linear positioning (UE166PP), a 3D positioning stage from Newport Irvine (USA) CA,tppe MMFN25PP, the bi potentiostat was EF437 from Elektroflex ltd,(Szeged Hungary) interfaced to the PC using a PCLab-812PG from Advantech,(USA) and a homemade software -that was written by Balazs Csóka- was used in making scanning electrochemical microscope (SECM) measurements. The smallest step for the linear motor was 75 nm.

3.2 Chemical modification of carbon electrodes

In this study, two descriptions of electrodes are adopted. This are the conventional size electrodes (1 mm to 5 mm OD) and micro electrodes (0.2 to 0.5 mm OD) or simply miniaturized electrodes.

GCepMBE and GCadsMBE denotes the conventional–size GCE modified with electropolymerised MB (epMB) and adsorbed MB (adsMB) respectively. Voltammetric working electrodes often get fouled by the products of electrochemical reactions at the electrode electrolyte interface. When this happens, the electrode cannot perform electroanalytical measurements due to loss of function as a result of obstruction of the electrochemically active sites. To overcome this challenge in electroanalytical work, the electrode is modified with an appropriate catalytic layer or mediator.

However, in this study, the purpose of chemical modification is to confine the electrocatalyst on the base electrode. In potentiometry the immobilized electrocatalyst layer increases the electrochemically active surface area, increases sensitivity to samples and improve on the repeatability of results. The Glassy carbon electrodes are modified through electropolymerization with $5x10^{-3}$ M MB or adsorption with $5x10^{-4}$ M MB. Exfoliated nano-size single layer graphene oxide is also electrodeposited on a functionalized GCE surface to form a GCGOadsMBE layer. The PGadsMBE film is made by adsorption of $5x10^{-4}$ M MB onto the functionalized surface of PGEs. The mediator acting as an electrocatalyst[165] is expected to lower the standard potential (E^o) of the analyte-product reaction to within the redox potential range of the mediator and sped up the rate of the reaction.

3.2.1 MB layer on conventional size Glassy carbon electrode

The new Pine instruments equipment had the advantage of a ready rotating disc GC electrode. Therefore, commercial tip of a Pine rotating disc electrode containing a central GC disc of 5 mm outer diameter is chemically modified and used in the experiments as working electrode. The Chrono-potentiometric experiments were done with rotating disc electrode (at 1000 RPM), while the CV-s were taken in quiescent solutions with stationary electrode. Before coating the surface with the MB redox mediator film the GCE disc is wet polished stepwise with different sizes of alumina polishing slurry. As follows 1 μm, followed with 0.3 μm and finalized with 0.05 μm size particles were used to remove any debris and ensure a clean shiny surface. Between the polishing steps, the alumina particles were removed by sonication in ion exchanged water.

A 50 ml beaker with 0.25 M phosphate buffer pH =7.0 served as the measuring cell. The 50 ml beaker is chosen to allow for sufficient space on the mouth of the beaker for the rotating electrode, counter electrode and the reference electrode. The electrode and the casing is 15 mm diameters.

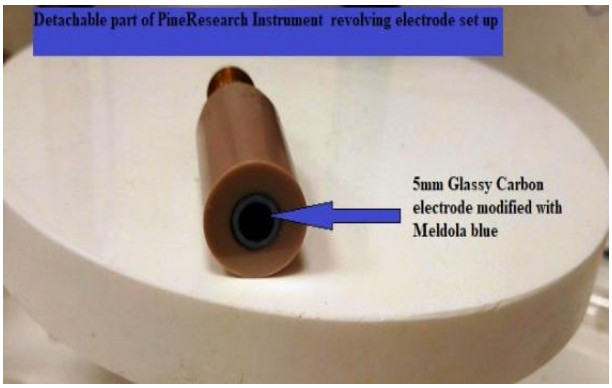

Fig. 9. The picture of a Pine research instrument Glassy carbon electrode disk, modified with MB

Electrochemical activation is carried out in order to enhance absorptivity character of GC. In this step the finely polished working electrode together with the Ag/AgCl reference- and platinum counter electrodes are placed in a 50 ml beaker containing 30 ml 0.1 M KCl solution and 120 polarization cycles with 5 V/s scanning rate are performed in the potential range of -0.5 to 3.0 V. After this, the electrode is kept for 60 s in the same solution at -0.5 V constant potential.

Before and after activation, CV-s are recorded with 100 mV/s scanning rate in 0.5 M H_2SO_4 solution containing 0.5 mM $K_4Fe(CN)_6$ /$K_3Fe(CN)_6$ for determination of the electrochemical surface area of the electrode.

The freshly activated and washed electrode is immersed for 60 s adsorption time into phosphate buffer pH=7.0 containing MB dye in $5X10^{-4}$ M concentration (see Fig. 9). The excess MB is removed by washing and rinsing with deionized water.

To determine the amount of immobilized MB and the number of layers, a baseline is obtained for the cyclic voltammogram under either the oxidation or reduction peaks. The

area under the curve between the baseline and the peak is determined by integration. This gives the charge (Q) in coulombs. Using the charge, Faraday constant and the Avogadro's number, the coverage density with material on the carbon surface is determined based on Faraday's first law of electrolysis.

3.2.2 Electropolymerized MB (epMB) layer formation

In the previous years, Yamaguchi et al[116]. as well as Vasilescu et al[166]. I successfully made a polymerized film of MB on a base electrode using multiple cycles of cyclic voltammetry. For a short period, the freshly polished GC electrode together with the reference and auxiliary electrodes is introduced in 20 ml pH=7.0 phosphate buffer containing MB in $5x10^{-3}$ M concentration. After purging out the oxygen from the solution with pure nitrogen gas, CV-s are recorded continuously in the range of -0.6 to 1.0 V, with 100 mVs^{-1} scanning rate. The increasing number of sequential voltammograms is an indication of the additive process from monolayer MB progressing into the polymerized form. Once the polymerization of the MB on the 5 mm outer diameter GCE is completed, it is then washed with ion exchanged water to remove any loosely attached MB monomer.

3.2.3 Stabilization of MB on GCE by a docking layer of graphene oxide

The stability of the MB on a bare functionalised carbon electrode can be made better, I had the idea to introduce another pure material as a docking layer for MB.

In creating a docking layer, one of the approaches is electrodeposition of graphene oxide followed by the adsorption of MB on Glassy carbon electrode. The polished GCE is activated by electrochemical pretreatment in 0.1 M KCl solution by continuous taking of CV-s with 5 V/s scanning rate in the range of -0.5 V to 3.0 V vs. Ag/AgCl reference for 120 s. After this activation the electrode surface is electrochemically coated with reduced graphene oxide (GO) layer employing the procedure of Cui and Zhang[134]. Accordingly a graphene oxide suspension with composition of 1 mg/cm^3 is made in 0.1 M, pH=8.0 phosphate buffer. Before electrochemical deposition, 4-hour long sonication of the suspension is employed to homogenize and exfoliate the particles. The electrode is then

immersed in the black graphene oxide suspension and 10 potential cycles between 0.5 to -1.8 V are imposed with scanning rate of 10 mV/s and 1000 r/m rotation rate.

The final step of electrode modification is done by MB adsorption on the surface of the GCGOE in $5x10^{-4}$ M solution of the MB freshly made in 0.25 M pH=7.0 phosphate buffer to obtain a GCGOMBE surface. This electrode is dipped in this solution and kept for given time in it. Before using it in experiments, the electrode is thoroughly rinsed with ion exchanged water to remove the free MB molecules. CV-s are taken in quiescent 0.25 M pH= 7.0 phosphate buffer to check for the presence and amount of the confined redox mediator layer. The redox capacity of it can be characterized by the charge under the MB peaks of the CV.

3.2.4 Adsorption of MB on various PGEs

Pencil graphite leads are affordable and readily available globally. To benefit from this, I sought to use a PGE as the base electrode to test how adaptable it was to the new chronopotentiometric method. In the adsorption process, characterization of PGEs in potassium ferricyanide/ ferrocyanide as the redox couple is done using the method described by R. N. Adams[96], as it is given in his book. The method is applied in the determination of the electrochemical surface area of the PGE-s. After the measurements are successful, the ready miniaturized PGE can be chemically modified by immobilizing a thin film of MB.

In practical antioxidant activity determination, the activity and stability of a redox mediator layer has an important role in the applicability of such an electrode. These parameters can be measured by fresh electrochemical activation of electrode followed by soaking for 60 s in $5x10^{-4}$ M MB solution prepared using 0.25 M phosphate buffer (pH=7.0) to adsorb a thin MB film. The electrodes are then washed thoroughly to remove the excess unadsorbed MB. CV-s are taken in phosphate buffer (pH=7.0) to check for successful attachment of MB and to quantify the amount in terms of the number of layers as described in section 3.2.1.

3.2.5 Calculated model of reagentless chronopotentiometric response

Hypothetically, it is expected that measurements using the chronopotentiometry with a confined mediator would relate to the theoretical model. The expected shape of chronopotentiometric function (E-t) and that of the calibration curve ($\Delta E/\Delta t_{initial} - C_{analyte}$) are estimated by mathematical calculation using a rough model and it is then compared to experimental measurements.

3.2.6 Tuning of the electrode depending on the amount of immobilised mediator

It is possible that the amount and number of layers of confined redox mediator on the surface of a working electrode would influence the signal based on theoretical calculations (see results section). In a reaction involving the mediator and an analyte, a decrease in the amount of the oxidized form of mediator is accompanied by an increase in the reduced form of the mediator. A smaller amount of the mediator would yield a higher potential change signal.

To study this dependence of the analytical signal to the amount of confined mediator, experiments are carried out using more amount and less amounts of MB on the electrode surface for comparison.

First the activated electrode is modified with the electrocatalytic layer as described in previous sections. To obtain a relatively thinner layer, the electrode is soaked in MB with a smaller concentration and for less time compared to the thicker layer. This is then quantified by use of CVs to determine the charge as described in the previous section 3.2.1. The electrodes with thick and thin layers are evaluated for the electrocatalytic response using a measurement method for the analyte activity.

3.2.7 Software used in model calculations, figures and evaluation of results

The data obtained from AfterMath 1.5.9644 software of Pine model AFMSRCE and GEPES 4.9.005 software was downloaded as notepad data sheet. The data is copy pasted onto a spread -sheet software and the appropriate evaluation and graphical outputs are made to obtain CV, DPV, E/t curves, $\Delta E/\Delta t$-c curves and SECM curves.

The model equations were worked out in Ms Excel spread sheet as well. A column for the formula is created and each of the dimensionless values in the equation obtained. The calculated value shows the expected response depending on the measurement (e.g E/t or $\Delta E/\Delta t$-c curves) type targeted in the model.

4 Results and discussion

4.1 Reagentless chronopotentiometric measurements using conventional-size GCE modified with an immobilised MB layer

To achieve fast reaction rate kinetics, a lower potential for electrochemical redox reactions and a larger electrochemical surface, I used MB as the electrocatalyst.

4.1.1 Investigation of the electrochemical responses of epMB and adsMB layers

In this study, I electropolymerized MB on an activated GCE surface using the method proposed by Yamaguchi[116] with slight modification. The 5 mm GCE was initially washed in deionized water. The polishing of the electrode and electrochemical was done as shown in section 3.2.2. The electrochemical cell includes a Ag/AgCl reference electrode and a 1 cm Pt electrode as the counter electrode. The activated GCE was therefore ready for electropolymerization. The same process of cleaning and activation was used in subsequent preparation for the adsorption of MB.

The electropolymerization process was set at a scan rate of 100 mV/s, in 5 mM MB in 0.25 M phosphate buffer pH=7.0 in the range -0.6 V to 1.0 V. Oxygen was purged from the electrochemical cell by bubbling with pure nitrogen. The process of electropolymerization is shown in Fig. 10. Multiple CV-s were recorded revealing the process of polymerized layer formation. When the monomer is subjected to controlled electrochemical heterogenous reactions, the product is a polymerized MB layer on the solid electrode surface. Hypothetically, the epMB was expected to have different characteristics compared to adsMB monomer. Polymerization results in Fig.10 shows that even with additional cycling, a limiting point is reached in the MB polymerization process where, the Ip_{ox} value did not indicate an increase anymore.

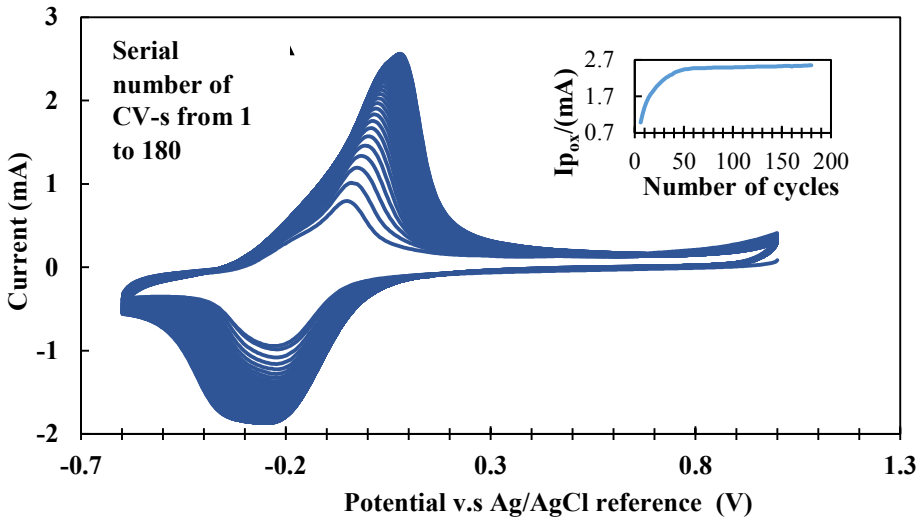

Fig. 10. CV-s recorded during electropolymerization in phosphate buffer (pH=7.0) containing 5 mM Meldola Blue. Scanning rate 100 mV/s. Inset shows, the oxidation peak current (ip_{ox}) plotted against the serial number of CVs.

Inset of this Fig. 10 is a plot revealing the dependence of oxidizing peak height (ip_{ox}) on the serial number of the CVs made from 1 to 180. Notably, the polymerization process indicated by the increase in the peak height after each cycle continued up to a limiting point of about 70 cycles. Yamaguchi et al.[116]. reported a simillar limit of the number of CV cycles The successfully electropolymerized GCE (epMB) was ready for subsequent tests. After polymerization, any excess MB on the surface was removed by washing thoroughly with deionized water.

The second approach was adsorption of MB layer onto the activated GCE. To achieve this, the activated GCE was immersed into 0.5 mM MB solution prepared in 0.25 M phosphate buffer pH=7.0. for 60 seconds. The unadsorbed MB was then washed off with deionised water. I tested for the successful electropolymerization and adsorption of MB using CV.

In order to determine the amount of active catalyst attached on the electrode surfaces using these two different methods, CV-s were recorded in pH 7.0 phosphate buffer, with 100 mV/s scanning rate. Fig. 11 shows the three CV-s for comparison.

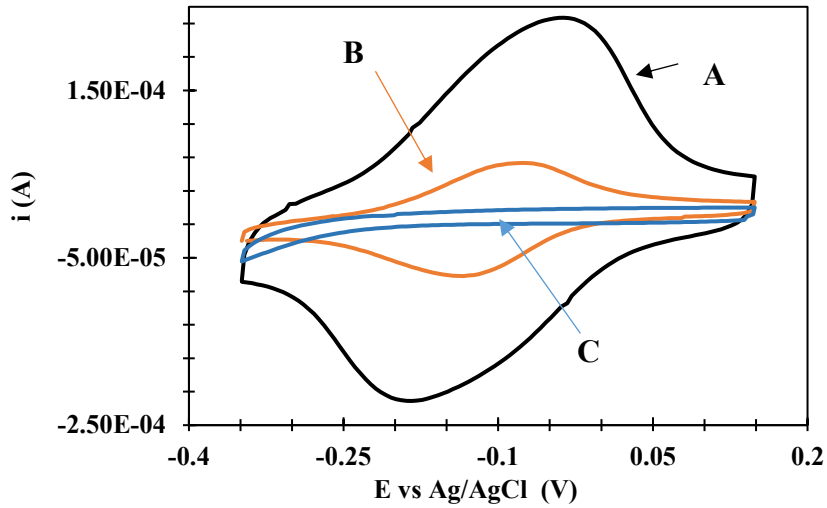

Fig. 11. CV-s recorded in phosphate buffer pH=7.0 using electrochemically pretreated GCE modified with an electropolymerized MB layer (A), pretreated GCE modified with an adsorbed MB layer (B). and pretreated bare GCE (C). 100 mV/s scanning rate.

As it was expected, the CV obtained with well-polished bare electrode (C) did not have peaks in the range studied, while the electrodes modified with adsorptive electro catalyst layer (B) and with polymerized catalytic layer (A), show well-formed peaks in both oxidation and reduction positions on the CV. The current peaks and the areas under these peaks are much smaller in the CV recorded with adsMB compared to the epMB modified electrode.

Table 2. A comparison of the main parameters of GCEs modified with MB layers prepared by absorption (adsMB) or electropolymerization (epMB). Scan rate: 100 mVs^{-1}.

#	Electrochemical parameter	Activated GCE with adsMB	Activated GCE with epMB (90 CV cycles)
1	Ep_{ox} vs. Ag/AgCl [mV]	−81.3	−41.2
2	Ep_{red} vs. Ag/AgCl [mV]	−133.8	−188.7
3	$Ep_{ox} - Ep_{red} = \Delta Ep$ [mV]	52.5	147.5
4	Ip_{ox} [µA]	55.0	190.8
5	Ip_{red} [µA]	−55.4	-162.6
6	Q_{ox} [Cb]	7.3×10^{-5}	3.22×10^{-4}
7	Q_{red} [Cb]	7.8×10^{-5}	3.13×10^{-4}
8	Ratio $Q_{ox}(ads)/Q_{ox}(pol)$,	0.23	
9	Ratio $Q_{red}(ads)/Q_{red}(pol)$,	0.25	
10	MB amount [mole]	3.79×10^{-10}	1.67×10^{-9}
11	Number of molecules	$2.28 \times 10^{+14}$	$1.01 \times 10^{+15}$
12	Geometric area (mm^2)	19.64	19.64
13	Electrochemically active area of the GC [mm^2]	9.9	9.9
14	MB density [mole/mm^2]	3.83×10^{-11}	1.69×10^{-10}
15	Estimated MB layer number (molecules/one layer)	5.67	25.00
16	Q/area [C/mm^2]	3.72×10^{-6}	1.64×10^{-5}

Table 2. further compares the most important characters like the peak potential (Ep_{ox}, Ep_{red}), peak current (Ip_{ox}, Ip_{red}) - values as well as the corresponding electric charges involved in redox reactions (Q_{ox}, Q_{red}). The coverage densities (mole/mm^2) could be estimated knowing the geometric surface area (19.625 mm^2) the number of electrons involved in redox reaction (n=2) and the electric charge values showing the amount of MB moles on the GC surface (the coverage). Furthermore we could make a rough estimate of the numbers of electro-active MB layers on the electrode surface based on the known estimated area (24.6 $Å^2$) [167] of one MB molecule.

From my results, it is demonstrated that the ratio of corresponding the peak current (ip) and charge (Q) values obtained from the electro-polymerization were higher than the values of the two parameters from the electrode adsorbed with the mediator. The higher amount of electrochemically accessible immobilized mediator on the GC surface of the epMB layer resulted to the distinctly higher values. As it was expected, the thicker

coverage of the polymer produced a higher ΔEp value between the oxidation and reduction peaks too. The charge which is measured in ampere seconds or Coulombs reveals the amount of MB. A higher value in ampere seconds or the area under curve implies a higher amount of the mediator on the working electrode surface.

What this important observation means is that, in the case of epMB, the redox reaction is more complex than the one in case of adsMB. Consequently, it is probable that the thicker epMB involves some relatively slow redox and chemical reaction steps.

4.1.2 Evaluation of the MB layer stability on GCepMBE and GCadsMBE

I needed to find out, between the adsMB and epMB, which modification retained or lost more of the MB over a series of 100 measurements. The measured baseline in this experiment was the CV of bare electrode. The oxidation current peak (Ip_{ox}) height after each modification was determined. The area under the Ip_{ox} is equivalent to the charge. Based on Faradays first laws of electrolysis, the amount of MB deposited on the electrode or the coverage can therefore be determined. This information was useful in evaluating the stability of the MB layer on the electrodes. The stability of the redox mediator on the electrode surface is an important parameter concerning the applicability of the modified electrode for measurement. The stability of the layer, possibly contributes to the repeatability of results. To verify this by measurement, potential scanning on the voltammetric behavior of the redox layer sequential CV-s were recorded in pH=7.0 phosphate buffer employing 100 mV/s scanning rate with the two differently made MB modified electrodes. In both cases 100 cycles were made. Fig.12 shows the peak values of oxidative current peak ($Ip_{ox\,(n)}$) as a percentage of the initial one ($Ip_{ox(n=1)}$).

$$Ip_{ox}(\%) = 100 * \left(\frac{Ip_{ox(n)}}{Ip_{ox(n=1)}}\right) \quad (11)$$

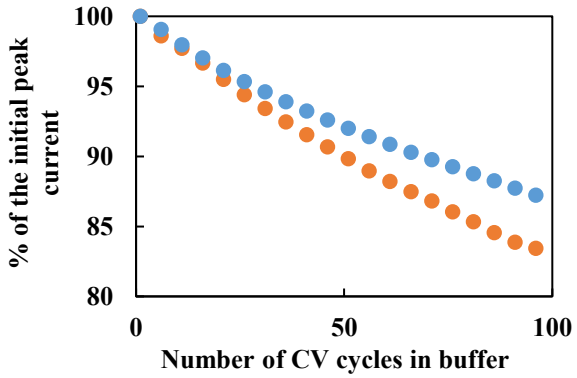

Fig. 12. A graph showing the effect of making multiple CV cycles to the oxidative current peak $Ip_{ox(n)}$ as a percentage of the initial peak current ($ip_{ox(n=1)}$) measured on adsMB (orange●) and epMB (blue●) modified GCE. The measurements were made in 0.25 M Phosphate buffer pH= 7.0 scan rate 100 mV/s.

Notably by observation of the graph in Fig. 12, it can be concluded that, from the scans that, the Ip_{ox} obtained with the epMB saved up to 88% and lost 12% of the original value. The adsMB however saved 83% and lost 17% of its original $Ip_{ox\ (n=1)}$ value. The difference is not extensive indicating that the polymerized layer is relatively more stable, though the stability of adsorptive mediator is almost closely similar retaining most of the MB activity. Therefore both modifications are is reliably stable for making electrochemical measurements.

4.1.3 Evaluation of antioxidant activity in the case of GCepMBE and GCadsMBE

The Fig.12 shows that more than 80% of MB layer was retained in both modifications. The other test was the antioxidant sensing nature of the MB modified GC electrodes by using the novel chronopotentiometric E/t curves recorded in pH=7.0 phosphate buffer. Three different concentrations (9.99 $x10^{-5}$ M, 4.99 $x10^{-4}$ M and 3.373$x10^{-3}$ M) of the antioxidant L-ascorbate were made in 0.25 M phosphate buffer pH=7.0. In these experiments 50 ml beaker served as measuring cell and the Pine instrument rotating disc electrode provided intensive convection. The freshly made chemically modified rotating disk GCadsMBE and GCepMBE were used as the working electrode in a three electrode set up that included Ag/AgCl reference electrode and an approximately 1 cm^2 Pt counter electrode.

The autolab potentiostat was set as follows,

Table 3. The set up for new chronopotentiometric measurements using the GEPES 4.9.005 software

Chrono method interval time (less than 0.1 s) Potentiometry (zero current)	
Pre-treatment	
First conditioning potential	0.2 V
Duration of oxidation	2 s
Interval time	0.001
Duration of measurement	2 s

In the first step, the electrode potential was controlled, and the surface linked mediator was bought to its oxidized state by employing 0.2 V vs. Ag/AgCl potential for 2 s. Immediately after, the open cell potential (OCP) was recorded in time. The electrode potential – time traces E/t are shown in Fig. 13.

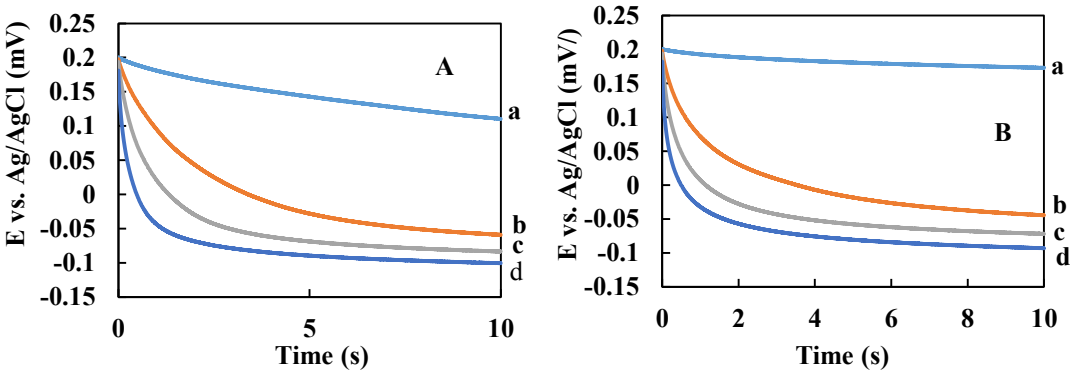

Fig. 13. Chrono-potentiometric electrode potential (OCP) - time traces (E/t) obtained with GCepMBE- (Fig.13 A) and GCadsMBE (Fig.13 B) in, (a)phosphate buffer pH= 7.0 containing L-ascorbate in different concentrations,(b) 9.99 x10^{-5} M, (c), 4.99 x10^{-4} M and (d) 3.373x10^{-3} M concentrations respectively.

It can be seen that at t= 0, when the activation step ends, the OCP starts decreasing. The reason is obvious. In the activation step, the potential 0.2 V vs. Ag/AgCl reference electrode, was set. The oxidation peak potential of MB is less than 0.2 V therefore, at that potential, the surface layer of immobilized MB was mainly in its oxidized state.

As the potential control was terminated, then reducing species in the solution change the aMB_{ox}/aMB_{red} activity ratio by reacting with the mediator in a heterogeneous redox reaction. This resulted in OCP change from the initial 0.2 V to a lower potential. Over some period, when the aMB_{ox} was reduced, the open circuit potential did not change any further. How fast the potential change happened depended on the amount of the reducing species (AA) concentration. The concentration is related to the activity based on the equation.

$$\left(\frac{\Delta E}{\Delta t}\right) = f(a_{antioxidant}) \qquad 12$$

For example in the case of a high concentration of the antioxidant or the reducing species, a faster potential change was obtained within the 1 ms initial part. In case of buffer without any antioxidant, the potential change was slow for both electrode modifications. The initial slope in buffer for the epMB modified electrodes was a little bigger than the one of adsMB. The differences seen in the Fig.13 are caused by the inertia of the electrochemical work station. Switching from potential control to open circuit can result in small systematic error.

Actually, by comparing the curves obtained at the same concentrations, no substantial differences could be seen between the ones recorded with polymerized layer (Fig. 13. A) and with an adsorbed layer (Fig. 13 B) on GC electrodes.

4.1.4 Assessment of the repeatability of chronopotentiometric measurements in case of the two differently MB modified GCEs

It was an important question how far the electrodes can retain the activity of the surface confined MB layer upon getting exposed to multiple activation - relaxation measuring steps. Would the results of measurements be accurate and repeatable? This was a valuable endeavor to determine how repeatable the results would be during measurement.

Having sufficient proof of a change in potential -time dependent signal, the initial slope ($\Delta E/\Delta t$) of the OCP curves could be used as an analytical signal for measuring concentration of antioxidant species. The two steps of the chronopotentiometric method could be repeated within short time intervals, one after the other in the same solution to follow changes in concentration in analyte.

In order to study the repeatability of results using the proposed method, 25 measurements were made one after the other. In experiments, using the two differently modified electrode surfaces, the rotating electrodes in phosphate buffer (pH=7.0) containing 2.49 mM concentration of L-ascorbate were utilized in both cases under similar conditions. In this case 0.2 V vs. Ag/AgCl reference activation potential step of 1 s was used. In the second OCP step, a 0.01 s section of the slope was taken from a recorded 2 s long section (see illustration of the method Fig. 41). Between measurements 60 s long, waiting time was employed. Fig. 14 shows the obtained results as the initial slope is plotted against the serial number of measurements.

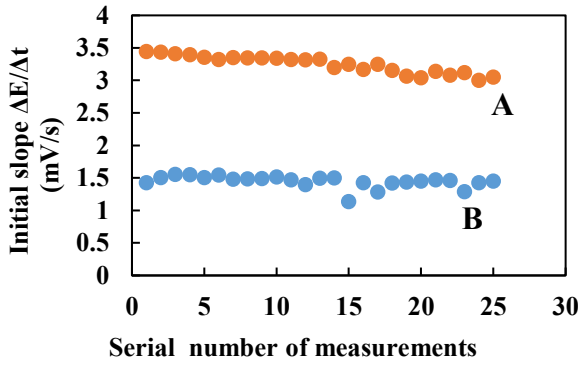

Fig. 14. The repeatability of chronopotentiometric measurements in the case of GCadsMBE (A) and GCepMBE (B) in phosphate buffer pH =7.0 containing 2.49 mM L-ascorbate. 1000 RPM electrode rotating rate, 0.2 V vs. Ag/AgCl activation potential, 1s activation time and 60s waiting time between the measurements were employed.

From the Fig.14, it can be observed that, after 25 repeated chronopotentiometric measurements, the adsorbed MB mediator layer lost about 14% of its original activity, while the slope values obtained with the electropolymerized MB layer did not show a steady decrease.

Based on results of these measurements we can conclude that the sensitivity of the chronopotentiometric antioxidant measurement is higher in case of GCadsMBE which gives a higher $\Delta E/\Delta t$ –c signal, therefore advantageous for short periods of measurements. On the other hand, the GCepMBE has a more stable layer of MB and can give accurate and repeatable analytical results for a slightly longer period compared to GCadsMBE.

4.1.5 Evaluation of the sensitivity of GCepMBE and GCadsMBE to L-ascorbate

The sensitivity of a sensor or electrode is determined from the slope of the calibration curve on the linear or dynamic range. A higher slope of the calibration curve implies better sensitivity compared to a sensor with a lower slope. For analytical measurements, it would be of interest to know what modification to use in order to suit the measurement conditions. Is there any difference between the sensitivity of GCadsMBE and GCepMBE to L-ascorbate?

To determine the modification that would give better sensitivity to an antioxidant /reducing species, I prepared a chronopotentiometric calibration curve under similar conditions using the differently modified electrodes. It was possible to deduce from the initial slope of chronopotentiometric curves, the activity of the antioxidant species L-ascorbate. The measurements were made in phosphate buffer pH=7.0 containing L-ascorbate in different concentrations. In these experiments the measuring parameters employed were the same as the ones used in obtaining the stability of the layer showed in Fig. 14. For every AA concentration, at least 5 measurements were performed and the average of the initial slopes were plotted against the L-ascorbate concentration. The deviation from the mean of each measurement was estimated from the repeated measurements (see the error bars on Fig. 15).

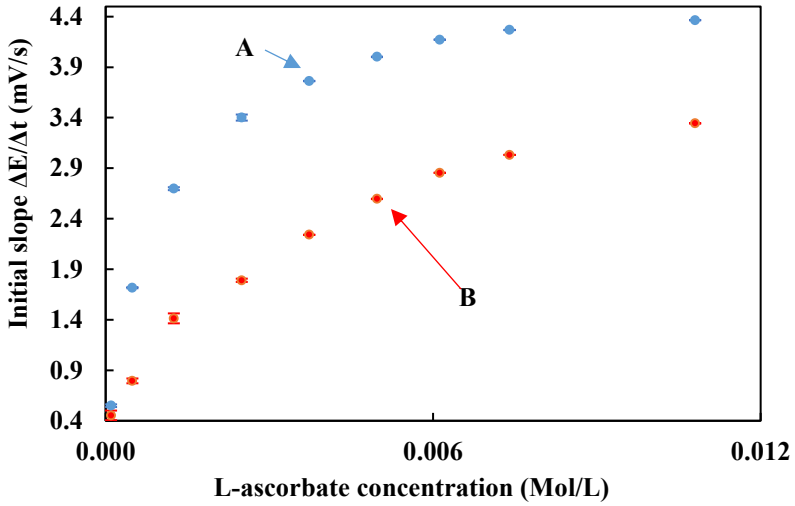

Fig. 15. Dependence of initial slopes of the chronopotentiometric curves on the L-ascorbate concentration obtained with GCadsMBE (blue markers●) and with GCepMBE layer (red makers ●) Measurements were made in pH=7.0 phosphate buffer with 1000 RPM rotation rate and 1s activation step of 0.2 V. The maximum standard deviation of five parallel measurements were under ±0.11 mV/s.

From the results in Fig. 15 it observed that the obtained dependences of the signal on concentration are monotonous in that a higher concentration results in higher slope in both cases. The GCadsMBE surface offered better sensitivity observed from the steeper slope against concentration of antioxidant (Fig. 15. A), within the dynamic range. The GCepMBE surface was less sensitive based on the slope of the calibration curve in the dynamic section (Fig.15B). Therefore for various concentrations of the antioxidant measured, the adsorbed MB layer was more sensitive. The applicability of the proposed chronopotentiometric method for testing antioxidants activity was therefore proved to be promising. However, it needed further research to find the optimal measuring conditions. My laboratory work intensively progressed to testing more capability of the novel technique.

4.2 Assessment of nano-size graphene oxide as a docking layer for adsorbed MB

From the investigations and evaluations in the previous sub-section 4.1, I had proof of the stability and activity of the electrode modified with immobilized redox mediator layers. The repeatability of results and sensitivity of the sensor was determined by making measurements with the newly introduced chronopotentiometric antioxidant measuring

method. These were important parameters for determining the applicability of the method in every day laboratory practice. Fig.16 A is an illustration of the adsorption process that results into a layer of MB on the activated GCE surface. To improve the properties of the electrode/sensor further, an idea to employ nano particles (GO) as a docking surface was worth testing (see illustration in Fig.16. B and Fig.17).

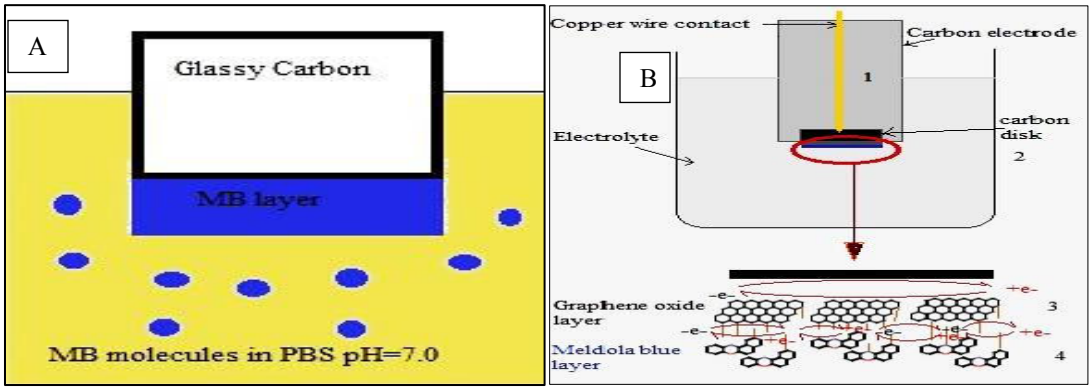

Fig. 16. (A) An illustration of adsorbed MB layer on a polished and activated GCE surface. (B) An illustration of MB layer docked on graphene oxide film on an activated GCE surface

The immobilization of graphene oxide that is shown in Fig. 16 B was done through direct electrodeposition method. Fig. 17 illustrates the rotating disk electrode that was electrodeposited with graphene oxide followed by adsorption of an MB layer.

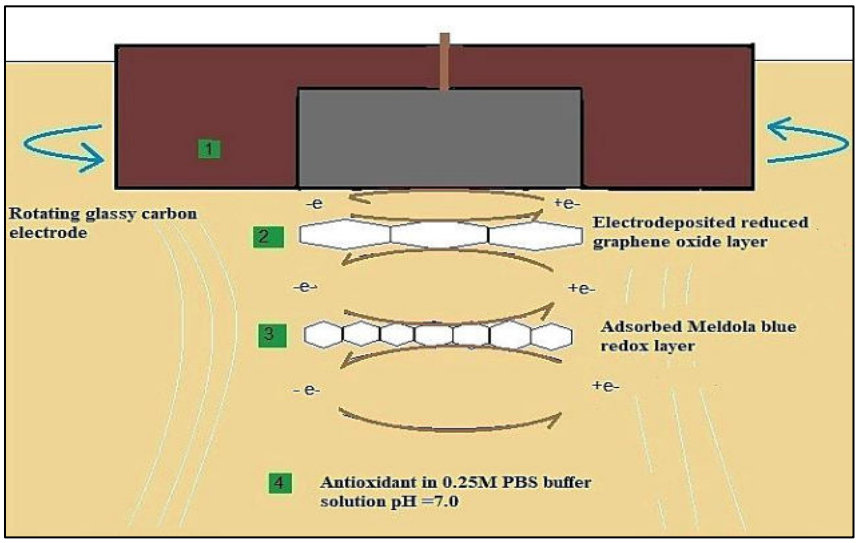

Fig. 17. A scheme of the rotating disk Glassy carbon electrode modified with a GO docking layer and adsorbed with MB.

4.2.1 Investigation of graphene oxide for enhanced stability of MB layer on GCE

Learning from all these aspects, the next obvious step was to test experimentally how far the activity and stability of the mediator layer could be improved by applying graphene oxide (GO) on the GCE as a docking layer for the adsMB mediator.

Consequently, I set up experiments that led to results that revealed an improvement in the analytical performance of the chronopotentiometric antioxidant measuring method. In these experiments, I depositing a thin reduced graphene oxide film onto the surface of a polished and electrochemically activated GC electrode using the method described under of electrode modification section of this thesis. It was expected, that some of the benefits of the grapheneous layer would be,

- An improved electron exchange rate between the mediator film and the GC phase or the base electrode,
- An increase in the activity through provision of good docking conditions for MB, as well as enhanced adherence to the base electrode,
- Provision of better working stability of the adsorbed MB mediator molecules on the stable GCGO surface.

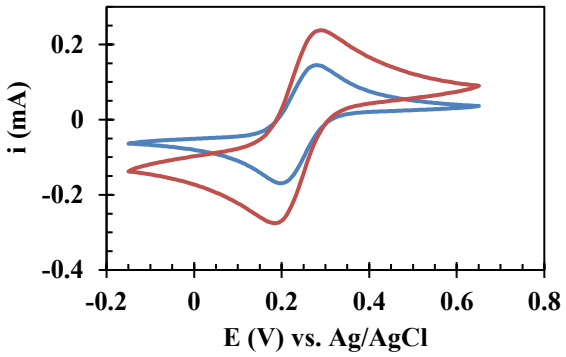

Fig. 18. Cyclic voltammograms recorded in 0.5 M KCl solution containing 5 mM $K_3[Fe(CN)_6]$/ $K_4[Fe(CN)_6]$ with electrochemically pretreated GCE with no GO layer (blue ●), with GO layer (red ●). Scanning rate = 50 mV/s.

In order to test the influence of a reduced graphene oxide layer on electrochemical activity, CVs were made in a quiescent solution of 5 mM $K_3[Fe(CN)_6]$/ $K_4[Fe(CN)_6]$ in

0.5 M KCl (see Fig.18). The two freshly polished and electrochemically functionalized 5mm GC electrodes were used in measurement. One was with and the other one without a reduced graphene oxide (GO) layer on the surface, at a scanning rate of 50 mV/s.

The current and change in peak potential characteristic values of the CV-s are showed in Table 4. From the results, it can be seen that the reduced graphene oxide layer substantially increased both the oxidation and reduction peak currents. Some changes of the ΔE_p were observed too.
We can conclude that the reduced graphene oxide has beneficial changes to the activity of the electrode.

Table 4. Characteristic values in the CV-s recorded with the differently modified electrodes.

Electrode surface	**ip_a (µA)**	**ip_r (µA)**	**ΔE_p (mV)**
GC no GO	180	184	56
GC with GO	290	290	81
Increase	110, (61%)	106, (57%)	25

From this study I concluded that, the electrochemically reduced graphene oxide film could be used as a docking film for immobilization of a mediator on GC working electrode. CV-s recorded in $K_3[Fe(CN)_6]$/ $K_4[Fe(CN)_6]$ indicated that the GO film increased the electrochemical surface area of the GC electrode.

The amount of the MB mediator adsorbed on the electrode surface and acting as confined reagent could be easily estimated too, in case of the two different electrodes. To do this, the electrochemically pretreated GCE and the GCGOE were soaked for 60 s in 0.25 M pH = 7.0 phosphate buffer containing MB in $5x10^{-4}$ M concentration. After through washing to remove excess MB on the surface, CV-s were recorded using the GCadsMBE and GCGOadsMBE in pure 0.25 M pH = 7.0 phosphate buffer employing 50 mV scanning rate. The charge was obtained by determining the area under the curve in Fig.19 A and Fig.19 B. The obtained CV-s are shown in Fig. 19. The charge on the surface of

the electrode depends on the amount of material deposited based on Faraday's first law of electrolysis.

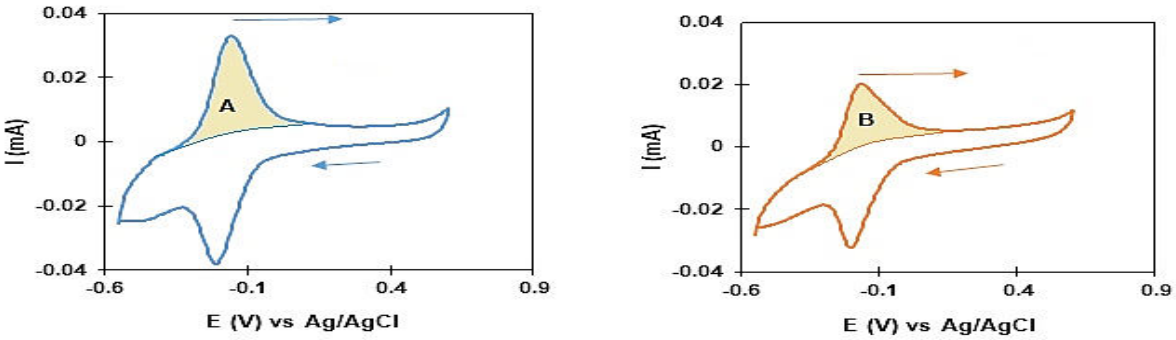

Fig. 19. Cyclic voltamograms of GCadsMBE and GCGOadsMBE in 0.25 M phosphate buffer pH=7.0, scan rate = 50 mV/s. A is the charge of GCadsMBE (Ox_{peak}), B the charge of GCGOadsMBE (Ox_{peak}).

I calculated the number of the adsorbed MB molecules taking part in redox reactions based on the charge values which is equivalent to the area under the curves or peaks. Knowing the geometric area of the GC surface and using the estimated geometric surface area of one MB molecule, I could determine the number of layers in the mediator film.

Table 5. Data about adsorbed mediator layer in case of different electrodes.

Main Parameters	GCMBE $_{(OX)}$	GCGOadsMBE $_{(OX)}$
Charge (Q) C	$8.44x10^{-5}$	$6.98x10^{-5}$
Geometrical area (A) mm^2	19.64	19.64
No of Moles of MB	$4.37x10^{-10}$	$3.62x10^{-10}$
Density of MB -Γ (Q/2FA) mol/mm^2	$2.23x10^{-11}$	$1.84x10^{-11}$
No. of MB molecules	$2.63x\ 10^{14}$	$2.1x\ 10^{14}$
No.of MB molecules on A of GCE	$7.98x\ 10^{13}$	$7.98x10^{13}$
Number of MB layers	3.3	2.73
Statistical analysis P-value (mean stability)		0.000154
Statistical analysis P-value (mean reproducibility of results)		$1.1x10^{-35}$

In doing these calculation, two electrons per MB molecule (n=2), Avogadro number of 6.02214 x10 ^{23}, Faraday of 96485.333 As/mol, geometric area of the electrode surface 19.643 mm^2, and geometric area of the one MB molecule 24.6 $Å^2$ [167] were used. The data obtained are listed in Table 5. In this way, the amounts of MB molecules adsorbed on bare GC and on GCGO electrode surfaces were measured.

It can be seen that a significantly higher amount of electric charge is involved in the redox reactions involving the GCadsMBE than in the redox reactions of GCGOadsMBE. This indicates that the electrochemically formed reduced GO layer takes up a high number of adsorption sites that were exclusively available for MB adsorption in the bare GCE. Interestingly, our further experiments established that a thinner mediator layer shows a higher chronopotentiometric analytical signal (see Fig. 22 in regard to number of layers). The chronopotentiometric antioxidant measuring activity was tested in the next step.

In a second test, using the calibration plot of one of the antioxidants tested, it was possible to evaluate changes in the stability, sensitivity and repeatability of reagentless chronopotentionmetry results.

To test the stability of the MB modified layer with reduced graphene oxide as a docking surface GCGOadsMBE, I compared it to the GCadsMBE without GO. For this, chronopotentiometric measurements were made in 0.25 M, pH=7.0 phosphate buffer solution containing L-ascorbate in different concentrations. In the case of both experimental electrodes, the MB layer was immobilized by adsorption. The results of the test in Fig. 20 from experimenting with 3.73 $x10^{-3}$ M L-ascorbate concentration and employing 0.2 V electrode potential (vs. Ag/AgCl reference) in controlled potential step of 2 s and 1000 RPM electrode rotation rate are revealed. In these experiments I continuously kept the electrodes in the measuring cell and the same two step measuring protocol was repeated one after the other leaving 2 minute time between them. The electrode potential – time curves were recorded for 2 s. The initial slopes or the signal of these recording were plotted against the serial number of the curves. In Fig. 20, the obtained results are shown. Fig. 20 A shows the values of the actual slopes in mV/10 ms, while in Fig. 20 B their change by the serial number of measurements can be seen in percentage.

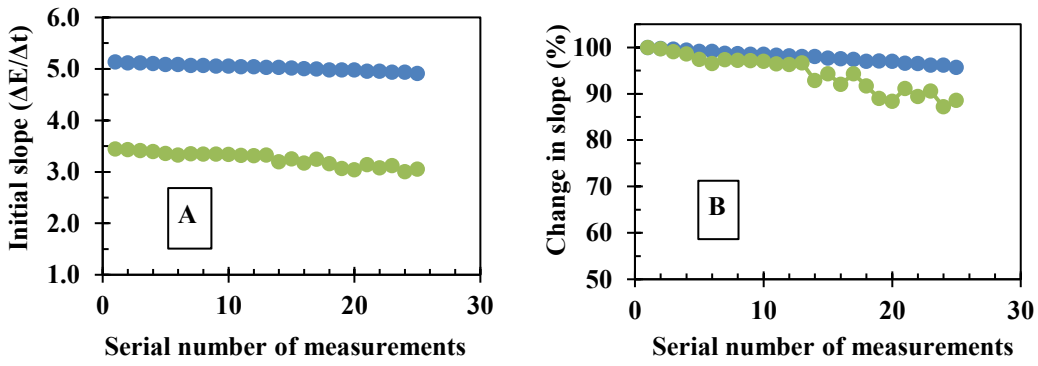

Fig. 20. Comparison of working stability of the two different GCEadsMBs, one made with reduced graphene oxide layer GCGOadsMBE, (blue●) and the other without it, GCadsMBE (green●).

Fig. 20. A, shows the initial slopes (ΔE_t/10ms) plotted against the serial number of experiment, Fig. 20. B reveals the change of the initial slopes in percentage of the measurements in Fig.20.A. The initial slope signal improved by increasing from 3.5 (GCadsMBE) to 5.1 (GCGOadsMBE) mV/10 ms (increase of ≈45.7%). The working stability also increased. Actually after 25 sequential measurements the electrode prepared with GO layer kept 98% of its original activity, while the electrode without it kept only 88% of it. The experimental findings clearly showed that the reduced graphene oxide layer improved the performance of the chemically modified GC electrode. The working stability of the mediator layer was challenged by serial antioxidant measurements. In these experiments slight increase of the working stability of the GCGOadsMB electrode was observed. On surface of GCGO electrode considerable less mediator molecule adsorbed than on the bare GC one, but interestingly higher antioxidant measuring sensitivity could be observed in case of GCGOadsMBE.

Statistical analysis for the two independent samples was done using the student t test. The number of measurements (n) was 25 each, therefore a parametric test was done by testing the following hypothesis,

H_0: There is no significant difference in the mean stability of MB between GCadsMBE and GCGOadsMBE during the chronopotentiometric measurement of antioxidant.

H_0: There is no significant difference in the mean repeatability of measurement results between GCadsMBE and GCGOadsMBE using the chronopotentiometric method

At $\alpha = 0.05$, the calculated P value for differences in the mean stability of MB layer between GCadsMBE and GCGOadsMBE was 0.000154 which is lower than $\alpha = 0.05$. Therefore the null hypothesis was rejected. The differences in the two sets of data is significant at 95% confidence interval. Similarly the calculated P value for differences in the mean repeatability of measurement results between GCGOMBE and GCGOadsMBE was 1.1×10^{-35}. This was lower than $\alpha = 0.05$. In that regard, the null hypothesis was rejected as well (see Table 5). Therefore the differences are significant at 95% confidence interval. In conclusion, the modifications with graphene oxide are recommended to improve on the stability MB and repeatability of measurements made using the sensor.

4.3 Evaluation of the sensitivity of GCGOadsMBE sensor depending on the amount of immobilized MB on the electrode surface

The analytical-signal-forming mechanism in the chronopotentiometric antioxidant measuring method is now known from theoretical calculation and experimental measurements, it could be expected that the amount of redox mediator confined on the surface of a working electrode will have a significant influence on the signal itself.

4.3.1 Tuning of the GCGOadsMBE by altering the amount of confined mediator

This being an heterogeneous reaction, the amount of the oxidized mediator will decrease and that of the reduced one increases simultaneously in the presence of an antioxidant. It therefore expected that the smaller the amount of mediator participating in the reaction, the higher the resulting potential change during the redox reaction (see equation 22).

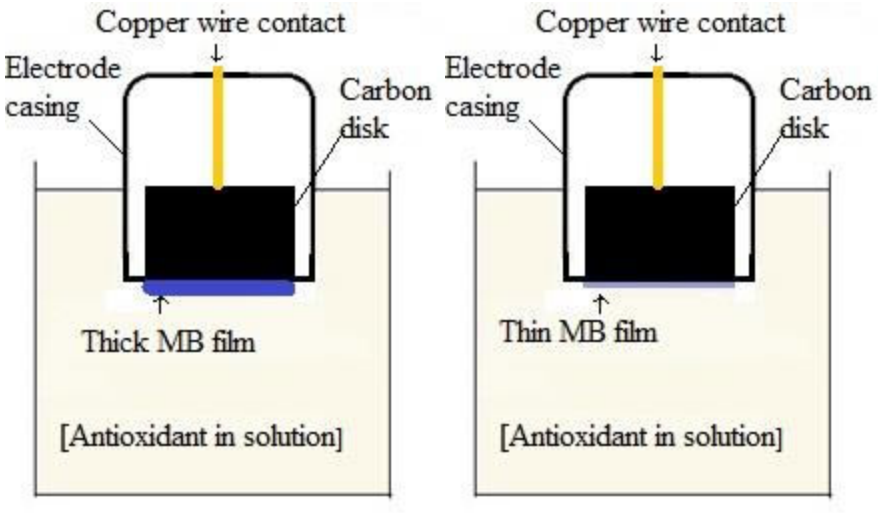

Fig. 21. An illustration of a thick and thin layer of the redox mediator MB on a functionalized carbon electrode base

In order to experimentally study the dependence of the analytical signal on the amount of active MB confined on the electrode surface, experiments were carried out using an electrodes with larger (thick) or smaller (thin) amounts of MB (Fig.21) on their surface. To prepare an electrode with the larger amount of mediator we soaked a freshly prepared GO-modified GC electrode in 5×10^{-4} M MB solution for 60 s, while a similar electrode was soaked in 1×10^{-6} M MB solution for 30 s to obtain an electrode with a smaller amount of mediator.

The number of MB layers was calculated from the CV peak values as discussed previously. The electrodes were washed with deionized water to remove excess MB from the surface. It was found that the electrode with the higher mediator coverage contained 2.55 MB layers while that with the lower coverage had only 0.77 of a layer. Chrono-potentiometric calibration curves of L-ascorbate were obtained with a 0.2 V oxidizing potential held for two seconds, using a rotation rate of 1000 RPM.

Table 6. Comparison of main parameters for thin and thick MB layers.

Parameter	**GCGOadsMBE (Thin layer) $1x10^{-6}$ M MB**	**GCGOadsMBE (Thick layer) $5x10^{-4}$ M MB**
Q (Charge) μC	9.91	32.955
Geometrical Area (A) mm^2	19.64	19.64
No. of Moles	$5.136x10^{-11}$	$1.708x10^{-10}$
Density of MB -Γ (Q/2FA) $mole/mm^2$	$2.614x10^{-12}$	$8.694x10^{-12}$
No. of MB molecules	$3.0927x10^{13}$	$1.028x10^{14}$
Number of layers	0.77	2.55
Dynamic range	$5x10^{-2}$ mM to 3.1 mM	$4x10^{-3}$ mM to 3.1 mM
Sensitivity (calibration curve slope)	2.6	0.8
Lower limit of detection (Buffer)	$4x10^{-3}$ mM	$4x10^{-3}$ mM
Lower limit of quantitation	$5x10^{-2}$ mM	$4x10^{-3}$ mM

Before making chronopotentiometric measurements with the electrodes, I washed with deionized water to remove excess MB from the surface.

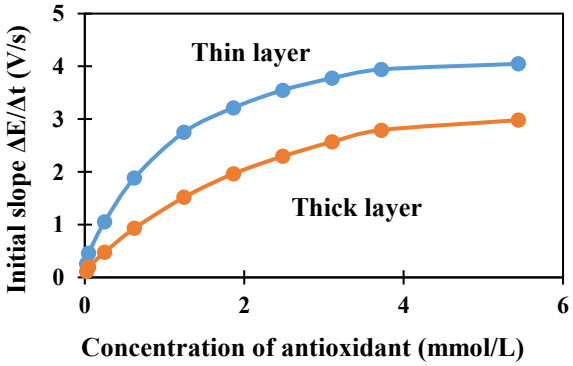

Fig. 22. Chronopotentiometric calibration curves of L-ascorbate analyte made with GCGOadsMBE electrodes holding thin and thick redox mediator layer. 0.2 V oxidizing potential was kept for two seconds and 1000 RPM.

Chronopotentiometric calibration curves of ascorbate were made with 0.2 V oxidizing potential kept for two seconds and using 1000 RPM rotation rate. The curves obtained are shown in Fig. 22. As it can be seen, the thin layer provided higher analytical signal especially, in the low analyte concentration range.

In conclusion, Fig. 22 shows that the quantity of the adsorbed mediator influences the sensitivity of the method. Knowing the estimated concentration range of the samples, the

performance of the method can be optimized by employing the right size of mediator film.

A comparison of the main parameters between a thin and thick layer of MB on GCGOadsMBE

4.4 Investigation of differences in antioxidant activity for selected pure species

Antioxidants with different chemical properties and structure are found in living things as endogenous antioxidants or in food (consumed by organisms) as exogenous antioxidants. From his review, Gulcin[76] points out that the differences in the antioxidant activity is known to be partly dependent on the chemical structure. Therefore based on this observation, it was obvious that different antioxidants would have different activities. The chronopotentiometric method has been proved well applicable for accessing antioxidant activity of L-ascorbate in the previous sections. To expand the scope by testing the applicability of the method for different analytes was an obvious step. In this regard, this method offered a perfect opportunity to test the variation in the antioxidant activity of different pure samples. It is fast, simple and no reagent is added into the antioxidant test sample.

To make the chronopotentiometric measurements, stock test solutions of analytical grade hydroquinone, L-ascorbate, gallic acid, pyro catechol, pyrogallic acid and resorcinol were prepared. The stock solutions were prepared in 0.25 M, pH=7.0 phosphate buffer. The same 5 mm GCGOadsMBE was used in as the electrode for all the different species. The chronopotentiometric process involving a two-step 0.2 V potential control for 2 s to oxidize the mediator surface followed by measurement of the open circuit potential was used. In all the measurements 1000 RPM electrode rotation rate was employed. Different E/t curves were obtained and evaluated to give calibration plots of each species.

In making the measurements a 20 ml volume of 0.25 M phosphate buffer pH=7.0, was accurately measured using a pipette and placed into an ordinary 50 ml beaker with a wide diameter. The wide beaker diameter provided sufficient space for the casing of the rotating disk GCE, the reference electrode and the counter electrode. This was the electrochemical cell in which all the measurements of the pure antioxidants samples were

made under the same experimental conditions. The initial measurements in buffer solution served as the baseline upon which the limit of detection, for the blank could be determined. All measurements were made by injecting small amounts of antioxidant from the stock solution into the 20 ml buffer solution for all the other antioxidant species. With each injection of additional antioxidant into the measuring cell, the concentration increased, and measurements were made. All the chronopotentiometric measurements were repeated 7 times at each antioxidant concentration.

Each of the initial slopes ($E/t_{initial}$) after 0.001 s for conventional size electrodes, was evaluated. Eventually, each antioxidant species had a chronopotentiometric calibration plot showing the response at different concentrations. The concentration of antioxidant in the bulk solution was made homogenous through convection of the rotating electrode. Fig. 23. shows the electrode potential – time curves recorded in gallic acid solutions at different concentrations. As it can be seen, the higher the concentration, the higher is the initial slope. It is expected that at t=0 s the potential value of 0.2 V is observed.

A further, 25 repeat measurements at $3.72x10^{-4}$ M were made to obtain sufficient results for for determination of gallic acid equivalent, assessment of repeatability of measurement results and evaluation of stability of the mediator. As an alternative, the gallic acid equivalent (GAE) could also be obtained based on the slope of the calibration curve (sensitivity) of each antioxidant compared to that of the measured gallic acid slope. The E/t curves of gallic acid at different concentrations are shown in the Fig.23.

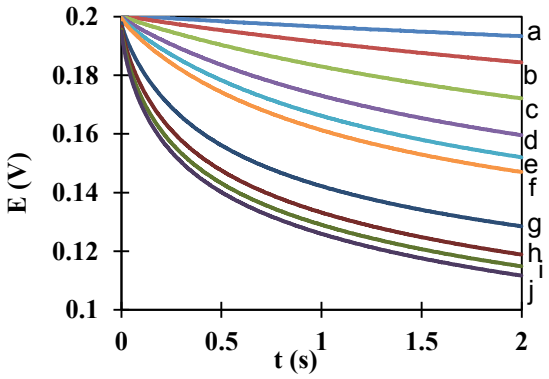

Fig. 23. Open circuit chronopotentiograms recorded in (a) $2x10^{-6}$ M, (b) $9.99x10^{-6}$ M, (c) $2.49x10^{-5}$ M, (d) $4.98x10^{-5}$ M, (e) $7.44x10^{-5}$ M, (f) $9.9x10^{-5}$ M, (g) $2.9x10^{-4}$ M, (h) $4.76x10^{-4}$ M, (i) $6.54x10^{-4}$ M and (j) $8.26x10^{-4}$ M concentrations of gallic acid in 0.25M phosphate pH=7.0 with GCGOadsMBE. The electrode rotation rate of 1000 RPM and 200 mV initial electrooxidation potential control for 2 s were employed.

Chrono-potentiometric response curves were recorded in buffer solution containing varying concentrations of several different analytes and the calibration plots are shown in Fig. 24. In these experiments the same parameters and the electrode were used as given in Fig. 23, and curves similar to the mathematically calculated and plotted ones shown in Fig. 26 were obtained.

From these recordings, calibration curves were prepared. Fig. 24 shows some of these curves. By utilizing either the slope or a particular antioxidant concentration, it was possible to determine the gallic acid equivalent of each species.

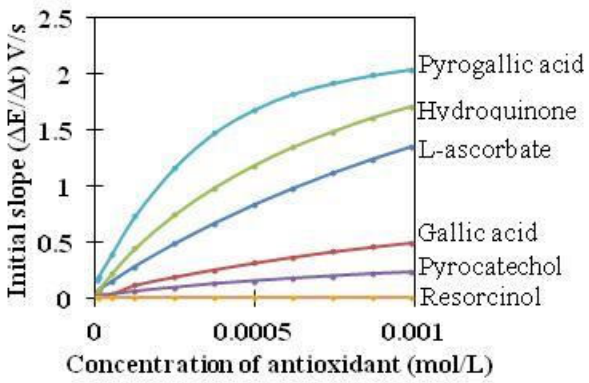

Fig. 24. Chrono-potentiometric calibration plots of different antioxidants obtained in 0.25 M phosphate pH=7.0, with GCGOMBE working electrode using 1000 RPM electrode rotation rate.

Looking at the calibration curves (Fig. 24) we can see that the antioxidant activity of the different species is substantially different. For illustration we recorded chronopotentiometric curves of solutions having different antioxidants in the same concentration. In these measurements

3.7×10^{-4} M concentration of the antioxidants in 0.25 M phosphate buffer pH=7.0 was employed together with 0.2 V potential control for 2 s, and 1000 RPM rotation rate. The initial slopes of the E/t curves obtained are compared in Table 7.

Based on Fig. 24 the chronopotentiometric response of the different species can be compared. In this we can use the initial slope values as well as the slope values obtained at certain concentration of the different species. Since gallic acid is often used as a reference material, in the Table, slope values are also compared to the slope values obtained in case of gallic acid.

Table 7. Comparison showing the slopes of (ΔE/Δt-c curve) for different antioxidant species, the ratio relative to gallic acid calibration slope, the (E/t) curve slopes of 0.37 mM of different antioxidants relative to the gallic acid slope at 0.37 mM concentration and the equivalent gallic acid concentration for the different antioxidant species

Antioxidant species	**Slope of ΔE/Δt-c (V/s-mM) (Sensitivity)**	**Ratio of ΔE/Δt-c slope to gallic acid slope**	**E/t slope at 0.37mM gallic acid**	**Ratio of E/t slope to gallic acid slope at 0.37mM**	**Equivalent gallic acid concentration in mM**
Pyrogallic acid	3.598	5.485	1.476	5.690	0.065
Hydroquinone	2.560	3.903	0.986	3.802	0.097
L-ascorbate	1.668	2.544	0.669	2.581	0.143
Gallic acid	0.656	1.000	0.259	1.000	0.37
Pyrocatechol	0.312	0.476	0.133	0.513	0.721
Resorcinol	0.005	0.008	0.005	0.019	19.473

The results in Fig. 24 show that the calibration plots differed in regard to sensitivity (the slope of the calibration plot) shown in Table.7 and from this, the equivalent sensitivities were determined based on the classical gallic acid equivalent concentration. Table 7. Shows gallic acid slope and ratios at 0.37mM relative to the test analytes. The results show the concentration of the different antioxidants that would give a signal equal to the chronopotentiometric signal of the measured 0.37mM gallic acid concentration. Pyrogallic acid has the lowest gallic acid equivalent concentration and resorcinol has the highest among the measured antioxidants.

In conclusion, the chronopotentiometric responses of different antioxidant species were tested by making calibration curves from the measured E/t curves. The antioxidant species tested have different reaction rate constants. Therefore selective measurement of individual antioxidant molecules present in complex matrices cannot be done without separation. The chronopotentiometric signal is a collective property of the sample. It indicates the complex antioxidant activity. It can be expressed in relative unit. This is subsequently evaluated for a collective sample of known antioxidants (see Fig. 32).

4.5 Estimation of the shapes of E-t and ΔE/Δt-c curves by model calculation

It is an obvious question how the $E = f(t)$ function or the $\Delta E/\Delta t_{initial}$ - $c_{analyte}$ calibration curve are expected to look. How the different experimental parameters influence these dependences.

Simple calculations based on a very rough model helped in finding approximate answers. The assumptions needed for the model calculations are the followings:

-we need to accept that the surface film with the mediator species is thin and that all sites in the confined mediator molecules are equally accessible to incoming analyte particles, and the reactivity of all these redox molecules is equal.

- A rotating working electrode is used therefore the diffusion layer of analyte transport is very thin. Consequently, the concentration of the sample at the reaction sites can be determined by competition of both the diffusion transport and the redox reaction.

- The electron exchange rate between the base conductive electrode materials (GC) and the redox mediator film is high. (Reduced graphene oxide was used for enhancing it).

-The stoichiometric coefficients of the reaction generating the signal are 1:1, and two electrons are exchanged by each interacting molecules (M_{ox} and M_{red} means the oxidized and reduced form of the mediator).

$$M_{ox} + 2e^- = M_{red}, \quad \text{and} \quad \text{Analyte}_{red} - 2e^- = \text{Product} \qquad (13)$$

From the above, we can assume that the total amount of confined mediator is constant. (Short time experimental findings (Fig 12.) about stability prove that this assumption is quite realistic).

-We can use the redox form of the Nernst equation for making estimates of the electrode potential dependence on surface concentration ratio of the both the oxidized [MB_{ox}] and the reduced [MB_{red}] forms of the Meldola Blue mediator.

$$E = E_0 + \frac{RT}{zF} \ln \frac{[MB_{ox}]}{[MB_{red}]} \qquad (14)$$

Where [MB_{ox}] and [MB_{red}] stand for concentration of oxidized or reduced form of the mediator in the surface film and other symbols have their usual meanings.

-The final assumption was that the redox reaction above follows the first order kinetics both for the confined mediator, as well as for the analyte.

From the acceptance of the conditions of the assumptions listed, we could write a conventional rate equation expressing the change of the concentration of the oxidized form (x) of the confined mediator.

In the equation *a,* is the two dimension concentration (2D) (mole/area) of the oxidized form of MB at t = 0, just after the controlled potential part of the measuring program

And c is the concentration of the reduced form of immobilized MB on the GCMBE. (The electrode potential imposed in controlled potential step determines the a/c ratio)

b is the (2D) analyte/sample concentration in the bulk. It is obvious that the analyte concentration at the surface will be determined by the competition of the chemical reaction and the diffusion.

The relatively high rotation rate results in a thin diffusion layer (Δy), therefore we can use Fick's I law for getting the contribution of diffusion transport. In the equation *dx* is the change in concentration of *a*.

If D stands for the diffusion- and k for the reaction rate coefficient, then the equation describing the rate of 2D concentration change will be

$$\frac{dx}{dt} = k(a-x)(b-x+\frac{D(b-x)}{\Delta y}) \qquad 15$$

$$\frac{dx}{dt} = k(a-x)*(b-x+\frac{D(b-x)}{\Delta y}) = k(a-x)*(b-x)(1+D/\Delta y) \qquad 16$$

Since D/Δy is constant in case of a particular analyte, at constant electrode rotation rate, then let be

(1+D/Δy)=Z

The reaction rate equation will be the following

$$\frac{dx}{dt} = k(a-x)*(b-x)*Z$$

17

Separating the variables we obtain that $$\frac{dx}{(a-x)*(b-x)*Z} = kdt$$

18

In the equation 19 and 20, the method of integration by partial fractions is use to get the integral form.

Let P and Q the numerators of the two fractions

$$\frac{dx}{(a-x)*(b-x)*Z} = kdt = \frac{Pdx}{(a-x)} + \frac{Qdx}{Z*(b-x)}$$

19

For getting the values of P and Q we use the usual treatment

$$\frac{1}{(a-x)*(b-x)*Z} = \frac{P}{(a-x)} + \frac{Q}{Z*(b-x)}$$

$$1 = \frac{P*(a-x)*(b-x)*Z}{(a-x)} + \frac{Q*(a-x)*(b-x)*Z}{Z*(b-x)}$$

$$1 = (P*(b-x)*Z) + (Q*(a-x))$$

Let x=b, then 1= 0+Q (a-b) and Q=1/ (a-b)

For obtaining P let be x= a, then 1= P*(b-a)*Z+0 and P=1/ (b-a)*Z

Substituting P and Q values into equation 18, we obtain

$$\frac{dx}{(a-x)*(b-x)*Z} = kdt = \frac{dx}{(a-x)*(b-a)*Z} + \frac{dx}{Z*(b-x)*(a-b)} = kdt$$

$$\frac{dx}{(a-x)*(b-a)*Z} - \frac{dx}{Z*(b-x)*(b-a)} = kdt$$

$$\frac{1}{(b-a)*Z}\left[\frac{dx}{(a-x)} - \frac{dx}{(b-x)}\right] = kdt$$

$$\frac{1}{(b-a)*Z}\left[\int_0^x \frac{dx}{(a-x)} - \int_0^x \frac{dx}{(b-x)}\right] = \int_0^t k\,dt$$

$$\frac{1}{(b-a)*Z}\left[-\ln\frac{(a-x)}{a} + \ln\frac{(b-x)}{b}\right] = kt$$

$$\frac{1}{(b-a)*Z}\left[\ln\frac{a(b-x)}{b(a-x)}\right] = kt$$

$$kt(b-a)Z = \ln\frac{a(b-x)}{b(a-x)}$$

$$e^{ktZ(b-a)} = \frac{a(b-x)}{b(a-x)}$$

$$b(a-x)e^{ktZ(b-a)} = a(b-x)$$

$$bae^{ktZ(b-a)} - be^{ktZ(b-a)}x = ab - ax$$

$$bae^{ktZ(b-a)} - ab = (be^{ktZ(b-a)} - a)x$$

$$x = \frac{bae^{ktZ(b-a)} - ab}{be^{ktZ(b-a)} - a} = \frac{ab(e^{ktZ(b-a)} - 1)}{be^{ktZ(b-a)} - a}$$

$$\frac{1}{(b-a)Z}\left[\ln\frac{a(b-x)}{b(a-x)}\right] = kt$$

20

4.5.1 Results from the calculation

From equation (20) the value of *x* can be obtained

$$x = \frac{ab(e^{ktZ(b-a)} - 1)}{be^{ktZ(b-a)} - a}$$

21

The change in the open cell electrode potential as a result of a heterogeneous reaction between the solid surface of modified electrode and the reactants in solution can be obtained from the Nernst equation by following the activity of the mediator on the electrode surface. A rough estimation can be obtained about influences of different

parameters (*a, b, c, k, D, Δy*) on the chronopotentiometric response ($E_{t>0)}$-*t*) curve and on the ($\Delta E_{t\,(initial)}$-$b_{analyte}$) calibration curve.

$$E_{t=0} = E_0 + S\log\frac{a}{c}, \qquad E_{t>0)} = E_0 + S\log\frac{a-x}{c+x}$$

$$\Delta E_t = S\log\frac{a-x}{c+x},$$

22

S is the slope of electrode response. For $n = 2; S = 29.5mV / decade_{T=25^oC}$

Equations (21) and (22) upon inserting dimensionless values for the different parameters can give the calculated chronopotentiometric response curves (E-*t*). Fig. 25 shows a few of them obtained in the case of *a*=1200, *c*= 120, *Z*= 1.001, *k*= 0.01 for different sample concentration values (*b*).

Comparing Fig. 25 the calculated values, and Fig. 23 from the actual laboratory measurements of the antioxidant gallic acid, the similarity is obvious. This proves that the rough model introduced can be used for understanding the working principle of the chronopotentiometric antioxidant measuring method.

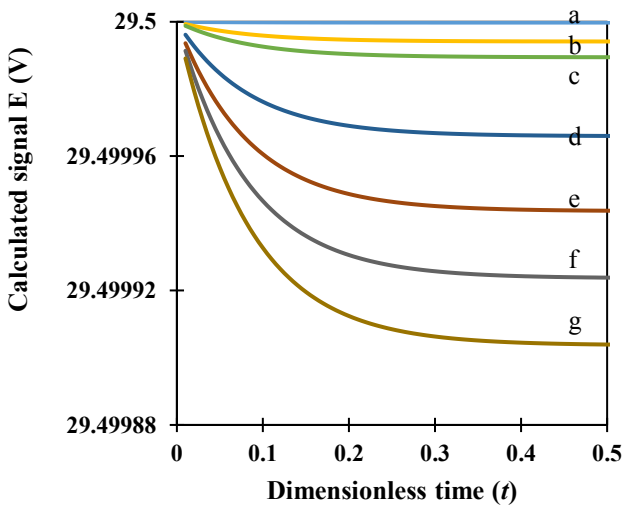

Fig. 25. Calculated chronopotentiometric response curves obtained in case of different dimensionless sample concentration (a) $2x10^{-6}$, (b) $9.9x10^{-6}$, (c) $2.5x10^{-6}$, (d) $4.98x10^{-5}$, (e) $9.9x10^{-5}$, (f) $2.9x10^{-4}$, (g) $8.2x10^{-4}$.

Plotting the initial slopes of the calculated response curves against sample concentration values we obtain the calculated calibration curves. Fig. 26 shows calculated calibration curves obtained with different reaction rate coefficients. The Fig. 26 indicates that separation and a different calibration curve is needed for assessing concentration of different species in a complex matrix. However, the method can give collective value for antioxidant activity of a sample expressed in a related scale. The shapes of the calculated (Fig. 26) and measured (Fig. 24) calibration curves are similar. The sensitivity slightly is decreasing as the concentration increases.

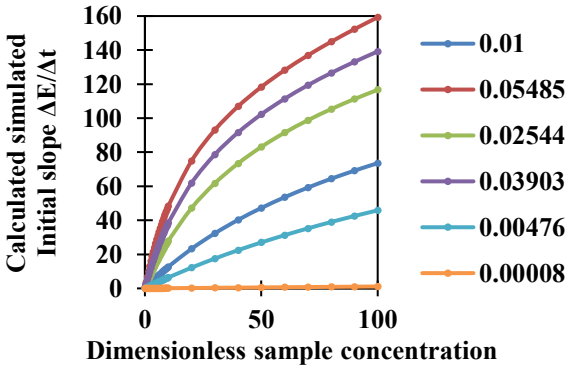

Fig. 26. Calculated calibration curves of analytes obtained with different reaction rate coefficients.

It is interesting to see how the amount of the confined redox mediator, that is the 2D concentration values (*a* and *c*) influence the calibration curves. Keeping in mind that the value of imposed electrode potential determines the concentration ratio of the oxidized and reduced forms, calibration curves were calculated for different mediator concentrations. Fig. 27 shows two of these curves. For the calculation, dimensionless values 0.01 and 1.001 were used for k and Z respectively, but different values for *a* and *c*. Curve A was obtained with (calculated thin layer) *a*=12 and *c*= 1.2, while B with (calculated thick layer) *a*=1200 and *c*= 120. Fig. 27 (2) shows the low concentration section enlarged. From the results, it can be seen that small mediator concentration is more sensitive to the antioxidant species. This is a useful characteristic for making measurements over a smaller sample concentrations in a limited concentration range. On the other hand, the calibration curve obtained with higher mediator concentration gives a broader range for assessing higher concentration but with less sensitivity. Therefore, the results of these calculations indicate an interesting character of the studied chronopotentiometric antioxidant measuring method. It seems very much likely that the analytical performance of the method can be optimized by employing the right amount of redox mediator confined on the electrode surface. This can be considered as tuning the electrode surface as fit for purpose. That means that by selecting the mediator amount, the method can be adjusted to the analytical task. Experimental calibration curves recorded for L-ascorbate (Fig. 22) with electrodes having different mediator films prove these.

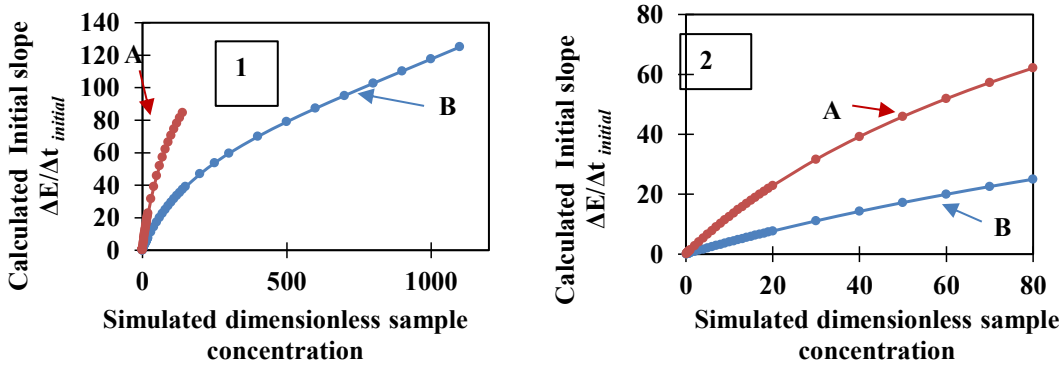

Fig. 27. (1).Calculated calibration curves obtained with thin (A) and thick mediator layers (B). (2).The curve at calculated calibration at low sample concentration.

From these measurements we can conclude that the performance of the method in case of different antioxidant species has been tested. Influence of redox layer thickness on the sensitivity has been checked. The expected shape of chronopotentiometric function (E-t) and that of the calibration curve ($\Delta E/\Delta t_{initial} - c_{analyte}$) were estimated using a rough model, and the calculated curves were compared to experimental ones.

4.6 Investigation of the applicability of miniaturised chemically modified PGadsMBE in antioxidant measurement

Learning from the literature about all advantages that application of electrodes fabricated from commercial pencil leads can provide, it was obvious to test how MB modified electrodes perform in the novel chronopotentiometric antioxidant assessing method. In my work electrodes from three different pencil graphite leads were fabricated. They were modified with MB layer and the PGMBE-s were used as working electrodes in different experiments. To measure the electrochemical surface areas of the PGEs voltammetric experiments were done with the bare, well-polished electrodes in aqueous 0.5 M KCl solution containing 0.5 mM $K_3[Fe(CN)_6]$/ $K_4[Fe(CN)_6]$, while the amount of MB on their surface was estimated from coulometrically taken values. Table 8 compares the characteristic values obtained for the three different electrodes modified with MB.

Table 8. Comparison of the main parameters for adsorbed MB layer on PGMBEs, the measurements were done at 50mV/s in 0.25M phosphate pH=7.0.

Parameter	**0.2 mm,HB**	**0.5 mm,2B**	**0.5 mm,HB**
Q (as) coulombs	$8.25x10^{-7}$	$1.04Ex10^{-5}$	$5.77x10^{-6}$
Electrochemically active surface area ECS (mm^2)	$9.98x10^{-2}$	$1.83x10^{-1}$	$2.65x10^{-1}$
Geometrical area (A) mm^2	$3.14x10^{-2}$	$1.96x10^{-1}$	$1.96x10^{-1}$
No.of Moles	$4.28x10^{-12}$	$5.38x10^{-11}$	$2.99x10^{-11}$
Density of MB -Γ (Q/2FA) mol/mm^2	$1.36x10^{-10}$	$2.74x10^{-10}$	$1.52x10^{-10}$
No. of MB molecules	$2.57x10^{12}$	$3.24x10^{13}$	$1.80x10^{13}$
Area of one molecule of MB 24.6 $Å^2$ in mm^2	$2.46x10^{-13}$	$2.46x10^{-13}$	$2.46x10^{-13}$
No.of MB molecules in one layer of MB on PGE	$1.28x10^{11}$	$7.98x10^{11}$	$7.99x10^{11}$
No.of molecules in one layer of MB on PGE ECS	$4.06x10^{11}$	$1.08x10^{12}$	$7.45x10^{11}$
Number of layers of MB (disk geometric surface)	20.15	40.59	22.55

Using the charge (Q) from the area under the peaks of each PGE (Fig 29), the numbers of adsorbed MB layers on the surfaces of the PGEs were determined (Table 8). It was noted that there were similarities in the number of layers, for HB that is 20.15 and 22.55 for the 0.2 mm and the bigger 0.5 mm electrode respectively. This shows that HB type of pencil graphite has similar adsorption properties. In contrast, the numbers of adsorbed layers on the 2B surface were found to be more than in HB. A total of 40.59 layers were obtained in regard to 0.5 mm 2B. This indicates that the different graphite composition of 2B pencil graphite has an influence on the adsorptive properties. In actual fact, the concentration of graphite in 2B is higher than in HB[103] as reported in literature. Of note too is that the 2B and HB of similar geometrical OD have different electrochemical surface area. The ECS of 0.5 mm HB electrode is slightly bigger than the ECS of 2B electrode of the same size (0.265 mm^2, 0.183 mm^2 respectively).

4.6.1 Adsorption of MB redox mediator layer on the PGE surface

It was questionable, how far the adsorbed MB layer stays attached on the electrochemically activated surface of different pencil electrode. In the study involving the use of 0.2 mm hard and black (HB) PGE, 0.5 mm hard and black (HB) PGE and 0.5 mm (soft black leads) 2B PGE, I successfully immobilized MB on the electrode surface.

Fig. 28. shows the small disc surface of the less than 0.6 mm of PGEs during adsorption with MB.

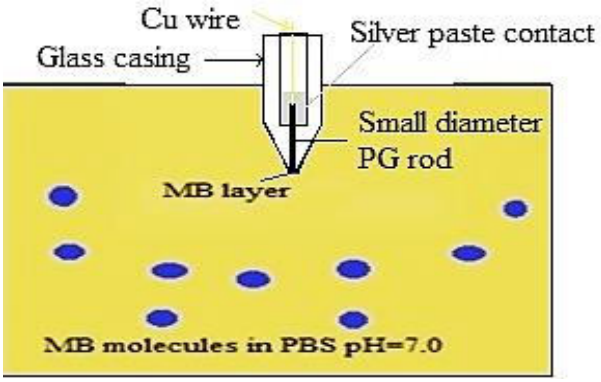

Fig. 28. Schematic drawing indicating the concept of adsorption of MB on pencil lead disk surface

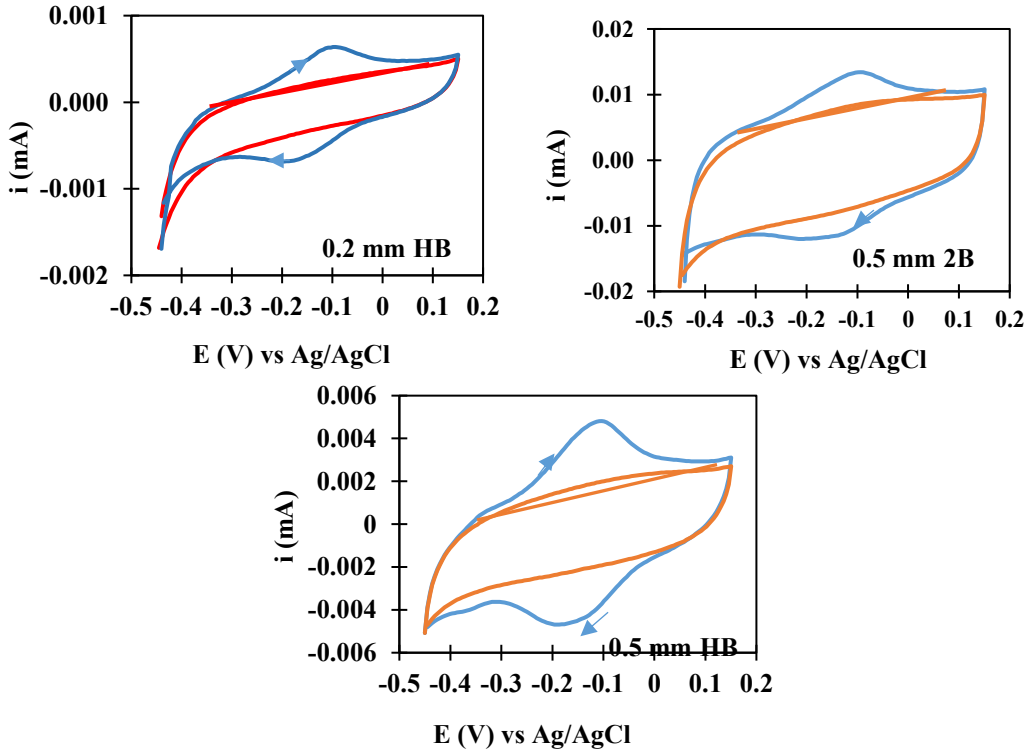

Fig. 29. CV-s taken with PGE (OD 0.2 mm HB, 0.5 mm 2B and 0.5 mm HB) in 0.25 M phosphate buffer pH=7.0 buffer. Scanning rate 50 mv/s. The PGE CVs with peaks are adsorbed with MB, the other curves without peaks are bare.

From the three electrodes, peak shaped curves with quasi reversible character were obtained. Peak separation ranged between 43-97 mV. The amount of MB adsorbed was determined from the area under the anodic peak. Fig. 29 shows the CVs taken with 0.2

mm HB, 0.5 mm 2B and 0.5 mm HB PGE. The peak shaped curves from the electrodes with an adsorbed MB film and the other CVs with no peaks were measured before the modification by adsorption with MB.

The conclusion from this is that, after the electrochemical activation, the three different pencil electrodes adsorbed substantial amount of MB. It follows that immobilization of MB redox mediator on PGE surface can be done. Therefore chemical modification of PGEs can be made without any challenge. The adsorbed mediator molecules readily took part in heterogeneous quasi reversible redox reactions. The estimated surface area of one MB molecule is 24.6 $Å^2$ as is available in publications. Since the area of one molecule is known, the thickness of a multi-layered redox mediator film can also be estimated.

4.6.2 Assessment of the stability of MB layer on the PGEs

In order to test the MB stability on the PG base electrode surface, serial CV-s were recorded with the three MB modified, different pencil electrodes in condition shown in legend of Fig. 29. Between each measurement, approximately five-minute waiting time was left between the measurements of CV-s. The areas under the anodic peaks were recorded followed by plotting of the values against the number of experiments. Comparison of the deviations from the mean value was expressed as a percentage.

Results shown in Fig. 30. (A-C) indicate that changes took place in the MB redox charges over 20 serial measurements. The three different PGMBEs each had a unique percentage deviation from the mean. The percentage was calculated as shown in equation 23. The deviation from the mean peak current (i) is given as a percentage. The uncertainty of setting the background lines under the peaks resulted in a high scattering however, the mean values did not show a big change. During the short period of time, minimal desorption occurred. The loss in MB did not cause a substantial systematic error of antioxidant activity measurements. In one working day the measurements were still repeatable.

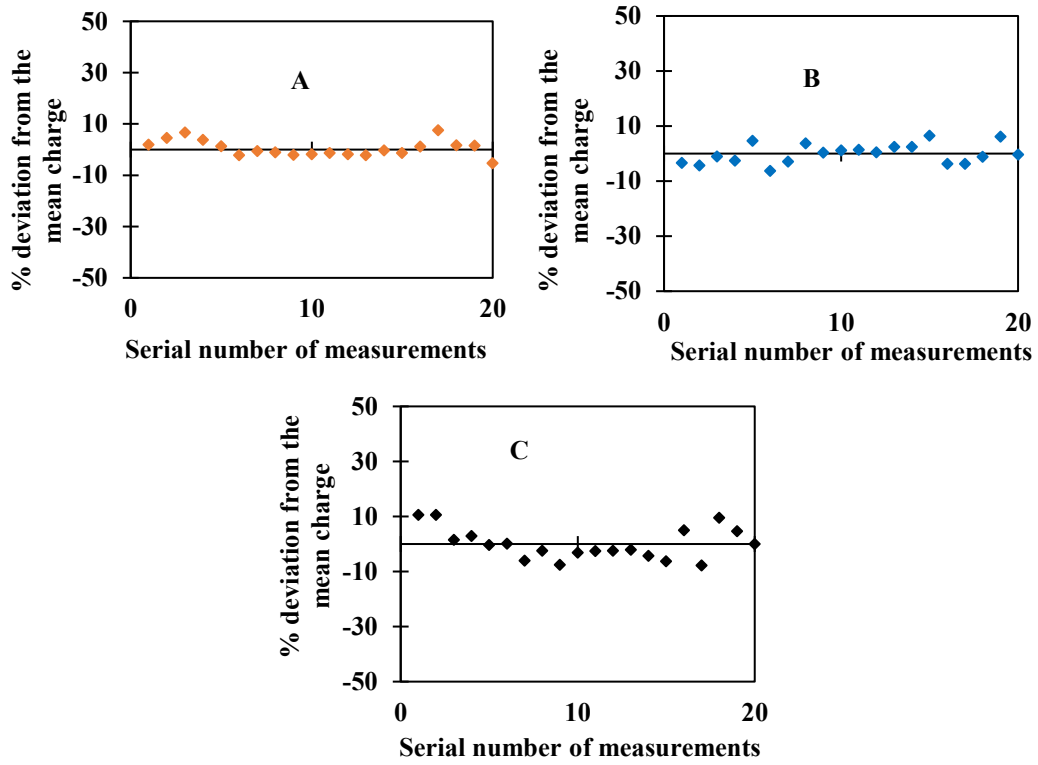

Fig. 30. The relative deviance of the area under CV peak from the average in percentage (equation 23) plotted against the serial number of experiments.

$$i\% = \sqrt{\left(\frac{Q_i - \frac{\sum Q_i}{n}}{\frac{\sum Q_i}{n}}\right)^2} * 100 \qquad (23)$$

A loss of 10% of the original MB redox charge was noted where the modified pencil electrodes were soaked in an aqueous solution overnight.

4.7 Testing the MB modified pencil electrodes in chronopotentiometric antioxidant assessments

4.7.1 Application of PGadsMBE in antioxidant activity experiments

To check the performance of the three different PGadsMBEs in antioxidant species measurements, the electrodes were used in various tests. In these tests, aqueous solutions of the antioxidants prepared with pH=7.0 0.25 M phosphate buffer .1 second long

electrode potential controlled step with 0.2 V vs. Ag/AgCl reference were used. The E/t curves were made in the open circuit The different sample solutions of known concentration gave results of the initial slope obtained after 0.01 s (see Fig.31 A). From the initial slope of E/t curves, calibration curves were made using the evaluation criteria of the method (see Fig.41). Fig. 31 shows some of the results obtained.

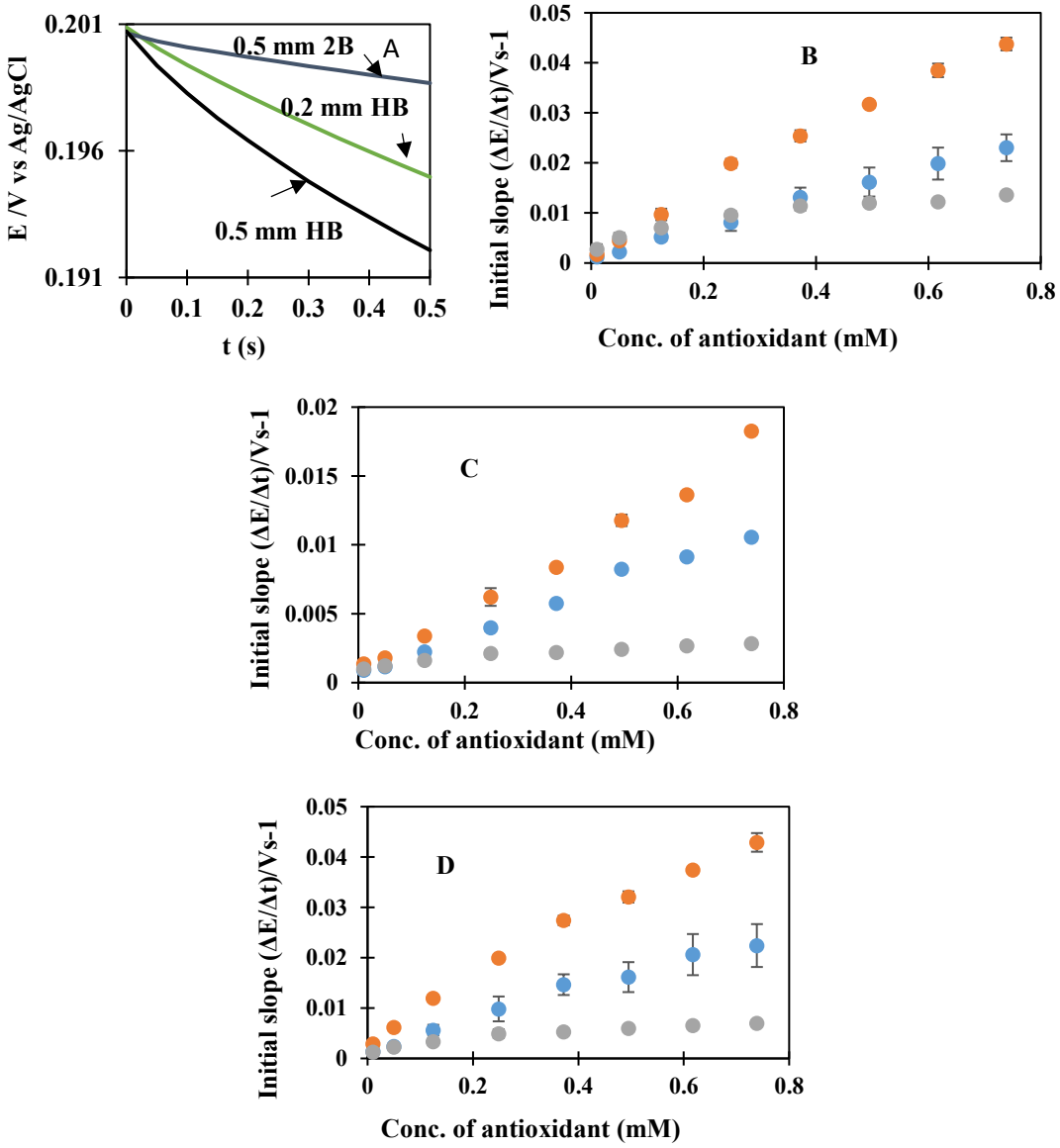

Fig. 31. (A) E-t curves obtained using the chemically modified 0.5 mm 2B, 0.2mm HB and 0.5 mm HB in the case of 1.25×10^{-4} M pyrogallic acid. ΔE/Δt-c calibration plot obtained using; (B) 0.2 mm HB PGMBE , (C) 0.5 mm 2B PGMBE and (D) 0.5 mm HB PGMBE for the antioxidants (orange ●) pyrogallicacid, (blue ●)L-ascorbate, and (grey ●) pyrocatechol in phosphate pH =7.0.

In Fig. 31 (A) the electrode potential – time recordings obtained with the three PGMBEs in case of $1.25x10^{-4}$ M pyrogallic acid are shown. It can be observed that, the potential changes follow the expected time dependences. In Fig. 31 (B-D) calibration curves of different antioxidant species were obtained for the three different PGMBE-s. (a) pyrogallic acid, (b) L-ascorbate and (c) pyrocatechol in 0.25 M phosphate pH=7.0). The shape of the curves correspond to the simulated calibration curves (see Fig. 29) in section dealing with, investigation of the amount of mediator in relation to basic characteristics of the novel reagentless chronopotentiometric method.

The main analytical parameters of the method in case of different pencil electrodes and analytes are listed in Table 9.

Table 9. Main analytical parameters of the method in case of different pencil electrodes and analytes

Parameter	**Antioxidant**	**0.2 mm, HB**	**0.5 mm, 2B**	**0.5 mm, HB**
Lower limit of detection 3δ (mol/L)	Pyrogallic acid	$1x10^{-5}$	$4.5x10^{-5}$	$4.8x10^{-5}$
	L-ascorbate	$4x10^{-5}$	$9.25x10^{-5}$	$1x10^{-5}$
	Pyrocatechol	$9.5x10^{-6}$	$5x10^{-5}$	$4x10^{-5}$
Dynamic range (mol/L)	Pyrogallic acid	$8x10^{-5}$ to $8x10^{-4}$	$5x10^{-5}$ to $8x10^{-4}$	$7x10^{-5}$ to $8x10^{-4}$
	L-ascorbate	$9.9x10^{-6}$ to $8x10^{-4}$	$7x10^{-5}$ to $8x10^{-4}$	$3x10^{-5}$ to $8x10^{-4}$
	Pyrocatechol	$9.5x10^{-6}$ to $3.5x10^{-4}$	$1.2x10^{-4}$ to $1.6x10^{-4}$	$7x10^{-5}$ to $2.5x10^{-4}$
lower Limit of quantification (mol/L)	Pyrogallic acid	$8x10^{-5}$	$5x10^{-5}$	$7x10^{-5}$
	L-ascorbate	$9.9x10^{-6}$	$7x10^{-5}$	$3x10^{-5}$
	Pyrocatechol	$9.5x10^{-6}$	$1.2x10^{-4}$	$7x10^{-5}$
Sensitivity[(V/s) / mol/L]	Pyrogallic acid	57	22	55
	L-ascorbate	30	13	29
	Pyrocatechol	26	4	14

It can be seen that the thickness or the number of mediator layers, the amount and nature of the binder materials used in making the pencil lead, as well as the size of the electrode surface can have significant influence on the various test parameters of stability, the repeatability of measurents using the electrode as well as on sensitivity and dynamic range of the chronopotentiometric method.

In conclusion, the PGEs were fabricated and chemically modified with a thin reversible MB redox mediator film immobilized on the measuring surface. The modified working electrodes were used in a novel, chronopotentiometric antioxidant activity measuring method and their performance was tested. The activity, stability and extent of the mediator film were found satisfactory for all the PGEs tested and could therefore be used for making measurements. In addition, calibration curves of pyrogallic acid, L-ascorbate and pyrocatechol were made. From these results, various analytical parameters, like lower limit of detection, dynamic range, lower limit of quantitation and the sensitivities of analysis were determined. Therefore the simple, chronopotentiometric method that gives collective response to antioxidant activity gets more cost efficient while retaining stability of the MB layer and repeatability of results if pencil based electrodes are used.

4.8 Investigation of the collective antioxidant activity in mixed solutions of reducing species

To determine the collective antioxidant activity in a sample of four different antioxidants, one solution was prepared from the four pure material to make 0.001 M concentration of each. The solution was made in 0.25 M phosphate buffer pH=7.0. The antioxidants were gallic acid, pyrocatechol, hyroquinone and L-ascorbate. The same mixed sample was tested using chronopotentiometry to obtain the E-t plot and compared to gallic acid.

A chronopotentiometric measurement was made in $2.5x10^{-5}$ M gallic acid solution. Another measurement of $2.5\ x10^{-6}$ M concentration of the mixed sample was also made under the same conditions as the pure gallic acid sample. In this way, it was possible to assess the collective activity of a mixed set of different antioxidant species,

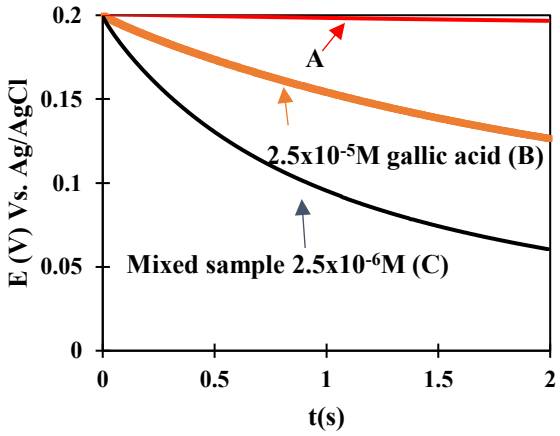

Fig. 32. The chronopotentiogram of (A●) buffer, (B●) 2.5 x 10^{-5} M gallic acid and (C●) 2.5 x10^{-6} M collective antioxidant sample

Fig. 32 shows the E-t curve at OCP of buffer (A), of gallic acid solution (B) and the solution containing four different antioxidants. As expected, initial slope was highest when the mixed solution with a higher collective activity of different antioxidants was tested. C is the total concentration of the mixed sample of various antioxidants. It is shown in section 4.4 that hydroquinone, and L-ascorbate would have a reaction rate that is 3.8 and 2.5 times faster than gallic acid as showed in Table 7. Therefore a higher E-t slope for the mixed sample is not unexpected. The chronopotentiometric method gives a single antioxidant activity value in cases of a samples containing several different antioxidants. For comparison of antioxidant activity of different complex samples the gallic acid equivalent of the obtained slope can be used. It means that the obtained initial slope value can show concentration. The gallic acid equivalent concentration can therefore be obtained for other samples from the calibration curve. ($\Delta E/\Delta t_{initial} - c_{gallic\ acid}$).

Table 10 shows the initial slope values of the collective sample. The gallic acid initial slope at 2.5x10^{-5} M and 2.5x10^{-6} M concentration of the mixed solution are shown for comparison.

Table 10. The comparison of the signal of gallic acid and a mixed antioxidant sample of L-ascorbate, gallic acid, hydroquinone, and pyrocatechol collective concentration ($2.5x10^{-6}$ M) concentration.

Sample	Initial slope ΔE/Δt-c (V/s/mol/L)
Buffer	0.003
Gallic acid (2.5×10^{-5} M)	0.0716
Mixed sample of L-ascorbate, pyrocatechol, hydroquinone and gallic acid ($2.5x10^{-6}$ M)	0.2151

4.9 Assessment of classical reagentless electroanalytical measurement of antioxidant by DPV parallel to chronopotentiometric measurements

To compare the classical voltammetric method to the novel regentless chronopotentiometry, an activated bare GCE was employed for voltammetric measurements. While for Chronopotentiometric measurements, the GCE 5 mm (OD) was modified with $5x10^{-4}$ M MB by adsorption followed by checking of the immobilization using cyclic voltammetry in phosphate buffer pH=7.0. The counter electrode was a Pt wire and the gel Ag/AgCl electrode was the reference. The differential pulse voltammetric (DPV) assay, involved making a calibration plot of gallic acid. The oxidation peak height (ipox) was the signal. Fig. 33 shows the recorded curves

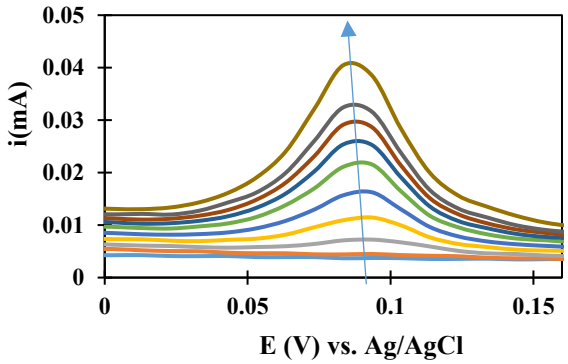

Fig. 33. Differential pulse voltammogram with different concentrations of gallic acid in 0.25 M phosphate buffer pH=7.0 using a bare 5 mm diameter GCE. The concentration in the direction of the arrow from buffer, lower to higher are $1x10^{-7}$ M, $5x10^{-7}$ M, $1.25x10^{-6}$ M, $2.49x10^{-6}$ M, $3.74x10^{-6}$ M, $4.98x10^{-6}$ M and $7.44x10^{-6}$ M gallic acid.

Fig. 33 suggests a method that is well applicable for measuring small concentrations of gallic acid. In this aspect, DPV would have a smaller lower limit of determination compared to chronopotentiometry.

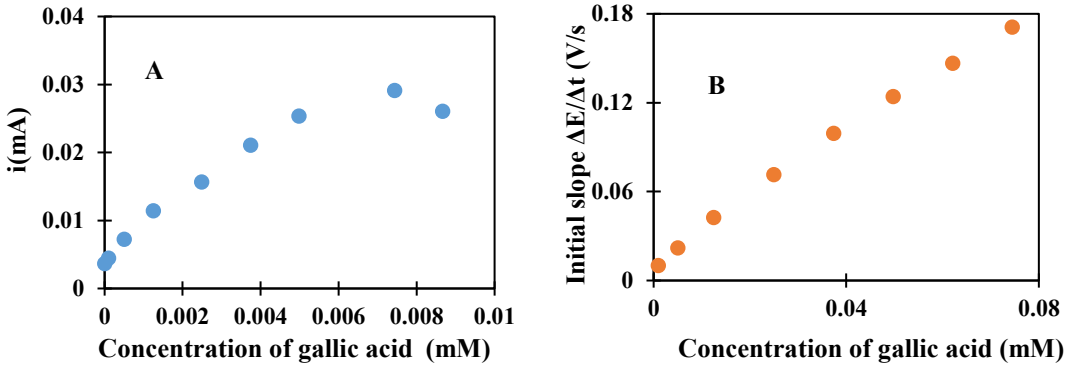

Fig. 34. (A) Calibration plot of gallic acid in 0.25 M phosphate buffer, PH=7.0, obtained from differential pulse voltammetric measurements with bare GCE. (B) Calibration plot of gallic acid with chronopotentiometry measurement.

Fig. 34 shows the calibration curves obtained by the two different methods. The measurements of different concentrations of gallic acid are compared. Table 11 shows the comparison of main parameters. The chronopotentiometric measurement in Fig. 34 (B) has a lower sensitivity for gallic acid than the DPV one (Fig 36 A and Table 11).

Table 11. A comparison of parameters of the parallel methods under equivalent conditions

Parameter	DPV method	New chronopotentiometric method
Dynamic range	$5x10^{-4}$ mM to $7x10^{-3}$ mM	$4x10^{-3}$ mM to $>8x10^{-2}$ mM
Sensitivity (calibration curve slope)	4.3	2.2
Lower limit of detection (Buffer)	$1x10^{-4}$ mM	$5x10^{-4}$ mM
Lower limit of quantitation	$5x10^{-4}$ mM	$4x10^{-3}$ mM

The very small lower limit of determination and the broad dynamic range provided by DPV are well known. It is questionable however, is that very low range necessary for antioxidant assessment in real samples. Most real samples such as fruit may have higher concentration of antioxidants than the dynamic range of DPV shown in Table 11.

Fig. 34. demonstrates the parallel measurements using both methods for a range of gallic acid concentration. The comparison reveals superiority of the new chronopotentiometric method for the measurement of antioxidant activity under high concentration of antioxidant.

4.9.1 Assessment of a real sample apple fruit extract by DPV

The juice from a fresh apple fruit was extracted by piercing and collection of the sap by suction using a micro-syringe. Using 0.25 M phosphate buffer as background electrolyte, a solution containing 0.05% and 0.25% of the collected juice were prepared and DPV measurements were carried out. The obtained voltammograms are shown in Fig.35.

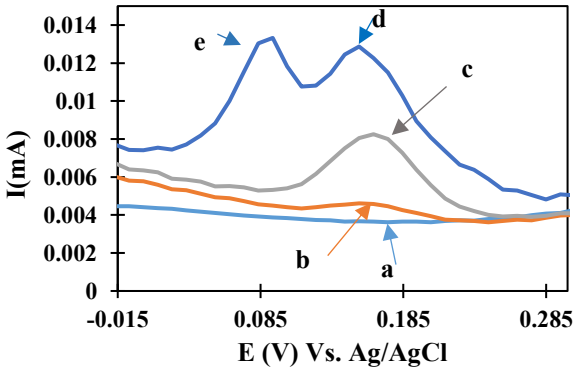

Fig 35. Differential pulse voltammetric curves of (a) 0.25M phosphate buffer, (b) 0.05% apple sap (c) 0.25% apple sap, (d) 2.5 x10^{-5}M ascorbic acid and (e) 1.5x10^{-5} M Gallic acid

Fig.35 shows the peaks at different peak potential for 2.5 x10^{-5}M ascorbic acid (d) and 1.5x10^{-5} M Gallic acid (e). At the peak potential of (b) and (c), a new peak was obtained upon introduction of the pure sample 2.5 x10^{-5} M ascorbic acid in the apple sap measurement cell. This was an indication of ascorbic acid in the apple fruit sap tested. On the other hand, the introduction of 1.5x10^{-5} M gallic acid into the apple sap measurement cell gave a new separate peak, at a different potential implying that gallic acid was not present in the apple sap sample.

In conclusion, reagentless DPV could be used to check for L-ascorbate and gallic acid samples as well as to indicate possible antioxidants in apple fruit. In that case DPV could be used as a complimentary method to the reagentless chronopotentiomentry measurement which is superior for quantitative analysis of antioxidant activity in a sample

4.10 Investigation of antioxidant activity in real samples by chronopotentiometry

4.10.1 Assessment of antioxidant activity in commercially available vitamin c using conventional size electrode

The tests using the chronopotentiometric method gave a consistent response signal as demonstrated by results in previous section. To challenge the method further, vitamin C tablets obtained commercially off the shelves were used. The tablets were a product of InnoPharm (Hungary).

The 1.293g tablet with 500 mg Vitamin C was crushed with a clean pestle and mortar. The fine powder was dissolved in 50 ml phosphate buffer pH=7.0 and stirred for one hour to achieve complete dissolution.

The chronopotentiometric measuring cell was set up as in previous sections and the measurement of buffer/blank, $2.5x10^{-5}$ M gallic acid and the dissolved vitamin C tablet sample concentration was $5x10^{-2}$M.

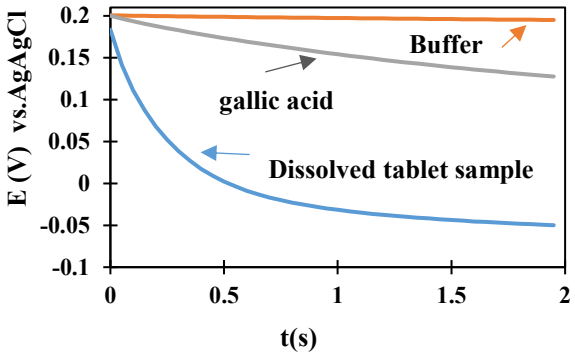

Fig. 36. Chronopotentiogram showing the response of $1.4x10^{-4}$ M commercial vitamin C extract, $2.5x10^{-5}$ M gallic acid and 0.25 M phosphate buffer/blank.

The Fig.36 shows the response to a 1.4 $x10^{-4}$ M concentration made from the $5x10^{-2}$ M stock solution of the whole dissolved vitamin C tablet. This is indicates that real samples for domestic use can be analysed for antioxidant activity using the chronopotentiometric method

4.10.2 Assessment of antioxidant activity in a complex matrix using miniaturized chemically modified PGEs

In order to test the applicability of the modified electrode and the method in a complex matrix of a real food sample, I opted for bell pepper. The bell pepper antioxidant activity can be estimated on the basis of gallic acid equivalent (GAE). The GAE concentration of the antioxidant activity in the pure sample were estimated. From the calibration curve, it was possible to determine the Gallic acid equivalent of the collective antioxidant activity in a red bell pepper (paprika) sample. The measurements were done using both the

PGadsMBE and GCadsMBE for testing samples made from the red pepper sap directly (using miniaturized PGEs) or after dilution with phosphate buffer.

In my studies, the red bell pepper obtained from the local market in Pécs was bled for collecting 10 µl neat sample of the sap. This was diluted 100 times. Fig. 37 shows the initial slope values obtained in serial chronopotentiometric measurements for antioxidant activity plotted against the serial number of the test. For making Fig. 37 A, the sample was $7x10^{-4}$ M gallic acid in 0.25 M phosphate buffer, for making Fig 37. B, red pepper juice diluted 100 times with phosphate buffer was the sample. In case of Fig. 37. C, the fruit juice directly on the fruit, without added background electrolyte was used as sample. The concentration of gallic acid was $7x10^{-4}$ M, the average chronopotentiometric signal [i.e. Initial slope $\Delta E/\Delta t$ (V/s)] for this concentration of gallic acid was 0.0593, therefore, the concentration of 10 % paprika juice extract signal (0.0056) and the direct red bell pepper fruit signal (0.1053) was determined to be $6.95x10^{-5}$ M and $1.25x10^{-3}$ M gallic acid equivalent respectively. Depending on the origin and season of harvest, red bell pepper total polyphenol 7.86 to 42.57 GAE mg/g[168] or $4.6x10^{-2}$ M to $2.5x10^{-1}$ M have been reported.

The measurements were intended to demonstrate the applicability of the MB modified electrodes in direct measurement of antioxidant species activity. The collective antioxidant activity is reported as gallic acid equivalent concentration. The measurements were made *in vivo* this shows that it is possible to make direct measurement on the fruit in the absence of buffer or special added analytical supporting electrolyte. The natural fruit fluid served as the background electrolyte. The stability of the mediator layer and the reproducibility of the measurements was acceptable.

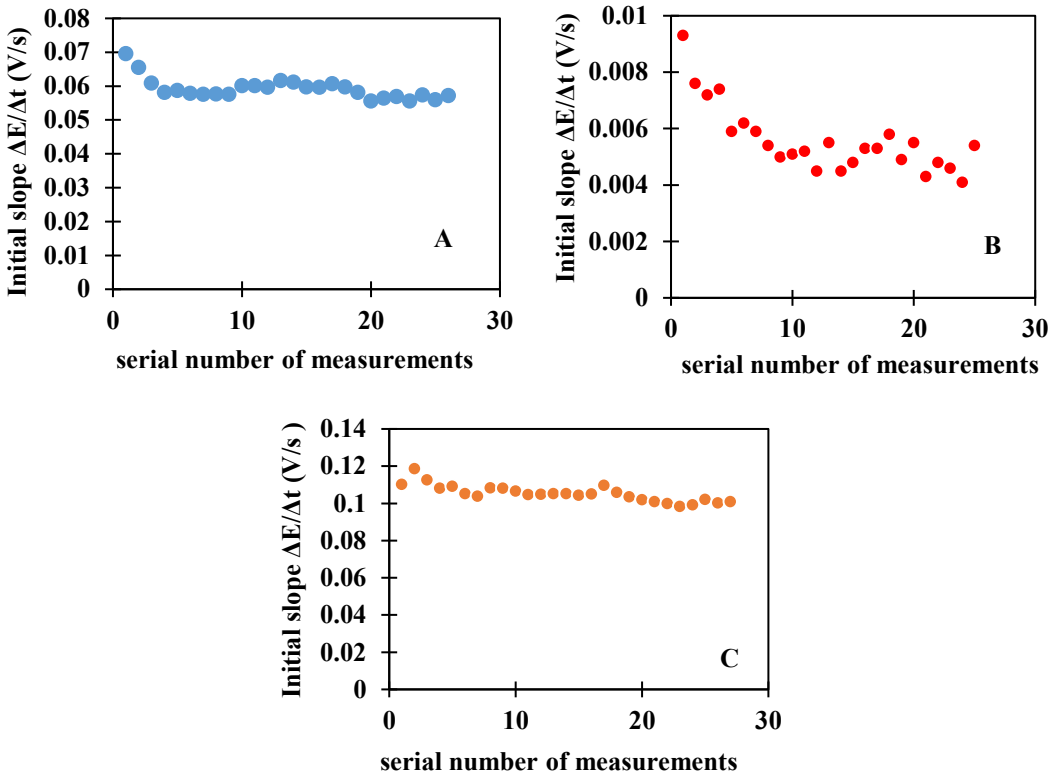

Fig. 37. A plot showing the chronopotentiometric signal stability and repeatability of measurements for a pure material (A) $7X10^{-4}$ M gallic acid in 0.25 M phosphate and 10 µl commercial bell pepper fruit sap extract (B) diluted 100 times in using 0.25 M phosphate. The 0.2 mm HB pencil graphite electrode was used. In both cases, measurements were done without stirring. (C) is the same bell pepper fruit with the measurements taken directly without any background electrolyte. No stirring was done since the miniaturized electrodes were inside the paprika fruit.

4.11 The dependence of SECM feedback signal on conducting spectral graphite carbon surface modified with MB

The Scanning Electrochemical Microscopy (SECM) is a powerful method for studying reactions on solid – liquid interfaces. It was expected that employing this method, information could be obtained about the change of redox activity resulted by confining redox mediator layer on the surface of carbon electrodes. Therefore in my experiments the electro-catalytic action of surfaces the chemically modified ones were compared using SECM. For these experiments about 15 mm long cylindrical section of pencil leads were cut and embedded in epoxy resin using a homemade cylindrical mold with diameter of 35 mm. The carbon surfaces were positioned to face the bottom of the mold. One day time was provided for the epoxy for curing. A hard plastic column of about 15 mm long containing the carbon samples were obtained. The cylindrical end plates were sanded and

polished. The carbon disc(s) were shaped up in line with the shining plastic surface. The chemical modifications with MB of the embedded sample surface were done as described before or left bare. Plastic tape was wrapped around the column sticking out for about 10 mm. In this way a small measuring cell was obtained that could hold 5-7 cm^3 volume of electrolyte.

Pt electrode with a 25 µm diameter as SECM measuring tip and Pt counter and Ag/AgCl reference electrodes were employed. pH = 7.0 phosphate buffer containing ferrocene methanol redox mediator in 2.5 mM concentration was introduced into the measuring cell and vertical approach curves were recorded over the horizontally set surfaces of plastic area and over that of the carbon sample discs. In these experiment 0.6 V (v.s. Ag AgCl) tip potential and 1 µm/s scanning rate were set. Fig. 38 shows how the current depends on the tip-sample distance. As usual in SECM the approach curves are presented in a form of as i_d/i_∞ -L recordings where i_d, i_∞ are the current vaue at d and at ∞ (that is fare from the surface) distances respectively and L = d/a, where d is the tip-surface distance and a is the radius of the tip (in this case 12.5 µm)

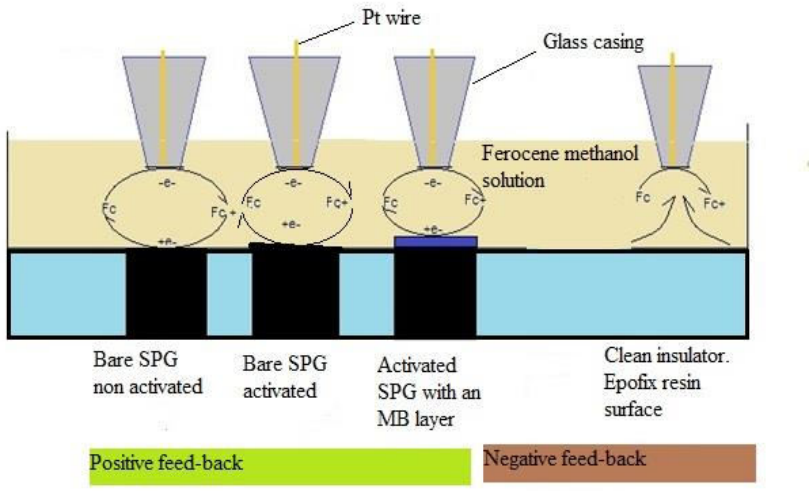

Fig. 38. A picture of the mould set up of bare polished SPGE, activated SPGE, SPGMBE, and a clean insulator surface.

The target was aligned to a level plane for SECM measurements and flooded with 2.5 mM FcMeOH electrolyte in 0.25 M PB pH=7.0. The amperometric measurements I/I_∞ against the Z (µm) on modified carbon targets and the insulator surface was determined

by SECM measurements. The SECM was set in amperometric mode with 1000 data points with a distance of 1uM between points. The potential was set at 600 mV and the current 200nA. The scanning data was recorded as the tip to the substrate distance Z direction in µm (d) and the current (I) at each Z position. For evaluation, the normalized tip distance L =d/a was used to determine the response against current I/I_{∞}, the tip radius (a) was 12.5µm and the I_{∞} was the initial Z position.

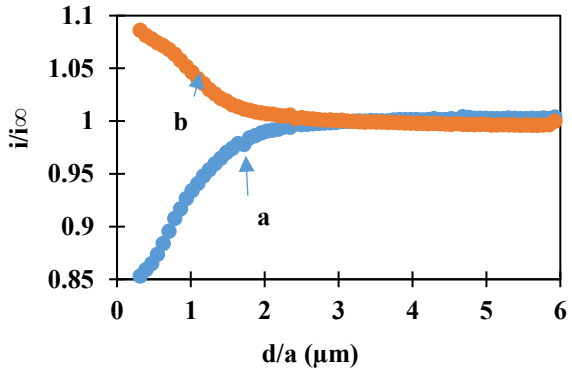

Fig. 39. (A) Plot of the SECM approach curves for plastic and SPGMBE surfaces in ferrocene methanol liquid interface. (a) plastic (b) SPGMBE

As it can be seen in Fig. 39, the approach curve over the plastic surface shows negative feedback effect. The current decreasing as the tip approaches to the surface. It is expected since the plastic surface is passive. It cannot regenerate the form of the mediator generated in the electrode reaction at the tip (oxidized ferrocene methanol). Furthermore the tip approaching hinders the diffusion transport of the form of the mediator reacting on the tip (reduced form).

The approach curves over the redox mediator (MB) modified electrode shows positive feedback effect. The current increases by the decrease of the distance. It means that the carbon surface can regenerate the oxidized mediator, so the reduced mediator diffusing back to the tip increases the concentration of the reacting species. This is shown as positive feedback. This means that the confined mediator layer substantially increases the rate of the heterogeneous redox reaction of reducing the oxidized ferrocene methanol (ferricinium methanol ion).

5 Conclusions

Antioxidant activity of physiologic, clinical, food, beverage etc. samples is a very important property that are more often measured.

In my work a novel measuring method has been worked out for assessing the collective antioxidant activity value of complex samples. The method employs carbon working electrode chemically modified with confined reversible redox mediator layer. Based on literature studies and preliminary experiments the Meldola Blue was selected for preparation of the mediator layer. The measuring procedure worked out is made of two steps. In one short controlled potential step the confined mediator is brought up to its oxidized state. In the second step the potential control is terminated and the open cell potential between the working electrode and a reference is followed in time. The initial slope of the open cell potential – time trace is used as analytical signal. The applicability of the method has been proved experimentally. The dependence of the signal on different parameters was checked experimentally. Using a rough model the theoretically expected dependence of the analytical signal was studied.

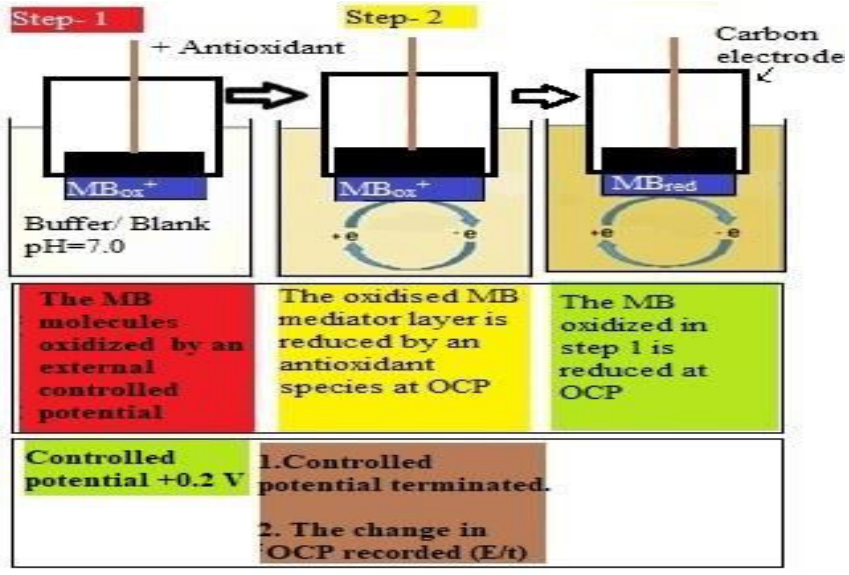

Fig. 40. Schematic drawing explaining the working concept of the novel reagentless chronopotentiometric method

Fig 40 shows schematically the steps and the processes that are involved during the chronopotentiometric measurement.

The working principle of this new method can be summarized as follows, firstly a working electrode is chemically modified with a very thin film acting as a reversible or just quasi reversible redox system. Potentiostatic control can set the redox state of the film.

In a short step the oxidized form can be made dominant. If after this step the electrode gets into contact with the sample, then the antioxidant species in the sample starts interacting with the film. A well-known electrocatalytic oxidation of the reducing components starts. If the potential control is kept, then Faraday current will flow. However, if the potentiostat is disconnected, then the activity ratio of the oxidized and reduced states of the surface film will change. The change of the open cell potential will indicate the change of activity ratio. Therefore, a higher antioxidant activity results in higher slope of the redox potential – time trace. The measured activity is related to the concentration using equation 12.

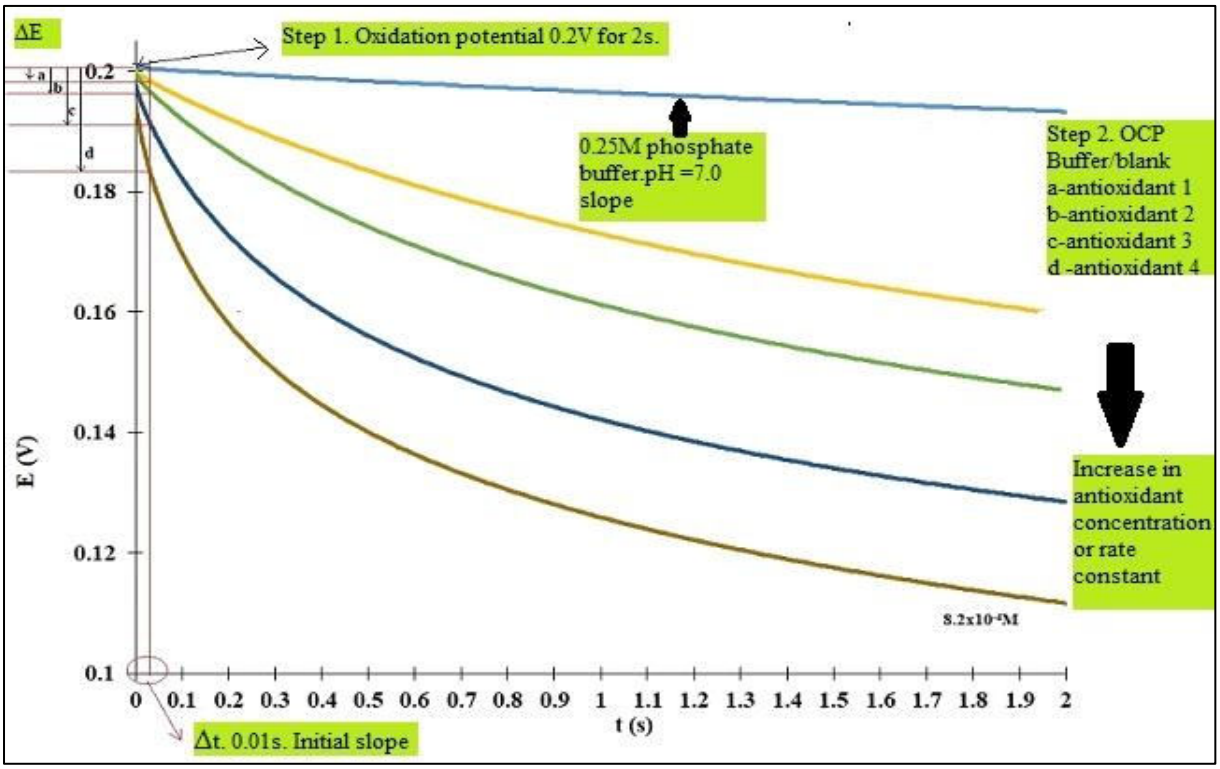

Fig. 41. An illustration of the analysis of results from the reagentless chronopotentiometric measurement

The stability and amount of the immobilized redox mediator layer confined on the electrode surface are important parameters in the new chronopotentiometric method. The applicability of the method in every day laboratory practice partly depends on that.

The new reagentless chronopotentiometric measuring technique has been employed in measuring the activity of L-ascorbate, pyrogallic acid, pyrocatechol, hydroquinone and gallic acid concentration in aqueous solutions. In addition real samples such as red pepper have been analyzed directly or in a support electrolyte solution.

Summarized in this thesis is the data obtained in further experiments with the new chronopotentiometric method. In this report, the redox mediator layer was deposited on a bare Glassy carbon electrode and tested. This was followed by improvement by electrochemically creating a graphene docking layer onto which the redox mediator was adsorbed. Further, the amount was varied by introducing a thick or thin layer which can be considered as tuning. In each subsequent investigation, performance was checked.

The carbon material was changed from GCE to PGE. The PGEs were miniaturized and the rotating GCE was replaced with this static PGE working electrode in the presence of a small stirrer. The stirring was eventually avoided after miniaturization. Finally direct measurements of a neat capsicum fruit sap was attempted. In addition, using this chemically modified working electrode, the chronopotentiometric response of different antioxidant species were measured and compared to that of gallic acid. Parallel measurements were made using classical reagentless DPV and compared to the reagentless chronopotentiometry. The analysis of results from measurements using the method is demonstrated in Fig. 41.

List of acronyms and abbreviations

AA	L-Ascorbate
AAPH	2,2′-Azobis(2-Amidinopropane) Dihydrochloride
ABTS	2, 2'-Azino-Bis (3-Ethylbenzthiazoline-6-Sulfonic Acid
adsMB	Adsorbed Meldola Blue
AOA	Antioxidant Activity
AOC	Antioxidant Capacity
CME	Chemically Modified Electrode
CP	Chronopotentiometry
CUPRAC	Cupric ion reducing antioxidant capacity
CV	Cyclic Voltammetry
DNA	Deoxyribonucleic Acid
DPPH	2, 2-Diphenyl-1-Picrylhydrazyl
EDTA	Ethylenediaminetetraacetic Acid
EI	Electrochemical Index
ELISA	Enzyme Linked Immunosorbent Assay
epMB	Electropolymerised Meldola Blue
ET	Electron Transfer
FC	Folin-Ciocalteau Reducing Capacity Assay
FRAP	Ferric Reducing Antioxidant Power
GAE	Gallic Acid Equivalent
GC	Glassy Carbon
GCGOE	Glassy Carbon, Graphene Oxide Modified Electrode
GCGOMBE	Glassy Carbon, Graphene Oxide MB Modified Electrode
GCMBE	Glassy Carbon, MB Modified Electrode
GO	Graphene Oxide
GRC	Graphite Reinforced Carbon
HAT	Hydrogen Atom Transfer
HOPG	Highly Oriented Pyrolytic Graphite
IC_{50}	Half maximal inhibitory capacity
ICP-MS	Inductively Coupled Plasma-Mass Spectroscopy

ICPS	Inductively Coupled Plasma Spectroscopy
IUPAC	International Union of Pure and Applied Chemistry
MB	Meldola Blue
OD	Outer Diameter
ORAC	Oxygen Radical Absorbance Capacity
PEDOT: PSS	Poly(2,3-Dihydrothieno-1,4-Dioxin)-Poly(Styrene Sulfonate)
PG	Pencil Graphite
PGE	Pencil Graphite Electrode
PGMBE	Pencil Graphite MB Electrode
PSA	Potentiometric Stripping Analysis
ROS	Reactive Oxygen Species
RPM	Rotations per Minute
SECM	Scanning Electrochemical Microscope
SEM	Scanning Electron Microscopy
SET	Single Electron Transfer
SPG	Spectral Graphite
SWV	Square Wave Voltammetry
TAC	Total Antioxidant Capacity
TE	Trolox Equivalent
TEAC	Trolox Equivalent Antioxidant Capacity
TPP	Total Polyphenol
TPTZ	Tripyridyltriazine
UV	Ultraviolet
XPS	X Ray Photoelectron Spectroscopy

List of figures.

List of tables

.

References

[1] W. Gibbs, *Z. für Anal. Chem.* **1864**, *3*, 387–402.

[2] A. Classen, *Quantitative Analyse durch Elektrolyse*, Springer Berlin Heidelberg, **2013**.

[3] E. Hart, *Journal of Analytical Chemistry*, Edward Hart, **1890**.

[4] L. Szebellédy, Z. Somogyi, *Z. für Anal. Chem.* **1938**, *112*, 391–395.

[5] F. Kohlrausch, W. Nippoldt, *Ann. Phys.* **1869**, *214*, 370–390.

[6] I. M. Kolthoff, I. Kolthoff, *Konduktometrische Titrationen*, Springer, **1932**.

[7] M. D. Archer, in *Electrochem. Past Present*, American Chemical Society, **1989**, pp. 115–126.

[8] M. Cremer, *Über Die Ursache der Elektromotorischen Eigenschaften der Gewebe, Zugleich Ein Beitrag zur Lehre von den Polyphasischen Elektrolytketten*, Oldenbourg, **1906**.

[9] F. Haber, Z. Hlemensiewicz, *Z. für Phys. Chem.* **1909**, *67*, 385–431.

[10] J. Heyrovsky, *Lond. Edinb. Dublin Philos. Mag. J. Sci.* **1923**, *45*, 303–315.

[11] R. Chillawar, K. Tadi, R. Motghare, *J. Anal. Chem.* **2015**, *70*, 399–418.

[12] L. Gorton, P. D. Hale, B. Persson, P. Hale, L. Boguslavsky, H. Karan, H. Lee, T. Skotheim, H. Lan, Y. Okamoto, *ACS Symp. Ser.* **1992**, *487*, 56–83.

[13] V. Lobo, A. Patil, A. Phatak, N. Chandra, *Pharmacogn. Rev.* **2010**, *4*, 118–26.

[14] B. Aslani, S. Ghobadi, *Life Sci.* **2016**, *146*, 163–173.

[15] S. Ali, H. Ahsan, M. Zia, T. Siddiqui, F. Khan, *J. Food Biochem.* **2020**, *44*, DOI 10.1111/jfbc.13145.

[16] A. Rizzo, P. Berselli, S. Zava, G. Montorfano, M. Negroni, P. Corsetto, B. Berra, in *Bio-Farms Nutraceuticals Funct. Food Saf. Control Biosens.* (Eds.: M. Giardi, G. Rea, B. Berra), **2010**, pp. 52–67.

[17] J. Kehrer, L. Klotz, *Crit. Rev. Toxicol.* **2015**, *45*, 765–798.

[18] R. Kaur, J. Kaur, J. Mahajan, R. Kumar, S. Arora, *Environ. Sci. Pollut. Res.* **2014**, *21*, 1599–1613.

[19] Y. Furukawa, *Chem. Lett.* **2021**, *50*, 331–341.

[20] R. Muijsers, G. Folkerts, P. Henricks, G. SadeghiHashjin, F. Nijkamp, *LIFE Sci.* **1997**, *60*, 1833–1845.

[21] M. Elhachem, P. Cayot, M. Abboud, N. Louka, R. G. Maroun, E. Bou-Maroun, *Antioxidants* **2021**, *10*, DOI 10.3390/antiox10030382.

[22] Z. Cai, in *Encycl. Toxicol. Second Ed.* (Ed.: P. Wexler), Elsevier, New York, **2005**, pp. 730–734.

[23] Y. Gilgun-Sherki, E. Melamed, D. Offen, *Neuropharmacology* **2001**, *40*, 959–975.

[24] S. B. Nimse, D. Pal, *RSC Adv* **2015**, *5*, DOI 10.1039/C4RA13315C.

[25] J. Flieger, W. Flieger, J. Baj, R. Maciejewski, *Mater. Basel Switz.* **2021**, *14*, DOI 10.3390/ma14154135.

[26] I. Munteanu, C. Apetrei, *Int. J. Mol. Sci.* **2021**, *22*, DOI 10.3390/ijms22073380.

[27] D. A. Belinskaia, P. A. Voronina, V. I. Shmurak, M. A. Vovk, A. A. Batalova, R. Jenkins, N. V. Goncharov, *Antioxidants* **2020**, *9*, DOI 10.3390/antiox9100966.

[28] F. L. Muller, Y. Liu, H. Van Remmen, *J. Biol. Chem.* **2004**, *279*, 49064–49073.

[29] H. M. Korashy, A. O. S. El-Kadi, *Chem. Biol. Interact.* **2006**, *162*, 237–248.

[30] M. Eggersdorfer, D. Laudert, U. Letinois, T. McClymont, J. Medlock, T. Netscher, W. Bonrath, *Angew. Chem.-Int. Ed.* **2012**, *51*, 12960–12990.

[31] J. L. Svirbely, A. Szent-Györgyi, *Biochem. J.* **1932**, *26*, 865–870.

[32] M. Moretti, A. L. S. Rodrigues, in *Pathology (Phila.)* (Ed.: V.R. Preedy), Academic Press, **2020**, pp. 159–167.

[33] J. M. Pullar, A. C. Carr, M. C. M. Vissers, *Nutrients* **2017**, *9*, DOI 10.3390/nu9080866.

[34] K. Yamagata, in *Stud. Nat. Prod. Chem.* (Ed.: Atta-ur-Rahman), Elsevier, **2018**, pp. 323–350.

[35] M. Rudrapal, S. Khairnar, J. Khan, A. Bin Dukhyil, M. Ansari, M. Alomary, F. Alshabrmi, S. Palai, P. Deb, R. Devi, *Front. Pharmacol.* **2022**, *13*, DOI 10.3389/fphar.2022.806470.

[36] C. Papuc, G. Goran, C. Predescu, V. Nicorescu, G. Stefan, *Compr. Rev. Food Sci. Food Saf.* **2017**, *16*, 1243–1268.

[37] X. Liu, C. Le Bourvellec, S. Guyot, C. Renard, *Compr. Rev. Food Sci. Food Saf.* **2021**, *20*, 4841–4880.

[38] M. Herrero, M. Plaza, A. Cifuentes, E. Ibáñez, in *Compr. Sampl. Sample Prep.* (Ed.: J. Pawliszyn), Academic Press, Oxford, **2012**, pp. 159–180.

[39] G. A. Burdock, *Food Chem. Toxicol.* **1998**, *36*, 347–363.

[40] R. Giner, J. Rios, S. Manez, *Antioxidants* **2022**, *11*, DOI 10.3390/antiox11020343.

[41] F. Shahidi, A. Chandrasekara, *Phytochem. Rev.* **2010**, *9*, 147–170.

[42] F. Tomas-Barberan, M. Clifford, *J. Sci. Food Agric.* **2000**, *80*, 1024–1032.

[43] K. B. Martinez, J. D. Mackert, M. K. McIntosh, in *Nutr. Funct. Foods Healthy Aging* (Ed.: R.R. Watson), Academic Press, **2017**, pp. 191–210.

[44] J. Fiedor, K. Burda, *Nutrients* **2014**, *6*, 466–488.

[45] T. Tanaka, M. Shnimizu, H. Moriwaki, *Molecules* **2012**, *17*, 3202–3242.

[46] L. Cai, J. Koropatnick, M. G. Cherian, *Chem. Biol. Interact.* **1995**, *96*, 143–155.

[47] C. Prescott, S. Bottle, *Cell Biochem. Biophys.* **2017**, *75*, DOI 10.1007/s12013-016-0759-0.

[48] G. Ye, N. S. Metreveli, J. Ren, P. N. Epstein, *Diabetes* **2003**, *52*, 777–783.

[49] N. Chiaverini, M. De Ley, *Free Radic. Res.* **2010**, *44*, 605–613.

[50] Z. Ďuračková, *Physiol. Res.* **2010**, *59*, 459–469.

[51] D. V. Ratnam, D. D. Ankola, V. Bhardwaj, D. K. Sahana, M. N. V. R. Kumar, *J. Control. Release Off. J. Control. Release Soc.* **2006**, *113*, 189–207.

[52] J. Hoyos-Arbeláez, M. Vázquez, J. Contreras-Calderón, *Food Chem.* **2017**, *221*, 1371–1381.

[53] J. Bouayed, T. Bohn, *Oxid. Med. Cell. Longev.* **2010**, *3*, 228–237.

[54] G. J. Burton, E. Jauniaux, *Placent. Bed Matern. - Fetal Disord.* **2011**, *25*, 287–299.

[55] M. Carocho, P. Morales, I. Ferreira, *Trends Food Sci. Technol.* **2018**, *71*, 107–120.

[56] M. Estévez, Z. Li, O. P. Soladoye, T. Van-Hecke, in *Adv. Food Nutr. Res.* (Ed.: F. Toldrá), Academic Press, **2017**, pp. 45–81.

[57] I. Bayram, E. A. Decker, *Trends Food Sci. Technol.* **2023**, *133*, 219–230.

[58] A. Somogyi, K. Rosta, P. Pusztai, Z. Tulassay, G. Nagy, *Physiol. Meas.* **2007**, *28*, R41–R55.

[59] F. Shahidi, Y. Zhong, *J. Funct. Foods* **2015**, *18*, 757–781.

[60] R. Nimal, O. Selcuk, S. Kurbanoglu, A. Shah, M. Siddiq, B. Uslu, *TrAC Trends Anal. Chem.* **2022**, *153*, 116626.

[61] E. Becker, L. Nissen, L. Skibsted, *Eur. Food Res. Technol.* **2004**, *219*, 561–571.

[62] R. van den Berg, G. Haenen, H. van den Berg, A. Bast, *Food Chem.* **1999**, *66*, 511–517.

[63] K. H. Musa, A. Abdullah, B. Kuswandi, M. A. Hidayat, *Food Chem.* **2013**, *141*, 4102–4106.

[64] D. W. Plank, J. Szpylka, H. Sapirstein, D. Woollard, C. M. Zapf, V. Lee, C. Y. O. Chen, R. H. Liu, R. Tsao, A. Düsterloh, S. Baugh, *J. AOAC Int.* **2012**, *95*, 1562–1569.

[65] S. Martinez, L. Valek, J. Resetic, D. F. Ruzic, *J. Electroanal. Chem.* **2006**, *588*, 68–73.

[66] M. Özyürek, K. Güçlü, R. Apak, *TrAC Trends Anal. Chem.* **2011**, *30*, 652–664.

[67] M. Moreno, R. Estevez-Brito, J. Mellado, *Comptes Rendus Chim.* **2020**, *23*, 395–401.

[68] M. Antolovich, P. D. Prenzler, E. Patsalides, S. McDonald, K. Robards, *The Analyst* **2002**, *127*, 183–198.

[69] G. Ziyatdinova, I. Salikhova, H. Budnikov, *Food Chem.* **2014**, *150*, 80–86.

[70] K. Brainina, D. Varzakova, E. Gerasimova, *J. Anal. Chem.* **2012**, *67*, DOI 10.1134/S1061934812020050.

[71] N. Ragubeer, D. R. Beukes, J. L. Limson, *Food Chem.* **2010**, *121*, 227–232.

[72] R. Karawita, N. Siriwardhana, K.-W. Lee, M. S. Heo, I.-K. Yeo, Y.-D. Lee, Y.-J. Jeon, *Eur. Food Res. Technol.* **2005**, *220*, 363–371.

[73] M. D. Rivero-Pérez, P. Muñiz, M. L. Gonzalez-Sanjosé, *J. Agric. Food Chem.* **2007**, *55*, 5476–5483.

[74] E. Pavlova, P. Genova-Kalou, G. Dyankov, *Anal. Biochem.* **2023**, *670*, 115137.

[75] J. Piljac-Zegarac, L. Valek, T. Stipcevic, S. Martinez, *Food Chem.* **2010**, *121*, 820–825.

[76] İ. Gulcin, *Arch. Toxicol.* **2020**, *94*, 651–715.

[77] F. Scholz, *Electroanalytical Methods*, **2010**.

[78] K. Z. Brainina, A. V. Ivanova, E. N. Sharafutdinova, E. L. Lozovskaya, E. I. Shkarina, *Talanta* **2007**, *71*, 13–18.

[79] J. Paré, J. Bélanger, *Instrumental Methods in Food Analysis*, Elsevier, **1997**.

[80] R. Abdel-Hamid, E. F. Newair, *J. Electroanal. Chem.* **2011**, *657*, 107–112.

[81] J. Hoyos-Arbelaez, M. Vazquez, J. Contreras-Calderon, *Food Chem.* **2017**, *221*, 1371–1381.

[82] J. Sochor, J. Dobes, O. Kryštofová, B. Ruttkay-Nedecky, P. Babula, M. Pohanka, T. Jurikova, O. Zitka, V. Adam, B. Klejdus, R. Kizek, *Int. J. Electrochem. Sci.* **2013**, *8*, 8464–8489.

[83] A. Pisoschi, C. Cimpeanu, G. Predoi, *Open Chem.* **2015**, *13*, DOI 10.1515/chem-2015-0099.

[84] Y. Wang, C. Calas-Blanchard, M. Cortina, L. Baohong, J. Marty, *Electroanalysis* **2009**, *21*, 1395–1400.

[85] A. J. Blasco, M. C. González, A. Escarpa, *Anal. Chim. Acta* **2004**, *511*, 71–81.

[86] M. Šeruga, I. Novak, L. Jakobek, *Food Chem.* **2011**, *124*, 1208–1216.

[87] S. Ignatov, D. Shishniashvili, B. Ge, F. W. Scheller, F. Lisdat, *Biosens. Bioelectron.* **2002**, *17*, 191–199.

[88] F. Lino, L. de Sa, I. Torres, M. Rocha, T. Dinis, P. Ghedini, V. Somerset, E. Gil, *Electrochimica Acta* **2014**, *128*, 25–31.

[89] A. M. Pisoschi, C. Cimpeanu, G. Predoi, *Open Chem.* **2015**, *13*, 824–856.

[90] I. de Macedo, L. Garcia, J. Neto, K. Leite, V. Ferreira, P. Ghedini, E. Gil, Food *Chem.* **2017**, *217*, 326–331.

[91] K. Z. Brainina, E. L. Gerasimova, D. P. Varzakova, S. L. Balezin, I. G. Portnov, V. A. Makutina, E. V. Tyrchaninova, *Open Chem. Biomed. Methods J.* **2012**, *5*, 1–7.

[92] K. Z. Brainina, L. G. Galperin, E. L. Gerasimova, M. Y. Khodos, *IEEE Sens. J.* **2012**, *12*, 527–532.

[93] R. L. McCreery, *Chem. Rev.* **2008**, *108*, 2646–2687.

[94] A. Rana, N. Baig, T. A. Saleh, *J. Electroanal. Chem.* **2019**, *833*, 313–332.

[95] R. C. A. Jacek Lipkowski, *Electrochemistry of Carbon Electrodes*, John Wiley & Sons, **n.d.**

[96] R. N. Adams, *Electrochemistry at Solid Electrodes*, N. Dekker, **1969**.

[97] P. Kissinger, W. R. Heineman, *Laboratory Techniques in Electroanalytical Chemistry, Revised and Expanded*, CRC Press, **2018**.

[98] C. M. A. Brett, A. M. O. Brett, *Electrochemistry: Principles, Methods, and Applications*, Oxford University Press, **1993**.

[99] R. N. Adams, *Anal. Chem.* **1958**, *30*, 1576–1576.

[100] W. E. Van der Linden, J. W. Dieker, *Anal. Chim. Acta* **1980**, *119*, 1–24.

[101] M. Armstrong-James, J. Millar, *J. Neurosci. Methods* **1979**, *1*, 279–287.

[102] A. Isa, N. Nosbi, M. Che Ismail, H. Md Akil, W. F. F. Wan Ali, M. F. Omar, *Mater. Basel Switz.* **2022**, *15*, DOI 10.3390/ma15144991.

[103] A. Pandey, S. Sharma, R. Jain, A. Raja, *J. Electrochem. Soc.* **2020**, *167*, 037501.

[104] H. T. Purushothama, Y. A. Nayaka, M. M. Vinay, P. Manjunatha, R. O. Yathisha, K. V. Basavarajappa, *J. Sci. Adv. Mater. Devices* **2018**, *3*, 161–166.

[105] I. David, D. Popa, M. Buleandra, *J. Anal. Methods Chem.* **2017**, *2017*, DOI 10.1155/2017/1905968.

[106] K. Aoki, T. Okamoto, H. Kaneko, K. Nozaki, A. Negishi, *J. Electroanal. Chem. Interfacial Electrochem.* **1989**, *263*, 323–331.

[107] J. Kariuki, *J. Electrochem. Soc.* **2012**, *159*, H747–H751.

[108] V. K. Sharma, F. Jelen, L. Trnkova, *Sensors* **2015**, *15*, 1564–1600.

[109] R. A. Durst, *Pure Appl. Chem.* **1997**, *69*, 1317–1324.

[110] R. W. Murray, *Acc. Chem. Res.* **1980**, *13*, 135–141.

[111] R. W. Murray, *Electroanal. Chem. Vol 13* **1984**, *191*.

[112] W. Boumya, N. Taoufik, M. Achak, N. Barka, *J. Pharm. Anal.* **2021**, *11*, 138–154.

[113] M. Coroş, F. Pogacean, A. Biris, A. Biris, S. Pruneanu, *Micro Nanosyst.* **2013**, *5*, 127.

[114] Md. Z. Khan, *J. Nanomater.* **2017**, *2017*, DOI 10.1155/2017/8178314.

[115] H. Beitollai, M. Safaei, S. Tajik, *Int. J. Nano Dimens.* **2019**, *10*, 125–140.

[116] T. Yamaguchi, T. Komura, S. Hayashi, M. Asano, G. Y. Niu, K. Takahashi, *Electrochemistry* **2006**, *74*, 32–41.

[117] A. D. Pournara, G. D. Tarlas, G. S. Papaefstathiou, M. J. Manos, *Inorg Chem Front* **2019**, *6*, 3440–3455.

[118] A. J. Bard, *J. Chem. Educ.* **1983**, *60*, 302–304.

[119] F. Mousazadeh, S. Mohammadi, S. Akbari, N. Mofidinasab, M. Aflatoonian, A. Shokooh-Saljooghi, *Curr. Anal. Chem.* **2022**, *18*, 6–30.

[120] L. Nagy, G. Nagy, R. E. Gyurcsányi, M. R. Neuman, E. Lindner, *Proc. 6th Symp. Instrum. Anal.* **2002**, *53*, 165–175.

[121] D. Centonze, C. Malitesta, F. Palmisano, P. G. Zambonin, *Electroanalysis* **1994**, *6*, 423–429.

[122] F. Mizutani, S. Yabuki, Y. Sato, T. Sawaguchi, S. Iijima, *Electrochimica Acta* **2000**, *45*, 2945–2952.

[123] F. Palmisano, Luisa. L.Torsi, P. Giorgio. P.G.Zambonin, *Anal. Chem.* **1990**, *62*, 2735–2740.

[124] R. J. Geise, J. M. Adams, N. J. Barone, A. M. Yacynych, *Biosens. Bioelectron.* **1991**, *6*, 151–160.

[125] R. N. Adams, *Anal. Chem.* **1976**, *48*, 1126A-1138A.

[126] G. A. Gerhardt, A. F. Oke, G. Nagy, B. Moghaddam, R. N. Adams, *Brain Res.* **1984**, *290*, 390–395.

[127] G. Nagy, G. A. Gerhardt, A. F. Oke, M. E. Rice, R. N. Adams, M. N. Szentirmay, C. R. Martin, *J. Electroanal. Chem. Interfacial Electrochem.* **1985**, *188*, 85–94.

[128] L. Xiang-Qin, K. Guang-Feng, C. Ying, *Chin. J. Anal. Chem.* **2008**, *36*, 157–161.

[129] H. Afsharara, E. Asadian, B. Mostafiz, K. Banan, S. A. Bigdeli, D. Hatamabadi, A. Keshavarz, C. M. Hussain, R. Keçili, F. Ghorbani-Bidkorpeh, *TrAC-Trends Anal. Chem.* **2023**, 116949.

[130] B. Csóka, B. Kovacs, G. Nagy, *Electroanalysis* **2003**, *15*, 1335–1342.

[131] N. Baig, M. Sajid, T. A. Saleh, *TrAC Trends Anal. Chem.* **2019**, *111*, 47–61.

[132] C. Liu, K. Wang, S. Luo, Y. Tang, L. Chen, *Small* **2011**, *7*, 1203–1206.

[133] H. Guo, X. Wang, Q. Qian, F. Wang, X. Xia, *ACS Nano* **2009**, *3*, 2653–2659.

[134] F. Cui, X. Zhang, *J. Solid State Electrochem.* **2013**, *17*, 167–173.

[135] Y. Wang, Y. Li, L. Tang, J. Lu, J. Li, *Electrochem Commun* **2009**, *11*, 889–892.

[136] L. Gorton, A. Torstensson, H. Jaegfeldt, G. Johansson, *J. Electroanal. Chem. Interfacial Electrochem.* **1984**, *161*, 103–120.

[137] A. V. Alex, R. Ciucu, *J. Biosens. Bioelectron.* **2014**, *5*, 1–10.

[138] D. Gligor, I. Craciunescu, I. C. Popescu, L. Gorton, *Electroanalysis* **2010**, *22*, 509–512.

[139] S. Kaya, T. Karabulut, S. Kurbanoglu, S. Ozkan, *Curr. Pharm. Anal.* **2020**, *16*, 641–660.

[140] M. Sajid, M. Nazal, M. Mansha, A. Alsharaa, S. Jillani, C. Basheer, *TrAC-Trends Anal. Chem.* **2016**, *76*, 15–29.

[141] R. W. Murray, A. G. Ewing, R. A. Durst, *Anal. Chem.* **1987**, *59*, 379A-390A.

[142] G. G. Wallace, in *Chem. Sens.* (Ed.: T.E. Edmonds), Springer Netherlands, Dordrecht, **1988**, pp. 132–154.

[143] J. Svitkova, T. Ignat, L. Svorc, J. Labuda, J. Barek, *Crit. Rev. Anal. Chem.* **2016**, *46*, 248–256.

[144] G. Nagy, I. Kapui, L. Gorton, *Fifth Eur. Conf. Electroanal.* **1995**, *305*, 65–73.

[145] S. Kochius, A. Magnusson, F. Hollmann, J. Schrader, D. Holtmann, *Appl. Microbiol. Biotechnol.* **2012**, *93*, 2251–64.

[146] L. Muthuri, L. Nagy, G. Nagy, *Electrochem. Commun.* **2021**, *122*, 106907.

[147] P. Endpoint, *Curr. Sep.* **2000**, *18*, 130.

[148] R. Pecsok, *Anal. Chem.* **1983**, *55*, A993–A993.

[149] C. Foulk, A. Bawden, *J. Am. Chem. Soc.* **1926**, *48*, 2045–2051.

[150] J. E. Baur, in *Handb. Electrochem.* (Ed.: C.G. Zoski), Elsevier, Amsterdam, **2007**, pp. 829–848.

[151] C. N. Reilley, W. G. Scribner, *Anal. Chem.* **1955**, *27*, 1210–1215.

[152] F. H. Beyerlein, R. S. Nicholson, *Anal. Chem.* **1968**, *40*, 286–288.

[153] H. B. Herman, A. J. Bard, *J. Electrochem. Soc.* **1968**, *115*, 1028.

[154] R. W. Murray, C. N. Reilley, *J. Electroanal. Chem. 1959* **1962**, *3*, 64–77.

[155] C. R. Christensen, F. C. Anson, *Anal. Chem.* **1963**, *35*, 205–209.

[156] J. M. Estela, C. Tomás, A. Cladera, V. Cerdà, *Crit. Rev. Anal. Chem.* **1995**, *25*, 91–141.

[157] D. Jagner, A. Graneli, *Anal. Chim. Acta* **1976**, *83*, 19–26.

[158] D. Jagner, *Analyst* **1982**, *107*, 593–599.

[159] S. Bruckenstein, J. W. Bixler, *Anal. Chem.* **1965**, *37*, 786–790.

[160] N. Serrano, J. M. Díaz-Cruz, C. Ariño, M. Esteban, *Electroanalysis* **2007**, *19*, 2039–2049.

[161] E. Beinrohr, J. Dzurov, J. Annus, J. A. C. Broekaert, *Fresenius J. Anal. Chem.* **1998**, *362*, 201–204.

[162] J. Švarc-Gajić, Z. J. Suturovic, N. J. Marjanovic, S. Kravić, *Asian J. Anim. Vet. Adv.* **2006**, *1*, 13–22.

[163] N. Meepan, S. Siriket, S. Dejmanee, R. Ratana-Ohpas, *Walailak J. Sci. Technol.* **2010**, *7*, 61–67.

[164] M. Pournaghi-Azar, H. Dastangoo, R. Baj, *J. Radioanal. Nucl. Chem.* **2010**, *283*, 75–81.

[165] L. Zhu, J. Zhai, R. Yang, C. Tian, L. Guo, *Biosens. Bioelectron.* **2007**, *22*, 2768–2773.

[166] A. Vasilescu, S. Andreescu, C. Bala, S. C. Litescu, T. Noguer, J.-L. Marty, *Sel. Pap. Seventh World Congr. Biosens. Kyoto Jpn. 15-17 May 2002* **2003**, *18*, 781–790.

[167] National Library of Medicine, National Center for Biotechnology Information, can be found under https://pubchem.ncbi.nlm.nih.gov/compound/Meldola-blue, **2023**.

[168] A.-E. Luis Miguel, Z. Villagran, O. Vázquez-Paulino, F. Ascencio, A. Villarruel-Lopez, *Molecules* **2021**, *26*, 5341.